

Daniel dos Santos Mota

Title of the Thesis

Subtitle if
it is needed

Thesis for the Degree of Philosophiae Doctor

Trondheim, January 2023

Norwegian University of Science and Technology
Faculty of Information Technology and Electrical Engineering
Department of Electric Power Engineering



Norwegian University of
Science and Technology

NTNU

Norges teknisk-naturvitenskapelige universitet
Norwegian University of Science and Technology

Thesis for the Degree of Philosophiae Doctor
Faculty of Information Technology and Electrical Engineering
Department of Electronic Systems

Submitted dd/mm/yyyy;
Approved dd/mm/yyyy;
Date of defense dd/mm/yyyy; Rådsrommet G144 | (time)

Supervisors
Prof. Supervisor & Prof. Co-supervisor

Assessment Committee

- 1st opponent
Dr. 1st opponent,
Name of the institute in the original language
Name of the institute in English
City, Country
- 2nd opponent
Dr. 2nd opponent,
Name of the institute in the original language
Name of the institute in English
City, Country
- Additional members of the committee and administrator
Prof. committee

TITLE OF THE THESIS

Chapters 1-3 © 2021 Author (unless otherwise stated)
Chapter 4 © 2017 Name of journal publisher 1
Chapter 5 © 2018 Name of journal publisher 2
Chapter 6 © 2020 Name of journal publisher 3
Chapter 7 © 2021 Author

ISBN 123-45-678-9101-2 (printed ver.)
ISBN 123-45-678-9101-2 (electronic ver.)
ISSN 1234-5678 (printed ver.)
ISSN 1234-5678 (online ver.)

Doctoral theses at NTNU, 2021:12

Printed by NTNU Grafisk senter

To my family

...

“Don’t Panic.”
The Hitchhiker’s Guide to the Galaxy
Douglas ADAMS



“O jogo só acaba quando termina”
frase atribuída a Vicente MATHEUS

Abstract

Lorem ipsum dolor sit amet, consectetuer adipiscing elit. Ut purus elit, vestibulum ut, placerat ac, adipiscing vitae, felis. Curabitur dictum gravida mauris. Nam arcu libero, nonummy eget, consectetuer id, vulputate a, magna. Donec vehicula augue eu neque. Pellentesque habitant morbi tristique senectus et netus et malesuada fames ac turpis egestas. Mauris ut leo. Cras viverra metus rhoncus sem. Nulla et lectus vestibulum urna fringilla ultrices. Phasellus eu tellus sit amet tortor gravida placerat. Integer sapien est, iaculis in, pretium quis, viverra ac, nunc. Praesent eget sem vel leo ultrices bibendum. Aenean faucibus. Morbi dolor nulla, malesuada eu, pulvinar at, mollis ac, nulla. Curabitur auctor semper nulla. Donec varius orci eget risus. Duis nibh mi, congue eu, accumsan eleifend, sagittis quis, diam. Duis eget orci sit amet orci dignissim rutrum.

Nam dui ligula, fringilla a, euismod sodales, sollicitudin vel, wisi. Morbi auctor lorem non justo. Nam lacus libero, pretium at, lobortis vitae, ultricies et, tellus. Donec aliquet, tortor sed accumsan bibendum, erat ligula aliquet magna, vitae ornare odio metus a mi. Morbi ac orci et nisl hendrerit mollis. Suspendisse ut massa. Cras nec ante. Pellentesque a nulla. Cum sociis natoque penatibus et magnis dis parturient montes, nascetur ridiculus mus. Aliquam tincidunt urna. Nulla ullamcorper vestibulum turpis. Pellentesque cursus luctus mauris.

Nulla malesuada porttitor diam. Donec felis erat, congue non, volutpat at, tincidunt tristique, libero. Vivamus viverra fermentum felis. Donec nonummy pellentesque ante. Phasellus adipiscing semper elit. Proin fermentum massa ac quam. Sed diam turpis, molestie vitae, placerat a, molestie nec, leo. Maecenas lacinia. Nam ipsum ligula, eleifend at, accumsan nec, suscipit a, ipsum. Morbi blandit ligula feugiat magna. Nunc eleifend consequat lorem. Sed lacinia nulla vitae enim. Pellentesque tincidunt purus vel magna. Integer non enim. Praesent euismod nunc eu purus. Donec bibendum quam in tellus. Nullam cursus pulvinar lectus. Donec et mi. Nam vulputate metus eu enim. Vestibulum pellentesque felis eu massa.

Preface

This thesis is submitted as a partial fulfillment of the requirements for acquiring a **Philosophiae Doctor (PhD)** Degree at the **Norwegian University of Science and Technology (NTNU)**. This doctoral work has been carried out at the **Power Electronic Systems and Components (PESC)** research group in the **Department of Electric Power Engineering (IEL)**, with Professor Elisabetta Tedeschi and Dr. Santiago Sanchez-Acevedo as main supervisor and co-supervisor, respectively.

This work was supported through the PETROENTER scheme, under the **LowEmission Research Centre (LowEmission)**, grant number 296207 and was carried out in the period between February 2020 and January 2023.

MOTIVATION

Nulla malesuada porttitor diam. Donec felis erat, congue non, volutpat at, tincidunt tristique, libero. Vivamus viverra fermentum felis. Donec nonummy pellentesque ante. Phasellus adipiscing semper elit. Proin fermentum massa ac quam. Sed diam turpis, molestie vitae, placerat a, molestie nec, leo. Maecenas lacinia. Nam ipsum ligula, eleifend at, accumsan nec, suscipit a, ipsum. Morbi blandit ligula feugiat magna. Nunc eleifend consequat lorem. Sed lacinia nulla vitae enim. Pellentesque tincidunt purus vel magna. Integer non enim. Praesent euismod nunc eu purus. Donec bibendum quam in tellus. Nullam cursus pulvinar lectus. Donec et mi. Nam vulputate metus eu enim. Vestibulum pellentesque felis eu massa.

Quisque ullamcorper placerat ipsum. Cras nibh. Morbi vel justo vitae lacus tincidunt ultrices. Lorem ipsum dolor sit amet, consectetur adipiscing elit. In hac habitasse platea dictumst. Integer tempus convallis augue. Etiam facilisis. Nunc elementum fermentum wisi. Aenean placerat. Ut imperdiet, enim sed gravida sollicitudin, felis odio placerat quam, ac pulvinar elit purus eget enim. Nunc vitae tortor. Proin tempus nibh sit amet nisl. Vivamus quis tortor vitae risus porta vehicula.

Fusce mauris. Vestibulum luctus nibh at lectus. Sed bibendum, nulla a faucibus semper, leo velit ultricies tellus, ac venenatis arcu wisi vel nisl. Vestibulum diam. Aliquam pellentesque, augue quis sagittis posuere, turpis lacus congue quam, in hendrerit risus eros eget felis. Maecenas eget erat in sapien mattis porttitor. Vestibulum porttitor. Nulla facilisi. Sed a turpis eu lacus commodo

facilisis. Morbi fringilla, wisi in dignissim interdum, justo lectus sagittis dui, et vehicula libero dui cursus dui. Mauris tempor ligula sed lacus. Duis cursus enim ut augue. Cras ac magna. Cras nulla. Nulla egestas. Curabitur a leo. Quisque egestas wisi eget nunc. Nam feugiat lacus vel est. Curabitur consectetur.

OBJECTIVES AND SCOPE

Nulla malesuada porttitor diam. Donec felis erat, congue non, volutpat at, tincidunt tristique, libero. Vivamus viverra fermentum felis. Donec nonummy pellentesque ante. Phasellus adipiscing semper elit. Proin fermentum massa ac quam. Sed diam turpis, molestie vitae, placerat a, molestie nec, leo. Maecenas lacinia. Nam ipsum ligula, eleifend at, accumsan nec, suscipit a, ipsum. Morbi blandit ligula feugiat magna. Nunc eleifend consequat lorem. Sed lacinia nulla vitae enim. Pellentesque tincidunt purus vel magna. Integer non enim. Praesent euismod nunc eu purus. Donec bibendum quam in tellus. Nullam cursus pulvinar lectus. Donec et mi. Nam vulputate metus eu enim. Vestibulum pellentesque felis eu massa.

Quisque ullamcorper placerat ipsum. Cras nibh. Morbi vel justo vitae lacus tincidunt ultrices. Lorem ipsum dolor sit amet, consectetur adipiscing elit. In hac habitasse platea dictumst. Integer tempus convallis augue. Etiam facilisis. Nunc elementum fermentum wisi. Aenean placerat. Ut imperdiet, enim sed gravida sollicitudin, felis odio placerat quam, ac pulvinar elit purus eget enim. Nunc vitae tortor. Proin tempus nibh sit amet nisl. Vivamus quis tortor vitae risus porta vehicula.

Fusce mauris. Vestibulum luctus nibh at lectus. Sed bibendum, nulla a faucibus semper, leo velit ultricies tellus, ac venenatis arcu wisi vel nisl. Vestibulum diam. Aliquam pellentesque, augue quis sagittis posuere, turpis lacus congue quam, in hendrerit risus eros eget felis. Maecenas eget erat in sapien mattis porttitor. Vestibulum porttitor. Nulla facilisi. Sed a turpis eu lacus commodo facilisis. Morbi fringilla, wisi in dignissim interdum, justo lectus sagittis dui, et vehicula libero dui cursus dui. Mauris tempor ligula sed lacus. Duis cursus enim ut augue. Cras ac magna. Cras nulla. Nulla egestas. Curabitur a leo. Quisque egestas wisi eget nunc. Nam feugiat lacus vel est. Curabitur consectetur.

OUTLINE

The thesis is divided in two part (clever references to the parts)...In the first part, I talk about this, in the second, first "n" chapters (clever references) introduce an overall... and provide... they all summarize...

The main results are

Suspendisse vel felis. Ut lorem lorem, interdum eu, tincidunt sit amet, laoreet vitae, arcu. Aenean faucibus pede eu ante. Praesent enim elit, rutrum at, molestie non, nonummy vel, nisl. Ut lectus eros, malesuada sit amet, fermentum eu, sodales cursus, magna. Donec eu purus. Quisque vehicula, urna sed ultricies auctor, pede lorem egestas dui, et convallis elit erat sed nulla. Donec luctus. Curabitur et nunc. Aliquam dolor odio, commodo pretium, ultricies non, pharetra in, velit. Integer arcu est, nonummy in, fermentum faucibus, egestas vel, odio.

Sed commodo posuere pede. Mauris ut est. Ut quis purus. Sed ac odio. Sed vehicula hendrerit sem. Duis non odio. Morbi ut dui. Sed accumsan risus eget odio. In hac habitasse platea dictumst. Pellentesque non elit. Fusce sed justo eu urna porta tincidunt. Mauris felis odio, sollicitudin sed, volutpat a, ornare ac, erat. Morbi quis dolor. Donec pellentesque, erat ac sagittis semper, nunc dui lobortis purus, quis congue purus metus ultricies tellus. Proin et quam. Class aptent taciti sociosqu ad litora torquent per conubia nostra, per inceptos hymenaeos. Praesent sapien turpis, fermentum vel, eleifend faucibus, vehicula eu, lacus.

Pellentesque habitant morbi tristique senectus et netus et malesuada fames ac turpis egestas. Donec odio elit, dictum in, hendrerit sit amet, egestas sed, leo. Praesent feugiat sapien aliquet odio. Integer vitae justo. Aliquam vestibulum fringilla lorem. Sed neque lectus, consectetur at, consectetur sed, eleifend ac, lectus. Nulla facilisi. Pellentesque eget lectus. Proin eu metus. Sed porttitor. In hac habitasse platea dictumst. Suspendisse eu lectus. Ut mi mi, lacinia sit amet, placerat et, mollis vitae, dui. Sed ante tellus, tristique ut, iaculis eu, malesuada ac, dui. Mauris nibh leo, facilisis non, adipiscing quis, ultrices a, dui.

Acknowledgements

Lorem ipsum dolor sit amet, consectetuer adipiscing elit. Ut purus elit, vestibulum ut, placerat ac, adipiscing vitae, felis. Curabitur dictum gravida mauris. Nam arcu libero, nonummy eget, consectetuer id, vulputate a, magna. Donec vehicula augue eu neque. Pellentesque habitant morbi tristique senectus et netus et malesuada fames ac turpis egestas. Mauris ut leo. Cras viverra metus rhoncus sem. Nulla et lectus vestibulum urna fringilla ultrices. Phasellus eu tellus sit amet tortor gravida placerat. Integer sapien est, iaculis in, pretium quis, viverra ac, nunc. Praesent eget sem vel leo ultrices bibendum. Aenean faucibus. Morbi dolor nulla, malesuada eu, pulvinar at, mollis ac, nulla. Curabitur auctor semper nulla. Donec varius orci eget risus. Duis nibh mi, congue eu, accumsan eleifend, sagittis quis, diam. Duis eget orci sit amet orci dignissim rutrum.

Nam dui ligula, fringilla a, euismod sodales, sollicitudin vel, wisi. Morbi auctor lorem non justo. Nam lacus libero, pretium at, lobortis vitae, ultricies et, tellus. Donec aliquet, tortor sed accumsan bibendum, erat ligula aliquet magna, vitae ornare odio metus a mi. Morbi ac orci et nisl hendrerit mollis. Suspendisse ut massa. Cras nec ante. Pellentesque a nulla. Cum sociis natoque penatibus et magnis dis parturient montes, nascetur ridiculus mus. Aliquam tincidunt urna. Nulla ullamcorper vestibulum turpis. Pellentesque cursus luctus mauris.

Nulla malesuada porttitor diam. Donec felis erat, congue non, volutpat at, tincidunt tristique, libero. Vivamus viverra fermentum felis. Donec nonummy pellentesque ante. Phasellus adipiscing semper elit. Proin fermentum massa ac quam. Sed diam turpis, molestie vitae, placerat a, molestie nec, leo. Maecenas lacinia. Nam ipsum ligula, eleifend at, accumsan nec, suscipit a, ipsum. Morbi blandit ligula feugiat magna. Nunc eleifend consequat lorem. Sed lacinia nulla vitae enim. Pellentesque tincidunt purus vel magna. Integer non enim. Praesent euismod nunc eu purus. Donec bibendum quam in tellus. Nullam cursus pulvinar lectus. Donec et mi. Nam vulputate metus eu enim. Vestibulum pellentesque felis eu massa.

Contents

ABSTRACT **VII**

PREFACE **IX**

ACKNOWLEDGEMENT **XIII**

LIST OF FIGURES **XIX**

LIST OF TABLES **XXI**

ABBREVIATIONS AND ACRONYMS **XXIII**

SYMBOLS AND UNITS **XXV**

PART I BACKGROUND 1

CHAPTER 1 INTRODUCTION 3

| | | |
|-------|--|----------|
| 1.1 | Section 1 in chapter 1 | 3 |
| 1.1.1 | Subsection 1.1 of section 1 in chapter 1 | 5 |
| 1.1.2 | Subsection 1.2 of section 1 in chapter 1 | 6 |
| 1.2 | Long section title displayed in the table of content | 7 |
| 1.2.1 | Subsection 1.2 of section 2 in chapter 1 | 9 |
| 1.3 | References | 9 |

CHAPTER 2 BACKGROUND 11

| | | |
|-----|------------|-----------|
| | Summary | 11 |
| 2.1 | Modelling | 11 |
| 2.2 | References | 11 |

CHAPTER 3 EXPERIMENTAL METHODS 13

| | | |
|-------|--|----|
| 3.1 | Section 1 in chapter 3 | 13 |
| 3.1.1 | Subsection 3.1 of section 1 in chapter 3 | 14 |
| 3.1.2 | Subsection 3.2 of section 1 in chapter 3 | 15 |
| 3.2 | Long section title displayed in the table of content | 16 |
| 3.2.1 | Subsection 3.2 of section 2 in chapter 3 | 18 |
| 3.3 | References | 18 |

PART II PUBLICATIONS 19

CHAPTER 4 OFFSHORE WIND AND O&G PLATFORMS 21

| | | |
|-------|--|----|
| | Abstract | 22 |
| 4.1 | Introduction | 22 |
| 4.2 | Frequency Control in Electromechanical Systems | 24 |
| 4.2.1 | Phases of the Frequency Control | 25 |
| 4.2.2 | Other Dynamics | 29 |
| 4.3 | Hybrid Energy Storage System | 30 |
| 4.3.1 | Power Balancing Within the ESS | 31 |
| 4.3.2 | ESS Control Structure | 32 |
| 4.4 | Perspectives and Possibilities | 35 |
| 4.4.1 | Frequency Support | 36 |
| 4.4.2 | DC Voltage Control within the ESS | 36 |
| 4.4.3 | Frequency as a Global Variable | 38 |
| 4.5 | Future Research | 38 |
| 4.6 | Conclusion | 39 |
| 4.7 | References | 40 |

CHAPTER 5 SIZING OF HYBRID ENERGY STORAGE SYSTEMS 43

| | | |
|--|----------|----|
| | Abstract | 44 |
|--|----------|----|

| | | |
|-------|--|----|
| 5.1 | Introduction | 44 |
| 5.2 | Materials and Methods | 47 |
| 5.2.1 | Frequency Control in ACPSs | 47 |
| 5.2.2 | Sizing of the Converter-Interfaced ESS Elements | |
| | | 53 |
| 5.3 | Results | 61 |
| 5.3.1 | Case study: a wind-powered offshore platform in the North Sea | 61 |
| 5.3.2 | Sizing of the Energy Storage System | 63 |
| 5.3.3 | Sizing validation | 65 |
| 5.4 | Conclusions | 70 |
| 5.5 | References | 71 |

**CHAPTER 6 TITLE OF THE CHAPTER 6 DISPLAYED
IN THE TABLE OF CONTENTS 79**

| | | |
|----------|--|----|
| Abstract | 80 | |
| 6.1 | Section 1 in chapter 6 | 80 |
| 6.1.1 | Subsection 6.1 of section 1 in chapter 6 | 82 |
| 6.1.2 | Subsection 6.2 of section 1 in chapter 6 | 83 |
| 6.2 | Long section title displayed in the table of content | 84 |
| 6.2.1 | Subsection 6.2 of section 2 in chapter 6 | 86 |
| 6.3 | References | 86 |

PART III EPILOGUE 87

CHAPTER 7 CONCLUSION 89

| | | |
|-------|--|----|
| 7.1 | Section 1 in chapter 7 | 89 |
| 7.1.1 | Subsection 7.1 of section 1 in chapter 7 | 90 |
| 7.1.2 | Subsection 7.2 of section 1 in chapter 7 | 91 |

| | |
|--|----|
| 7.2 Long section title displayed in the table of content | 92 |
| 7.2.1 Subsection 7.2 of section 2 in chapter 7 | 93 |
| 7.3 References | 94 |

APPENDIX A SUPPLEMENTARY INFORMATION FOR CHAPTER 4 **A-1**

| | |
|---------------------------------|-----|
| A.1 Detailed growth information | A-1 |
|---------------------------------|-----|

APPENDIX B SUPPLEMENTARY INFORMATION FOR CHAPTER 5 **A-3**

| | |
|--|-----|
| B.1 Additional micro-Raman spectroscopy measurements | A-3 |
|--|-----|

APPENDIX C SUPPLEMENTARY INFORMATION FOR CHAPTER 6 **A-5**

| | |
|-------------------------|-----|
| C.1 micro-PL spectra | A-5 |
| C.2 micro-Raman spectra | A-6 |

CURRICULUM VITAE **L-1**

DISSEMINATION OF RESEARCH **L-3**

COPYRIGHT PERMISSIONS **L-7**

List of Figures

CHAPTER 1

- 1.1 SEM images of AlN on graphene formed via different MEE cycles 4

CHAPTER 2

- 2.1 WT model type 4 11
2.2 Simplified WT model type 4 12

CHAPTER 3

- 3.1 Cross-sectional SEM images of GaN nanocolumns on graphene formed via different AlN MEE cycles 13

CHAPTER 4

- 4.1 Prospective scenario of a wind farm and an ESS connected to an existing O&G platform. 23
4.2 Aggregated rotating mass model. 24
4.3 Frequency response phases. 26
4.4 Inertia and governor roles in the frequency control. 28
4.5 Control dynamics in an AC electrical system 30
4.6 Schematic diagram of a hybrid energy storage system. 31
4.7 Control structures of a hybrid energy storage system. 33
4.8 ESS providing inertia and primary reserves 37
4.9 Case 3, DC voltage with (blue) and without (red) feed-forward scheme. 38
4.10 Case 3, mechanical speed and electrical frequency. 39

CHAPTER 5

- 5.1 Frequency droop. 49
- 5.2 The three periods of frequency variation and the control actions. 51
- 5.3 Elements of a converter-interfaced ESS. 53
- 5.4 Schematic representation of the DC link, grid converter, and LC filter. 59
- 5.5 Schematic representation of the case study ACPS. 61
- 5.6 Histogram of the platform active power demand. 63
- 5.7 Overview of the MATLAB Simulink model. 65
- 5.8 Generalized nonlinear droop controller. 66
- 5.9 Case-study behavior during a load increase with and without the proposed ESS. 67
- 5.10 Case-study behavior during the wind farm disconnection with and without the proposed ESS. 69

CHAPTER 6

- 6.1 HRXRD measurements of the nanocolumns 81

APPENDIX C

- C.1 RT micro-photoluminescence spectra of reference sample (HVPE-freestanding GaN), samples G1, G2 and G3 A-5
- C.2 Micro-Raman spectroscopy of the nanocolumn samples, including the graphene for each respective sample A-6

DISSEMINATION OF RESEARCH

- D.1 Cover image/featured article in Nanotechnology L-4

List of Tables

CHAPTER 3

- 3.1 Experimental conditions described in the ToC 14

CHAPTER 5

- 5.1 Parameters of the ACPS and the requirements for its ESS 64
5.2 Parameters of the primary controllers. 66

CHAPTER 6

- 6.1 Al-content of each axial nanocolumn segment for the vertical
GaN/AlGaN nanocolumn ensemble obtained from fitting the
simulation model to the HRXRD $2\theta-\omega$ scan data 85

APPENDIX A

- A.1 Detailed growth conditions of nanocolumns A-2

APPENDIX B

- B.1 Summary of micro-Raman spectroscopy measurements for the
as-grown nanocolumn sample A-3

Abbreviations and Acronyms

A list of abbreviations and acronyms used in this doctoral dissertation is presented below. Ambiguities and double meaning of abbreviations and acronyms have been avoided as much as possible. However, the notations might be re-defined in the accepted manuscripts presented from Chapters x to x, as those are presented in the form they were accepted for publication. The manuscript under review in Chapter x also has notations that differ from the ones defined herein. Notwithstanding, it is the author's intention to use the notation as consistently as possible throughout the text.

| | |
|---------|---|
| AC | Alternate current <i>30, 36–40, 42, 45</i> |
| ACPS | AC power system <i>50–60, 64, 67, 68, 70, 74</i> |
| AGC | Automatic generation control <i>35</i> |
| BC | Battery converter <i>38–42</i> |
| CIG | Converter-interfaced generator <i>50–52, 55, 56, 58, 65</i> |
| CR | Capacitive-resistive <i>40</i> |
| DC | Direct current <i>28, 36–38, 40–42, 45, 46, 63–66, 70, 77</i> |
| EMS | Energy management system <i>68, 71, 72</i> |
| ES | Energy storage <i>59, 60, 63, 64, 66, 73, 75</i> |
| ESD | Energy storage device <i>30, 36–41, 44, 45, 52, 59, 60, 63, 66, 68–71, 74</i> |
| ESS | Energy storage system <i>28–30, 36–38, 40–42, 44–46, 50–52, 58–60, 65–76</i> |
| FCC | Fuel cell converter <i>42</i> |
| FCR | Frequency containment reserves <i>55, 58</i> |
| FFR | Fast frequency reserves <i>55, 58</i> |
| FRR | Fast restoration reserves <i>55, 58, 72, 75</i> |
| FSM | Frequency sensitivity mode <i>54</i> |
| GC | Grid converter <i>36–38, 40–42, 45</i> |
| GHG | Greenhouse gas <i>28, 29</i> |
| GT | Gas turbine <i>28–31, 35, 39, 42, 44, 45</i> |
| HES-OFF | Innovative Hybrid Energy System for Stable Power and Heat Supply in Offshore O&G Installation Project <i>28, 30, 36, 38, 41, 42, 46, 77</i> |
| HV | High-voltage <i>36, 41, 42, 44</i> |
| IE | Faculty of Information Technology and Electrical Engineering <i>5</i> |

| | |
|-----------------|--|
| IEL | Department of Electric Power Engineering ix |
| IGBT | Insulated-gate bipolar transistor 5, 40 |
| LC | Inductive-capacitive 59, 64–66, 70, 72, 77 |
| LCL | Inductive-capacitive-inductive 5, 40, 65, 66 |
| LowEmission | LowEmission Research Centre ix, 28, 30, 36–38, 40–42, 44, 46, 77 |
| LPF | Low-pass filter 40 |
| LV | Low-voltage 44 |
| MG | microgrid 50–52, 55, 56, 58, 65 |
| NCS | Norwegian continental shelf 28, 70 |
| NO _x | Nitrogen oxides 28, 29 |
| NTNU | Norwegian University of Science and Technology ix, 5, 27, 49 |
| O&G | Oil and gas 28, 29, 31, 32, 35, 45 |
| PEC | Power electronic converter 31, 35, 37, 38, 41, 45 |
| PEM | Proton exchange membrane 67, 68, 74, 75 |
| PESC | Power Electronic Systems and Components ix |
| PhD | Philosophiae Doctor ix |
| PI | Proportional and integral 40 |
| PID | Proportional, integral, and derivative 30, 38, 46 |
| PLL | Phase-locked loop 40, 44 |
| PMS | Power management system 30, 31, 35, 38, 39, 46 |
| PWM | Pulse-width modulation 38, 40, 41 |
| RES | Renewable energy source 29 |
| RoCoF | Rate of change of frequency 31, 33, 56, 57, 60, 61 |
| RRF | Rotating reference frame 40, 41 |
| SCADA | Supervisory control and data acquisition 68 |
| SM | Synchronous machine 50, 54, 56, 57 |
| SOC | State of charge 39, 40 |
| WF | Wind farm 29, 30, 35, 42, 45 |
| WT | Wind turbine 31, 35, 41, 42, 44, 45 |

Symbols and Units

A list of symbols, operators, and units used in this doctoral dissertation is presented below. Ambiguities and double meaning of symbols and operators have been avoided as much as possible. However, the notations might be redefined in the accepted manuscripts presented from Chapters x to x, as those are presented in the form they were accepted for publication. The manuscript under review in Chapter x also has notations that differ from the ones defined herein. Notwithstanding, it is the author's intention to use the notation as consistently as possible throughout the text.

Mathematical operators

Capitalized and lowercase Latin and Greek letters, as well as stylized characters, are used to represent mathematical operators.

\mathcal{C} matrix used an the $abc \leftrightarrow \alpha\beta0$ transformation.

* for any complex number $a + jb$, its complex conjugate is represented as $(a + jb)^*$ and is equal to $a - jb$.

d infinitesimal variation of a variable, i.e., dx .

∂ infinitesimal variation of a variable, i.e., ∂x ; used in the context of partial derivatives.

Δ finite variation of a variable, i.e., Δx .

• dot product of two column vectors \mathbf{x} and \mathbf{y} is $\mathbf{x} \bullet \mathbf{y} = \mathbf{x}^\top \mathbf{y}$.

\int integral.

\times multiplication of scalars, vectors or matrices; however, in most cases the multiplication is indicated without any symbol, $x \times y = xy$.

\parallel paralleling of two impedances, $Z_1 \parallel Z_2 = (Z_1^{-1} + Z_2^{-1})^{-1}$.

\mathcal{P} matrix used in the $\alpha\beta0 \leftrightarrow dq0$ transformation.

Π product.

Σ sum.

• time derivative, $\frac{dx}{dt} = \dot{x}$.

\mathcal{T} matrix used in the $abc \leftrightarrow dq0$ transformation.

\top the transpose of a matrix \mathbf{T} is represented as \mathbf{T}^\top .

Units

Mostly **SI** units from the Bureau International des Poids et Mesures **BIPM** with nomenclature adapted from the International Electrotechnical Vocabulary (**IEV**) of the International Electrotechnical Commission (**IEC**).

- A ampere, SI base unit of electric current, IEV 112-02-07.
- F farad, capacitance, in SI base units $F = m^{-2} s^4 kg^{-1} A^2$, IEV 131-12-90.
- H henry, inductance, in SI base units $H = m^2 s^{-2} kg A^{-2}$, IEV 131-12-91.
- h hour, time, sixty minutes.
- m metre, SI unit of length, IEV 112-02-05.
- min minute, time, sixty seconds.
- N newton, force, in SI base units $N := kg m s^{-2}$, IEV 113-03-15.
- pu per unit, a quantity in a given unit that is divided by a constant expressed in the same unit.
- s second, SI unit of time, IEV 112-02-04.
- V volt, unit of the scalar quantity equal to the line integral of the electric field strength along a specific path, IEV 121-11-27.
- VA voltampere, product of the rms voltage between the terminals of an element by the rms current through the element.
- var voltampere reactive, special name of voltampere, 1 var $:= 1 VA$, IEV 131-11-45.
- W watt, power, time derivative of energy being transferred or transformed, IEV 113-03-52.
- Wh watt hour, convenient unit of energy, IEV 131-11-58.
- Ω ohm, unit of resistance defined $\Omega := V A^{-1}$, IEV 131-12-88.

Latin Variables and Constants

Variables in Latin letters can be capitalized or not depending on the context, they are mostly represented in italic, whereas constants are represented in roman (upright) form, matrices are represented in bolded roman.

a, b, c axes of the natural reference frame for three-phase measurements.

B conductance.

C capacitance.

d, q axes of the rotating reference frame for three-phase measurements.

e Euler's number given by $\lim_{n \rightarrow \infty} \left(1 + \frac{1}{n}\right)^n$.

E, e, V, v, U, u voltage.

F, f frequency or a generic function.

G, g conductance or a generic function.

I, i current.

L inductance.

j complex number equal to $\sqrt{-1}$.

J moment of inertia.

K, k an index or a gain.

n usually an integer number.

P, p power.

S apparent power.

s complex frequency in the Laplace domain.

t time.

T torque.

X, x reactance, state variable, or a generic variable.

Y, y admittance, output variable, or a generic variable.

Z, z impedance.

Greek Variables and Constants

Variables and constants in Greek letters can be capitalized or not depending on the context. Notice that some capitalized Greek letter may be used as mathematical operators.

$\alpha, \beta, \gamma, \delta, \theta, \varphi$ angle.

α, β axes of the stationary reference frame for three-phase measurements.

ζ damping coefficient.

η efficiency.

π well known transcendental constant.

τ time.

ω angular frequency.

Part I

BACKGROUND

CHAPTER 1

Introduction

Lorem ipsum dolor sit amet, consectetuer adipiscing elit [1]. Ut purus elit, vestibulum ut, placerat ac, adipiscing vitae, felis 1. Curabitur dictum gravida mauris. Nam arcu libero, nonummy eget, consectetuer id, vulputate a, magna. Donec vehicula augue eu neque [2]. Pellentesque habitant morbi tristique senectus et netus et malesuada fames ac turpis egestas 2. Mauris ut leo. Cras viverra metus rhoncus sem [3]. Nulla et lectus vestibulum urna fringilla ultrices. Phasellus eu tellus sit amet tortor gravida placerat 3. Integer sapien est, iaculis in, pretium quis, viverra ac, nunc. Praesent eget sem vel leo ultrices bibendum [4]. Aenean faucibus. Morbi dolor nulla, malesuada eu, pulvinar at (1.1), mollis ac, nulla. Curabitur auctor semper nulla 4. Donec varius orci eget risus. Duis nibh mi, congue eu, accumsan eleifend, sagittis quis, diam. Duis eget orci sit amet orci dignissim rutrum [1–6].

1.1 SECTION 1 IN CHAPTER 1

Nam dui ligula, fringilla a, euismod sodales, sollicitudin vel, wisi. Morbi auctor lorem non justo. Nam lacus libero, pretium at, lobortis vitae, ultricies et, tellus. Donec aliquet, tortor sed accumsan bibendum, erat ligula aliquet magna, vitae ornare odio metus a mi. Morbi ac orci et nisl hendrerit mollis. Suspendisse ut massa. Cras nec ante. Pellentesque a nulla. Cum sociis natoque penatibus et magnis dis parturient montes, nascetur ridiculus mus. Aliquam tincidunt urna. Nulla ullamcorper vestibulum turpis. Pellentesque cursus luctus mauris.

$$EQE = \frac{q \times P_{opt}}{I \times h\nu} \quad (1.1)$$

Nulla malesuada porttitor diam. Donec felis erat, congue non, volutpat at, tincidunt tristique, libero. Vivamus viverra fermentum felis. Donec nonummy pellentesque ante. Phasellus adipiscing semper elit. Proin fermentum massa ac quam. Sed diam turpis, molestie vitae, placerat a, molestie nec, leo. Maecenas lacinia. Nam ipsum ligula, eleifend at, accumsan nec, suscipit a, ipsum. Morbi blandit ligula feugiat magna. Nunc eleifend consequat lorem. Sed lacinia nulla vitae enim. Pellentesque tincidunt purus vel magna. Integer non enim. Praesent

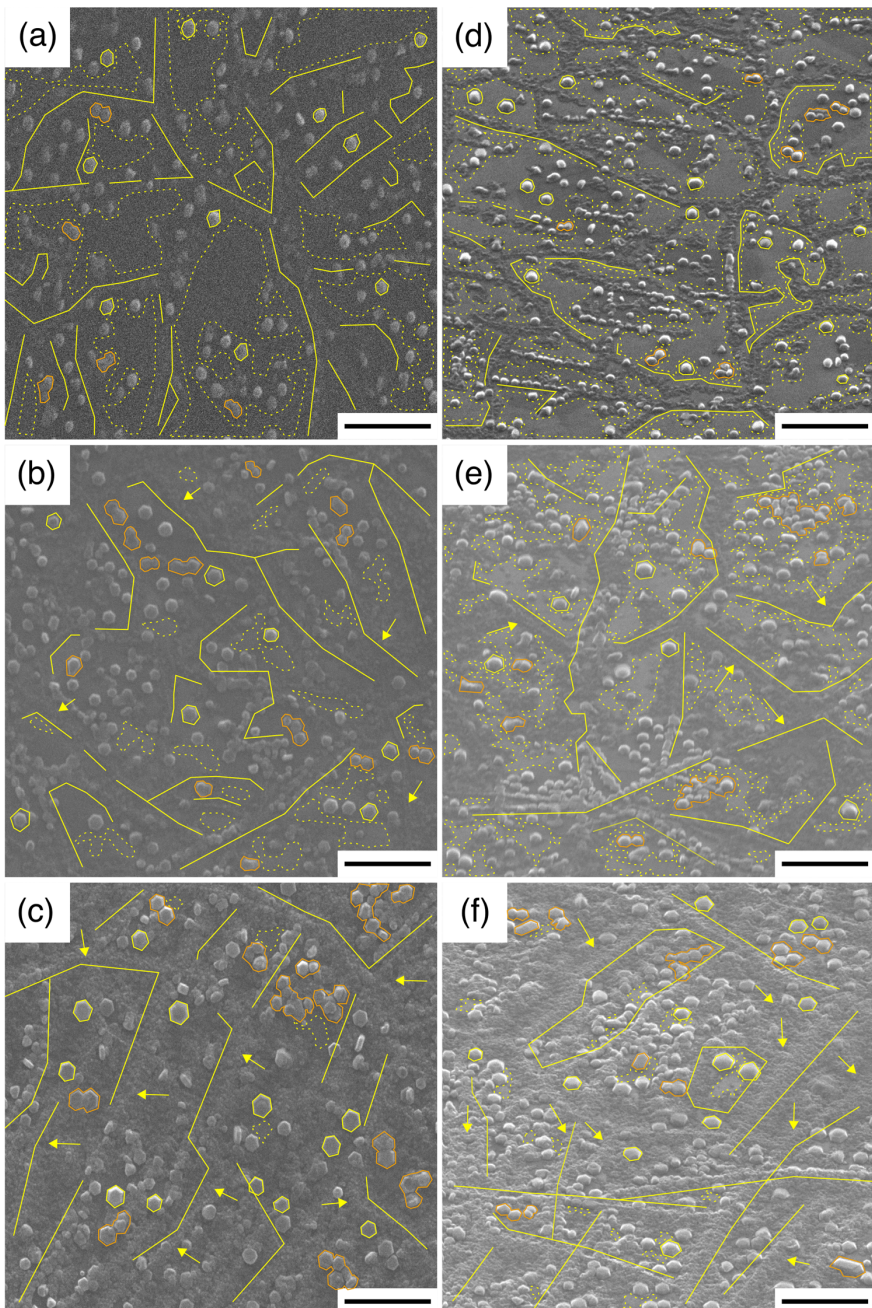


FIGURE 1.1 | SEM images of AlN on graphene formed via different MEE cycles. (a,d), (b,e) and (c,f) are (top-, bird's eye-view) SEM images of samples A1, A2 and A3, respectively. Scale bars are 1 μm . Features marked with yellow lines, yellow (orange) contours and yellow dashed outlines are high-density AlN nanostructures grown along line defects of graphene, individual (coalesced) AlN islands and areas of exposed graphene, respectively. Yellow arrows in samples A2 and A3 show the lateral growth of AlN nanostructures that initially nucleate at the line defects of graphene in sample A1 (adapted with permission from ref. 4 © Liudi Mulyo et al, 2020).

euismod nunc eu purus. Donec bibendum quam in tellus. Nullam cursus pulvinar lectus. Donec et mi. Nam vulputate metus eu enim. Vestibulum pellentesque felis eu massa.

Quisque ullamcorper placerat ipsum. Cras nibh. Morbi vel justo vitae lacus tincidunt ultrices. Lorem ipsum dolor sit amet, consectetur adipiscing elit. In hac habitasse platea dictumst. Integer tempus convallis augue. Etiam facilisis. Nunc elementum fermentum wisi. Aenean placerat. Ut imperdiet, enim sed gravida sollicitudin, felis odio placerat quam, ac pulvinar elit purus eget enim. Nunc vitae tortor. Proin tempus nibh sit amet nisl. Vivamus quis tortor vitae risus porta vehicula.

[Inductive-capacitive-inductive \(LCL\)](#) and [LCL](#). Also, [NTNU](#) and [NTNU](#). But, not to forget, [Faculty of Information Technology and Electrical Engineering \(IE\)](#) and [IE](#). However, [insulated-gate bipolar transistor \(IGBT\)](#) and [IGBT](#).

1.1.1 Subsection 1.1 of section 1 in chapter 1

Fusce mauris. Vestibulum luctus nibh at lectus. Sed bibendum, nulla a faucibus semper, leo velit ultricies tellus, ac venenatis arcu wisi vel nisl. Vestibulum diam. Aliquam pellentesque, augue quis sagittis posuere, turpis lacus congue quam, in hendrerit risus eros eget felis. Maecenas eget erat in sapien mattis porttitor. Vestibulum porttitor. Nulla facilisi. Sed a turpis eu lacus commodo facilisis. Morbi fringilla, wisi in dignissim interdum, justo lectus sagittis dui, et vehicula libero dui cursus dui. Mauris tempor ligula sed lacus. Duis cursus enim ut augue. Cras ac magna. Cras nulla. Nulla egestas. Curabitur a leo. Quisque egestas wisi eget nunc. Nam feugiat lacus vel est. Curabitur consectetur.

Suspendisse vel felis. Ut lorem lorem, interdum eu, tincidunt sit amet, laoreet vitae, arcu. Aenean faucibus pede eu ante. Praesent enim elit, rutrum at, molestie non, nonummy vel, nisl. Ut lectus eros, malesuada sit amet, fermentum eu, sodales cursus, magna. Donec eu purus. Quisque vehicula, urna sed ultricies auctor, pede lorem egestas dui, et convallis elit erat sed nulla. Donec luctus. Curabitur et nunc. Aliquam dolor odio, commodo pretium, ultricies non, pharetra in, velit. Integer arcu est, nonummy in, fermentum faucibus, egestas vel, odio.

Sed commodo posuere pede. Mauris ut est. Ut quis purus. Sed ac odio. Sed vehicula hendrerit sem. Duis non odio. Morbi ut dui. Sed accumsan risus eget odio. In hac habitasse platea dictumst. Pellentesque non elit. Fusce sed justo eu urna porta tincidunt. Mauris felis odio, sollicitudin sed, volutpat a, ornare ac, erat. Morbi quis dolor. Donec pellentesque, erat ac sagittis semper, nunc dui lobortis purus, quis congue purus metus ultricies tellus. Proin et quam. Class aptent taciti sociosqu ad litora torquent per conubia nostra, per inceptos

hymenaeos. Praesent sapien turpis, fermentum vel, eleifend faucibus, vehicula eu, lacus.

1.1.2 Subsection 1.2 of section 1 in chapter 1

Pellentesque habitant morbi tristique senectus et netus et malesuada fames ac turpis egestas. Donec odio elit, dictum in, hendrerit sit amet, egestas sed, leo. Praesent feugiat sapien aliquet odio. Integer vitae justo. Aliquam vestibulum fringilla lorem. Sed neque lectus, consectetur at, consectetur sed, eleifend ac, lectus. Nulla facilisi. Pellentesque eget lectus. Proin eu metus. Sed porttitor. In hac habitasse platea dictumst. Suspendisse eu lectus. Ut mi mi, lacinia sit amet, placerat et, mollis vitae, dui. Sed ante tellus, tristique ut, iaculis eu, malesuada ac, dui. Mauris nibh leo, facilisis non, adipiscing quis, ultrices a, dui.

Morbi luctus, wisi viverra faucibus pretium, nibh est placerat odio, nec commodo wisi enim eget quam. Quisque libero justo, consectetur a, feugiat vitae, porttitor eu, libero. Suspendisse sed mauris vitae elit sollicitudin malesuada. Maecenas ultricies eros sit amet ante. Ut venenatis velit. Maecenas sed mi eget dui varius euismod. Phasellus aliquet volutpat odio. Vestibulum ante ipsum primis in faucibus orci luctus et ultrices posuere cubilia Curae; Pellentesque sit amet pede ac sem eleifend consectetur. Nullam elementum, urna vel imperdiet sodales, elit ipsum pharetra ligula, ac pretium ante justo a nulla. Curabitur tristique arcu eu metus. Vestibulum lectus. Proin mauris. Proin eu nunc eu urna hendrerit faucibus. Aliquam auctor, pede consequat laoreet varius, eros tellus scelerisque quam, pellentesque hendrerit ipsum dolor sed augue. Nulla nec lacus.

Suspendisse vitae elit. Aliquam arcu neque, ornare in, ullamcorper quis, commodo eu, libero. Fusce sagittis erat at erat tristique mollis. Maecenas sapien libero, molestie et, lobortis in, sodales eget, dui. Morbi ultrices rutrum lorem. Nam elementum ullamcorper leo. Morbi dui. Aliquam sagittis. Nunc placerat. Pellentesque tristique sodales est. Maecenas imperdiet lacinia velit. Cras non urna. Morbi eros pede, suscipit ac, varius vel, egestas non, eros. Praesent malesuada, diam id pretium elementum, eros sem dictum tortor, vel consectetur odio sem sed wisi.

1.2 SHORT SECTION TITLE IN THE CHAPTER

Sed feugiat. Cum sociis natoque penatibus et magnis dis parturient montes, nascetur ridiculus mus. Ut pellentesque augue sed urna. Vestibulum diam eros, fringilla et, consectetur eu, nonummy id, sapien. Nullam at lectus. In sagittis ultrices mauris. Curabitur malesuada erat sit amet massa. Fusce blandit. Aliquam erat volutpat. Aliquam euismod. Aenean vel lectus. Nunc imperdiet justo nec dolor.

Etiam euismod. Fusce facilisis lacinia dui. Suspendisse potenti. In mi erat, cursus id, nonummy sed, ullamcorper eget, sapien. Praesent pretium, magna in eleifend egestas, pede pede pretium lorem, quis consectetur tortor sapien facilisis magna. Mauris quis magna varius nulla scelerisque imperdiet. Aliquam non quam. Aliquam porttitor quam a lacus. Praesent vel arcu ut tortor cursus volutpat. In vitae pede quis diam bibendum placerat. Fusce elementum convallis neque. Sed dolor orci, scelerisque ac, dapibus nec, ultricies ut, mi. Duis nec dui quis leo sagittis commodo.

Aliquam lectus. Vivamus leo. Quisque ornare tellus ullamcorper nulla. Mauris porttitor pharetra tortor. Sed fringilla justo sed mauris. Mauris tellus. Sed non leo. Nullam elementum, magna in cursus sodales, augue est scelerisque sapien, venenatis congue nulla arcu et pede. Ut suscipit enim vel sapien. Donec congue. Maecenas urna mi, suscipit in, placerat ut, vestibulum ut, massa. Fusce ultrices nulla et nisl.

Etiam ac leo a risus tristique nonummy. Donec dignissim tincidunt nulla. Vestibulum rhoncus molestie odio. Sed lobortis, justo et pretium lobortis, mauris turpis condimentum augue, nec ultricies nibh arcu pretium enim. Nunc purus neque, placerat id, imperdiet sed, pellentesque nec, nisl. Vestibulum imperdiet neque non sem accumsan laoreet. In hac habitasse platea dictumst. Etiam condimentum facilisis libero. Suspendisse in elit quis nisl aliquam dapibus. Pellentesque auctor sapien. Sed egestas sapien nec lectus. Pellentesque vel dui vel neque bibendum viverra. Aliquam porttitor nisl nec pede. Proin mattis libero vel turpis. Donec rutrum mauris et libero. Proin euismod porta felis. Nam lobortis, metus quis elementum commodo, nunc lectus elementum mauris, eget vulputate ligula tellus eu neque. Vivamus eu dolor.

Nulla in ipsum. Praesent eros nulla, congue vitae, euismod ut, commodo a, wisi. Pellentesque habitant morbi tristique senectus et netus et malesuada fames ac turpis egestas. Aenean nonummy magna non leo. Sed felis erat, ullamcorper in, dictum non, ultricies ut, lectus. Proin vel arcu a odio lobortis euismod. Vestibulum ante ipsum primis in faucibus orci luctus et ultrices posuere cubilia Curae; Proin ut est. Aliquam odio. Pellentesque massa turpis, cursus eu, euismod nec, tempor congue, nulla. Duis viverra gravida mauris. Cras tincidunt. Curabitur eros ligula, varius ut, pulvinar in, cursus faucibus,

augue.

Nulla mattis luctus nulla. Duis commodo velit at leo. Aliquam vulputate magna et leo. Nam vestibulum ullamcorper leo. Vestibulum condimentum rutrum mauris. Donec id mauris. Morbi molestie justo et pede. Vivamus eget turpis sed nisl cursus tempor. Curabitur mollis sapien condimentum nunc. In wisi nisl, malesuada at, dignissim sit amet, lobortis in, odio. Aenean consequat arcu a ante. Pellentesque porta elit sit amet orci. Etiam at turpis nec elit ultricies imperdiet. Nulla facilisi. In hac habitasse platea dictumst. Suspendisse viverra aliquam risus. Nullam pede justo, molestie nonummy, scelerisque eu, facilisis vel, arcu.

Curabitur tellus magna, porttitor a, commodo a, commodo in, tortor. Donec interdum. Praesent scelerisque. Maecenas posuere sodales odio. Vivamus metus lacus, varius quis, imperdiet quis, rhoncus a, turpis. Etiam ligula arcu, elementum a, venenatis quis, sollicitudin sed, metus. Donec nunc pede, tincidunt in, venenatis vitae, faucibus vel, nibh. Pellentesque wisi. Nullam malesuada. Morbi ut tellus ut pede tincidunt porta. Lorem ipsum dolor sit amet, consectetur adipiscing elit. Etiam congue neque id dolor.

Donec et nisl at wisi luctus bibendum. Nam interdum tellus ac libero. Sed sem justo, laoreet vitae, fringilla at, adipiscing ut, nibh. Maecenas non sem quis tortor eleifend fermentum. Etiam id tortor ac mauris porta vulputate. Integer porta neque vitae massa. Maecenas tempus libero a libero posuere dictum. Vestibulum ante ipsum primis in faucibus orci luctus et ultrices posuere cubilia Curae; Aenean quis mauris sed elit commodo placerat. Class aptent taciti sociosqu ad litora torquent per conubia nostra, per inceptos hymenaeos. Vivamus rhoncus tincidunt libero. Etiam elementum pretium justo. Vivamus est. Morbi a tellus eget pede tristique commodo. Nulla nisl. Vestibulum sed nisl eu sapien cursus rutrum.

Nulla non mauris vitae wisi posuere convallis. Sed eu nulla nec eros scelesque pharetra. Nullam varius. Etiam dignissim elementum metus. Vestibulum faucibus, metus sit amet mattis rhoncus, sapien dui laoreet odio, nec ultricies nibh augue a enim. Fusce in ligula. Quisque at magna et nulla commodo consequat. Proin accumsan imperdiet sem. Nunc porta. Donec feugiat mi at justo. Phasellus facilisis ipsum quis ante. In ac elit eget ipsum pharetra faucibus. Maecenas viverra nulla in massa.

Nulla ac nisl. Nullam urna nulla, ullamcorper in, interdum sit amet, gravida ut, risus. Aenean ac enim. In luctus. Phasellus eu quam vitae turpis viverra pellentesque. Duis feugiat felis ut enim. Phasellus pharetra, sem id porttitor sodales, magna nunc aliquet nibh, nec blandit nisl mauris at pede. Suspendisse risus risus, lobortis eget, semper at, imperdiet sit amet, quam. Quisque scelerisque dapibus nibh. Nam enim. Lorem ipsum dolor sit amet, consectetur adipiscing elit. Nunc ut metus. Ut metus justo, auctor at, ultrices eu, sagittis ut,

purus. Aliquam aliquam.

1.2.1 Subsection 1.2 of section 2 in chapter 1

Aliquam lectus. Vivamus leo. Quisque ornare tellus ullamcorper nulla. Mauris porttitor pharetra tortor. Sed fringilla justo sed mauris. Mauris tellus. Sed non leo. Nullam elementum, magna in cursus sodales, augue est scelerisque sapien, venenatis congue nulla arcu et pede. Ut suscipit enim vel sapien. Donec congue. Maecenas urna mi, suscipit in, placerat ut, vestibulum ut, massa. Fusce ultrices nulla et nisl.

Etiam ac leo a risus tristique nonummy. Donec dignissim tincidunt nulla. Vestibulum rhoncus molestie odio. Sed lobortis, justo et pretium lobortis, mauris turpis condimentum augue, nec ultricies nibh arcu pretium enim. Nunc purus neque, placerat id, imperdiet sed, pellentesque nec, nisl. Vestibulum imperdiet neque non sem accumsan laoreet. In hac habitasse platea dictumst. Etiam condimentum facilisis libero. Suspendisse in elit quis nisl aliquam dapibus. Pellentesque auctor sapien. Sed egestas sapien nec lectus. Pellentesque vel dui vel neque bibendum viverra. Aliquam porttitor nisl nec pede. Proin mattis libero vel turpis. Donec rutrum mauris et libero. Proin euismod porta felis. Nam lobortis, metus quis elementum commodo, nunc lectus elementum mauris, eget vulputate ligula tellus eu neque. Vivamus eu dolor.

1.3 REFERENCES

- [1] A. Liudi Mulyo, Y. Konno, J. S. Nilsen, A. T. J. van Helvoort, B.-O. Fimland, H. Weman, and K. Kishino. [Growth study of self-assembled GaN nanocolumns on silica glass by plasma assisted molecular beam epitaxy](#). *Journal of Crystal Growth* **480**, 67–73 (2017). Cited on page/s 3.
- [2] A. Liudi Mulyo, M. K. Rajpalke, H. Kuroe, P.-E. Vullum, H. Weman, B.-O. Fimland, and K. Kishino. [Vertical GaN nanocolumns grown on graphene intermediated with a thin AlN buffer layer](#). *Nanotechnology* **30** (1), 015604 (2018). Cited on page/s 3.
- [3] I. M. Hoiaas, A. Liudi Mulyo, P. E. Vullum, D.-C. Kim, L. Ahtapodov, B.-O. Fimland, K. Kishino, and H. Weman. [GaN/AlGaN Nanocolumn Ultraviolet Light-Emitting Diode Using Double-Layer Graphene as Substrate and Transparent Electrode](#). *Nano Letters* **19** (3), 1649–1658 (2019). Cited on page/s 3.
- [4] A. Liudi Mulyo, M. K. Rajpalke, P. E. Vullum, H. Weman, K. Kishino, and B.-O. Fimland. [The influence of AlN buffer layer on the growth of self-assembled GaN nanocolumns on graphene](#). *Scientific Reports* **10** (1), 853 (2020). Cited on page/s 3, 4.
- [5] A. Liudi Mulyo *et al.* [The Influence of AlN Buffer Layer on the Growth of Self-Assembled GaN Nanocolumns on Graphene](#). *Unpublished* (n.d.). Cited on page/s 3.
- [6] A. Liudi Mulyo *et al.* [Utilization of Graphene as Substrate and Bottom Electrode for High-Density and Vertically-Aligned GaN/AlGaN Nanocolumns](#). *Unpublished* (n.d.). Cited on page/s 3.

CHAPTER 2

Background

SUMMARY

In this chapter, the modelling is done, something else is also done...

2.1 MODELLING

Modern wind turbines (WTs) are equipped with full scale back-to-back power electronic converters (PECs), as shown in figure 2.1. The machine converter runs in an optimum power point tracking mode and transfers power from the generator to the direct current (DC) link for attaining the optimum angular speed of the WT rotor for a given wind speed.

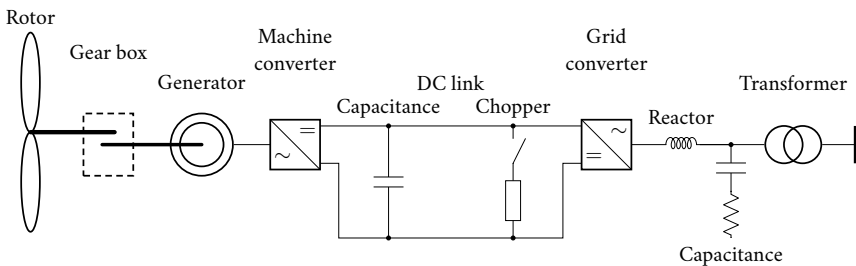


FIGURE 2.1 | WT model type 4 from [1].

Citing [2, 3]

2.2 REFERENCES

- [1] IEC 61400-27-1:2015. Wind turbines - Part 27-1: Electrical simulation models - Wind turbines. International Electrotechnical Commission (IEC) Geneva, Switzerland (February 2015). Cited on page/s 11.

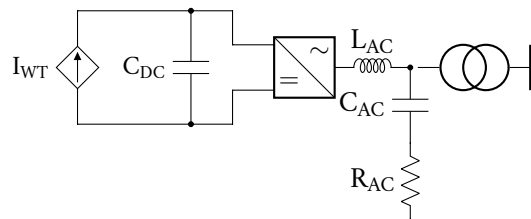


FIGURE 2.2 | Simplified WT model.

- [2] EU Comission Regulation. Guideline on capacity allocation and congestion management. EU 2015/1222. Technical report European Union (2015). eur-lex.europa.eu/eli/reg/2015/1222/oj. Accessed 2020-07-17. Cited on page/s 11.
- [3] ENTSO-E. Fast Frequency Reserve – Solution to the Nordic inertia challenge. Technical report ENTSO-E (December 2019). Cited on page/s 11.

CHAPTER 3

Experimental methods

Lorem ipsum dolor sit amet, consectetuer adipiscing elit [1]. Ut purus elit, vestibulum ut, placerat ac, adipiscing vitae, felis 1. Curabitur dictum gravida mauris. Nam arcu libero, nonummy eget, consectetuer id, vulputate a, magna. Donec vehicula augue eu neque [2]. Pellentesque habitant morbi tristique senectus et netus et malesuada fames ac turpis egestas 2. Mauris ut leo. Cras viverra metus rhoncus sem [3]. Nulla et lectus vestibulum urna fringilla ultrices. Phasellus eutellus sit amet tortor gravida placerat 3. Integer sapien est, iaculis in, pretium quis, viverra ac, nunc. Praesent eget sem vel leo ultrices bibendum [4]. Aenean faucibus. Morbi dolor nulla, malesuada eu, pulvinar at (3.1), mollis ac, nulla. Curabitur auctor semper nulla 4. Donec varius orci eget risus. Duis nibh mi, congue eu, accumsan eleifend, sagittis quis, diam. Duis eget orci sit amet orci dignissim rutrum [1–6].

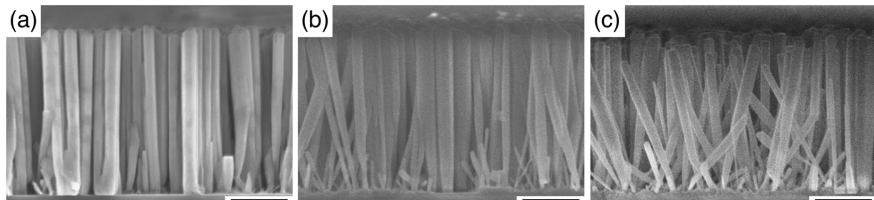


FIGURE 3.1 | Cross-sectional SEM images of GaN nanocolumns on graphene formed via different AlN MEE cycles. Samples (a) G1, (b) G2, and (c) G3. Scale bars are 500 nm (adapted with permission from ref. 4 © Liudi Mulyo et al, 2020).

3.1 SECTION 1 IN CHAPTER 3

Nam dui ligula, fringilla a, euismod sodales, sollicitudin vel, wisi. Morbi auctor lorem non justo. Nam lacus libero, pretium at, lobortis vitae, ultricies et, tellus. Donec aliquet, tortor sed accumsan bibendum, erat ligula aliquet magna, vitae ornare odio metus a mi. Morbi ac orci et nisl hendrerit mollis. Suspendisse ut massa. Cras nec ante. Pellentesque a nulla. Cum sociis natoque penatibus et magnis dis parturient montes, nascetur ridiculus mus. Aliquam tincidunt urna. Nulla ullamcorper vestibulum turpis. Pellentesque cursus luctus mauris.

$$EQE = \frac{q \times P_{opt}}{I \times h\nu} \quad (3.1)$$

Nulla malesuada porttitor diam. Donec felis erat, congue non, volutpat at, tincidunt tristique, libero. Vivamus viverra fermentum felis. Donec nonummy pellentesque ante. Phasellus adipiscing semper elit. Proin fermentum massa ac quam. Sed diam turpis, molestie vitae, placerat a, molestie nec, leo. Maecenas lacinia. Nam ipsum ligula, eleifend at, accumsan nec, suscipit a, ipsum. Morbi blandit ligula feugiat magna. Nunc eleifend consequat lorem. Sed lacinia nulla vitae enim. Pellentesque tincidunt purus vel magna. Integer non enim. Praesent euismod nunc eu purus. Donec bibendum quam in tellus. Nullam cursus pulvinar lectus. Donec et mi. Nam vulputate metus eu enim. Vestibulum pellentesque felis eu massa. 3.1 lists the experimental conditions of each sample synthesized in this study.

TABLE 3.1 | Experimental conditions.

| Sample ID | A1 | A2 | A3 | A4 | A5 | A6 | A7 |
|-----------------------|-----------------------|-----------------------|-----------------------|-----------------------|-----------------------|-----------------------|-----------------------|
| T _{sub} (°C) | 100 | 110 | 120 | 130 | 140 | 150 | 160 |
| Φ _{Ga} (Pa) | 1.0×10 ⁻¹⁰ | 1.0×10 ⁻¹¹ | 1.0×10 ⁻¹² | 1.0×10 ⁻¹³ | 1.0×10 ⁻¹⁴ | 1.0×10 ⁻¹⁵ | 1.0×10 ⁻¹⁵ |
| Q _N (sccm) | 1.5 | 1.6 | 1.7 | 1.8 | 1.9 | 2.00 | 2.1 |

3.1.1 Subsection 3.1 of section 1 in chapter 3

Fusce mauris. Vestibulum luctus nibh at lectus. Sed bibendum, nulla a faucibus semper, leo velit ultricies tellus, ac venenatis arcu wisi vel nisl. Vestibulum diam. Aliquam pellentesque, augue quis sagittis posuere, turpis lacus congue quam, in hendrerit risus eros eget felis. Maecenas eget erat in sapien mattis porttitor. Vestibulum porttitor. Nulla facilisi. Sed a turpis eu lacus commodo facilisis. Morbi fringilla, wisi in dignissim interdum, justo lectus sagittis dui, et vehicula libero dui cursus dui. Mauris tempor ligula sed lacus. Duis cursus enim ut augue. Cras ac magna. Cras nulla. Nulla egestas. Curabitur a leo. Quisque egestas wisi eget nunc. Nam feugiat lacus vel est. Curabitur consectetur.

Suspendisse vel felis. Ut lorem lorem, interdum eu, tincidunt sit amet, laoreet vitae, arcu. Aenean faucibus pede eu ante. Praesent enim elit, rutrum at, molestie non, nonummy vel, nisl. Ut lectus eros, malesuada sit amet, fermentum eu, sodales cursus, magna. Donec eu purus. Quisque vehicula, urna sed ultricies auctor, pede lorem egestas dui, et convallis elit erat sed nulla. Donec luctus. Curabitur et nunc. Aliquam dolor odio, commodo pretium, ultricies non, pharetra in, velit. Integer arcu est, nonummy in, fermentum faucibus, egestas vel, odio.

Sed commodo posuere pede. Mauris ut est. Ut quis purus. Sed ac odio. Sed vehicula hendrerit sem. Duis non odio. Morbi ut dui. Sed accumsan risus eget odio. In hac habitasse platea dictumst. Pellentesque non elit. Fusce sed justo eu urna porta tincidunt. Mauris felis odio, sollicitudin sed, volutpat a, ornare ac, erat. Morbi quis dolor. Donec pellentesque, erat ac sagittis semper, nunc dui lobortis purus, quis congue purus metus ultricies tellus. Proin et quam. Class aptent taciti sociosqu ad litora torquent per conubia nostra, per inceptos hymenaeos. Praesent sapien turpis, fermentum vel, eleifend faucibus, vehicula eu, lacus.

3.1.2 Subsection 3.2 of section 1 in chapter 3

Pellentesque habitant morbi tristique senectus et netus et malesuada fames ac turpis egestas. Donec odio elit, dictum in, hendrerit sit amet, egestas sed, leo. Praesent feugiat sapien aliquet odio. Integer vitae justo. Aliquam vestibulum fringilla lorem. Sed neque lectus, consectetur at, consectetur sed, eleifend ac, lectus. Nulla facilisi. Pellentesque eget lectus. Proin eu metus. Sed porttitor. In hac habitasse platea dictumst. Suspendisse eu lectus. Ut mi mi, lacinia sit amet, placerat et, mollis vitae, dui. Sed ante tellus, tristique ut, iaculis eu, malesuada ac, dui. Mauris nibh leo, facilisis non, adipiscing quis, ultrices a, dui.

Morbi luctus, wisi viverra faucibus pretium, nibh est placerat odio, nec commodo wisi enim eget quam. Quisque libero justo, consectetur a, feugiat vitae, porttitor eu, libero. Suspendisse sed mauris vitae elit sollicitudin malesuada. Maecenas ultricies eros sit amet ante. Ut venenatis velit. Maecenas sed mi eget dui varius euismod. Phasellus aliquet volutpat odio. Vestibulum ante ipsum primis in faucibus orci luctus et ultrices posuere cubilia Curae; Pellentesque sit amet pede ac sem eleifend consectetur. Nullam elementum, urna vel imperdiet sodales, elit ipsum pharetra ligula, ac pretium ante justo a nulla. Curabitur tristique arcu eu metus. Vestibulum lectus. Proin mauris. Proin eu nunc eu urna hendrerit faucibus. Aliquam auctor, pede consequat laoreet varius, eros tellus scelerisque quam, pellentesque hendrerit ipsum dolor sed augue. Nulla nec lacus.

3.2 SHORT SECTION TITLE IN THE CHAPTER

Sed feugiat. Cum sociis natoque penatibus et magnis dis parturient montes, nascetur ridiculus mus. Ut pellentesque augue sed urna. Vestibulum diam eros, fringilla et, consectetur eu, nonummy id, sapien. Nullam at lectus. In sagittis ultrices mauris. Curabitur malesuada erat sit amet massa. Fusce blandit. Aliquam erat volutpat. Aliquam euismod. Aenean vel lectus. Nunc imperdiet justo nec dolor.

Etiam euismod. Fusce facilisis lacinia dui. Suspendisse potenti. In mi erat, cursus id, nonummy sed, ullamcorper eget, sapien. Praesent pretium, magna in eleifend egestas, pede pede pretium lorem, quis consectetur tortor sapien facilisis magna. Mauris quis magna varius nulla scelerisque imperdiet. Aliquam non quam. Aliquam porttitor quam a lacus. Praesent vel arcu ut tortor cursus volutpat. In vitae pede quis diam bibendum placerat. Fusce elementum convallis neque. Sed dolor orci, scelerisque ac, dapibus nec, ultricies ut, mi. Duis nec dui quis leo sagittis commodo.

Aliquam lectus. Vivamus leo. Quisque ornare tellus ullamcorper nulla. Mauris porttitor pharetra tortor. Sed fringilla justo sed mauris. Mauris tellus. Sed non leo. Nullam elementum, magna in cursus sodales, augue est scelerisque sapien, venenatis congue nulla arcu et pede. Ut suscipit enim vel sapien. Donec congue. Maecenas urna mi, suscipit in, placerat ut, vestibulum ut, massa. Fusce ultrices nulla et nisl.

Etiam ac leo a risus tristique nonummy. Donec dignissim tincidunt nulla. Vestibulum rhoncus molestie odio. Sed lobortis, justo et pretium lobortis, mauris turpis condimentum augue, nec ultricies nibh arcu pretium enim. Nunc purus neque, placerat id, imperdiet sed, pellentesque nec, nisl. Vestibulum imperdiet neque non sem accumsan laoreet. In hac habitasse platea dictumst. Etiam condimentum facilisis libero. Suspendisse in elit quis nisl aliquam dapibus. Pellentesque auctor sapien. Sed egestas sapien nec lectus. Pellentesque vel dui vel neque bibendum viverra. Aliquam porttitor nisl nec pede. Proin mattis libero vel turpis. Donec rutrum mauris et libero. Proin euismod porta felis. Nam lobortis, metus quis elementum commodo, nunc lectus elementum mauris, eget vulputate ligula tellus eu neque. Vivamus eu dolor.

Nulla in ipsum. Praesent eros nulla, congue vitae, euismod ut, commodo a, wisi. Pellentesque habitant morbi tristique senectus et netus et malesuada fames ac turpis egestas. Aenean nonummy magna non leo. Sed felis erat, ullamcorper in, dictum non, ultricies ut, lectus. Proin vel arcu a odio lobortis euismod. Vestibulum ante ipsum primis in faucibus orci luctus et ultrices posuere cubilia Curae; Proin ut est. Aliquam odio. Pellentesque massa turpis, cursus eu, euismod nec, tempor congue, nulla. Duis viverra gravida mauris. Cras tincidunt. Curabitur eros ligula, varius ut, pulvinar in, cursus faucibus,

augue.

Nulla mattis luctus nulla. Duis commodo velit at leo. Aliquam vulputate magna et leo. Nam vestibulum ullamcorper leo. Vestibulum condimentum rutrum mauris. Donec id mauris. Morbi molestie justo et pede. Vivamus eget turpis sed nisl cursus tempor. Curabitur mollis sapien condimentum nunc. In wisi nisl, malesuada at, dignissim sit amet, lobortis in, odio. Aenean consequat arcu a ante. Pellentesque porta elit sit amet orci. Etiam at turpis nec elit ultricies imperdiet. Nulla facilisi. In hac habitasse platea dictumst. Suspendisse viverra aliquam risus. Nullam pede justo, molestie nonummy, scelerisque eu, facilisis vel, arcu.

Curabitur tellus magna, porttitor a, commodo a, commodo in, tortor. Donec interdum. Praesent scelerisque. Maecenas posuere sodales odio. Vivamus metus lacus, varius quis, imperdiet quis, rhoncus a, turpis. Etiam ligula arcu, elementum a, venenatis quis, sollicitudin sed, metus. Donec nunc pede, tincidunt in, venenatis vitae, faucibus vel, nibh. Pellentesque wisi. Nullam malesuada. Morbi ut tellus ut pede tincidunt porta. Lorem ipsum dolor sit amet, consectetur adipiscing elit. Etiam congue neque id dolor.

Donec et nisl at wisi luctus bibendum. Nam interdum tellus ac libero. Sed sem justo, laoreet vitae, fringilla at, adipiscing ut, nibh. Maecenas non sem quis tortor eleifend fermentum. Etiam id tortor ac mauris porta vulputate. Integer porta neque vitae massa. Maecenas tempus libero a libero posuere dictum. Vestibulum ante ipsum primis in faucibus orci luctus et ultrices posuere cubilia Curae; Aenean quis mauris sed elit commodo placerat. Class aptent taciti sociosqu ad litora torquent per conubia nostra, per inceptos hymenaeos. Vivamus rhoncus tincidunt libero. Etiam elementum pretium justo. Vivamus est. Morbi a tellus eget pede tristique commodo. Nulla nisl. Vestibulum sed nisl eu sapien cursus rutrum.

Nulla non mauris vitae wisi posuere convallis. Sed eu nulla nec eros scelesque pharetra. Nullam varius. Etiam dignissim elementum metus. Vestibulum faucibus, metus sit amet mattis rhoncus, sapien dui laoreet odio, nec ultricies nibh augue a enim. Fusce in ligula. Quisque at magna et nulla commodo consequat. Proin accumsan imperdiet sem. Nunc porta. Donec feugiat mi at justo. Phasellus facilisis ipsum quis ante. In ac elit eget ipsum pharetra faucibus. Maecenas viverra nulla in massa.

Nulla ac nisl. Nullam urna nulla, ullamcorper in, interdum sit amet, gravida ut, risus. Aenean ac enim. In luctus. Phasellus eu quam vitae turpis viverra pellentesque. Duis feugiat felis ut enim. Phasellus pharetra, sem id porttitor sodales, magna nunc aliquet nibh, nec blandit nisl mauris at pede. Suspendisse risus risus, lobortis eget, semper at, imperdiet sit amet, quam. Quisque scelesque dapibus nibh. Nam enim. Lorem ipsum dolor sit amet, consectetur adipiscing elit. Nunc ut metus. Ut metus justo, auctor at, ultrices eu, sagittis ut,

purus. Aliquam aliquam.

3.2.1 Subsection 3.2 of section 2 in chapter 3

Aliquam lectus. Vivamus leo. Quisque ornare tellus ullamcorper nulla. Mauris porttitor pharetra tortor. Sed fringilla justo sed mauris. Mauris tellus. Sed non leo. Nullam elementum, magna in cursus sodales, augue est scelerisque sapien, venenatis congue nulla arcu et pede. Ut suscipit enim vel sapien. Donec congue. Maecenas urna mi, suscipit in, placerat ut, vestibulum ut, massa. Fusce ultrices nulla et nisl.

Etiam ac leo a risus tristique nonummy. Donec dignissim tincidunt nulla. Vestibulum rhoncus molestie odio. Sed lobortis, justo et pretium lobortis, mauris turpis condimentum augue, nec ultricies nibh arcu pretium enim. Nunc purus neque, placerat id, imperdiet sed, pellentesque nec, nisl. Vestibulum imperdiet neque non sem accumsan laoreet. In hac habitasse platea dictumst. Etiam condimentum facilisis libero. Suspendisse in elit quis nisl aliquam dapibus. Pellentesque auctor sapien. Sed egestas sapien nec lectus. Pellentesque vel dui vel neque bibendum viverra. Aliquam porttitor nisl nec pede. Proin mattis libero vel turpis. Donec rutrum mauris et libero. Proin euismod porta felis. Nam lobortis, metus quis elementum commodo, nunc lectus elementum mauris, eget vulputate ligula tellus eu neque. Vivamus eu dolor.

3.3 REFERENCES

- [1] A. Liudi Mulyo, Y. Konno, J. S. Nilsen, A. T. J. van Helvoort, B.-O. Fimland, H. Weman, and K. Kishino. [Growth study of self-assembled GaN nanocolumns on silica glass by plasma assisted molecular beam epitaxy](#). *Journal of Crystal Growth* **480**, 67–73 (2017). Cited on page/s 13.
- [2] A. Liudi Mulyo, M. K. Rajpalke, H. Kuroe, P.-E. Vullum, H. Weman, B.-O. Fimland, and K. Kishino. [Vertical GaN nanocolumns grown on graphene intermediated with a thin AlN buffer layer](#). *Nanotechnology* **30** (1), 015604 (2018). Cited on page/s 13.
- [3] I. M. Hoiaas, A. Liudi Mulyo, P. E. Vullum, D.-C. Kim, L. Ahtapodov, B.-O. Fimland, K. Kishino, and H. Weman. [GaN/AlGaN Nanocolumn Ultraviolet Light-Emitting Diode Using Double-Layer Graphene as Substrate and Transparent Electrode](#). *Nano Letters* **19** (3), 1649–1658 (2019). Cited on page/s 13.
- [4] A. Liudi Mulyo, M. K. Rajpalke, P. E. Vullum, H. Weman, K. Kishino, and B.-O. Fimland. [The influence of AlN buffer layer on the growth of self-assembled GaN nanocolumns on graphene](#). *Scientific Reports* **10** (1), 853 (2020). Cited on page/s 13.
- [5] A. Liudi Mulyo *et al.* [The Influence of AlN Buffer Layer on the Growth of Self-Assembled GaN Nanocolumns on Graphene](#). *Unpublished* (n.d). Cited on page/s 13.
- [6] A. Liudi Mulyo *et al.* [Utilization of Graphene as Substrate and Bottom Electrode for High-Density and Vertically-Aligned GaN/AlGaN Nanocolumns](#). *Unpublished* (n.d). Cited on page/s 13.

Part II

PUBLICATIONS

CHAPTER 4

Offshore Wind Farms and Isolated Oil and Gas Platforms: Perspectives and Possibilities

Daniel dos Santos Mota¹, Erick Fernando Alves¹, Santiago Acevedo-Sanchez², Harald G. Svendsen², and Elisabetta Tedeschi^{1,3}

First published in: *The ASME 2022 41st International Conference on Ocean, Offshore & Arctic Engineering (OMAE)*, 2022.

DOI: [to-be-defined](#)

© ASME, 2022.

Contributions

DM, EA, SA, and HS conceptualized the idea. DM developed the software and performed the formal analysis and investigation. DM developed the methodology, validated the results, curated the data, wrote the original draft, and produced figures and tables. ET acquired the funding. DM, EA, and ET reviewed and edited this paper.

¹[NTNU](#), Trondheim, Norway. ²SINTEF Energi AS, Trondheim, Norway. ³University of Trento, Trento, Italy.

ABSTRACT

Single-cycle gas turbines operating at low-efficiency ranges due to redundancy concerns in offshore oil and gas platforms are responsible for considerable amounts of [nitrogen oxides](#) and [greenhouse gas](#) emissions in some countries. The abundant resource of offshore wind energy constitutes an extraordinary opportunity for reducing such emissions. However, new challenges are introduced when gas-powered generation is partially replaced by wind power. This paper investigates the possibilities provided by a centralized hybrid [energy storage system \(ESS\)](#) for addressing these challenges. It reviews frequency control concepts for isolated grids and discusses the analogous problem of power balancing within the [ESS](#) itself. A set of structures for control of the grid frequency and the [ESS DC](#) voltage are described and evaluated. All illustrated by results obtained within the frameworks of the [Innovative Hybrid Energy System for Stable Power and Heat Supply in Offshore O&G Installation Project](#) and the [LowEmission Research Centre](#).

4.1 INTRODUCTION

Rapid climate change is among the biggest global challenges today. The general road-map to tackle this challenge includes country-specific paths that depend on the types of national energy resources. The petroleum sector accounts for a considerable part of [nitrogen oxides \(NO_x\)](#) and [greenhouse gas \(GHG\)](#) emissions of many countries and, at the same time, is a key element of their socio-economic development. In Norway, for instance, 20% of the [GHG](#) emissions come from [gas turbines \(GTs\)](#) in operation in the [oil and gas \(O&G\)](#) fields in the [Norwegian continental shelf \(NCS\)](#) [1]. A similar situation with considerable emissions from the offshore [O&G](#) sector is observed in other European states, such as the United Kingdom [2] and the Netherlands [3].

Feasible approaches for reducing emissions related to offshore [O&G](#) production include the optimization of energy efficiency, carbon capture and storage, electrification from cleaner sources located onshore, and use of renewable energy sources. In this context, the abundant resource provided by offshore wind [4] is extremely promising when economic and environmental aspects are considered. However, technical challenges shall be addressed when integrating wind energy to the isolated power system of an [O&G](#) platform. Such platforms rely, typically, on compact single-cycle aeroderivative turbines for electricity generation [5]. Those turbines operate at a relatively stable load, however out of their best efficiency points due to redundancy requirements. Introducing a new but intermittent energy source as wind has positive and

negative consequences for the GTs [6, 7]. Among the consequences, one can mention:

- (+) operation of one GT at a higher load and better efficiency range if the redundant one can stay in cold standby;
- (-) increased number of start-stop operations and more variable load profile for the GTs, i.e., higher wear and tear and NO_x emissions;
- (-) overall degradation of the electric power quality and grid frequency stability, resulting in higher wear and tear of motors without variable frequency drives.

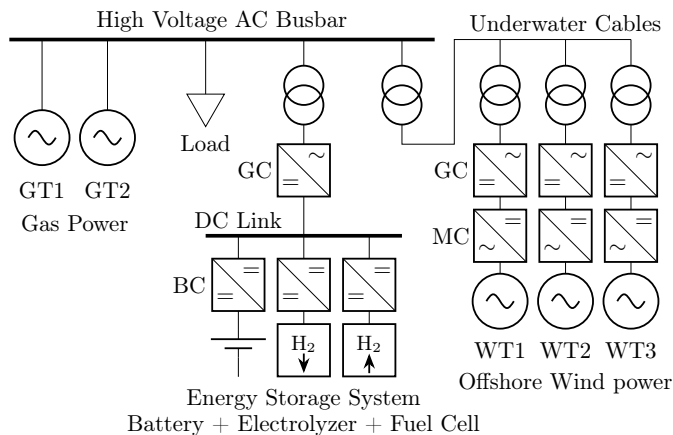


FIGURE 4.1 | Prospective scenario of a wind farm and an ESS connected to an existing isolated O&G platform, adapted from [8].

The diagram in figure 4.1 stems from a prospective scenario involving an existing O&G platform isolated from the continental electrical grid. This platform is fed by two 35 MW gas-powered generators. Currently, it does not feature an ESS and is not connected to any renewable energy source (RES). A techno-economical assessment [7] estimated that a reduction of approximately 30 % in GHG emissions would be possible if the platform were connected to a 12 MW offshore wind farm (WF). With this assessment as background, a novel sizing methodology for ESSs was proposed in [9]. A set of simulation models [10] of the platform and prospective WF were developed to validate the sizing methodology. These models were further developed [11] and are used in this paper for illustrating fundamental concepts and evaluating the dynamic behavior of the ESS.

In summary, this paper focuses on the frequency control of an isolated O&G platform equipped with a centralized hybrid ESS and connected to an offshore

WF. The overall mechanical and electrical power balancing problem of the platform is discussed from a fast frequency support perspective. The analogous electrical power balancing issue of the **ESS** is also presented. A control strategy applied to the **ESS** for **alternate current (AC)** frequency support is described. This strategy is based on established **proportional, integral, and derivative (PID)** techniques. It does not rely on fast communication links between different **energy storage devices (ESDs)** or with the platform's **power management system (PMS)**. Potential challenges are identified and future research paths are discussed. All this is illustrated by previous and current results obtained by **Innovative Hybrid Energy System for Stable Power and Heat Supply in Offshore O&G Installation Project (HES-OFF)** and **LowEmission** research projects.

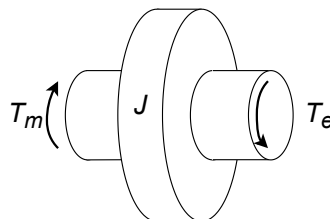


FIGURE 4.2 | Aggregated rotating mass model, adapted from [12, 13].

4.2 FREQUENCY CONTROL IN ELECTROMECHANICAL SYSTEMS

The control of the frequency of an **AC** electrical grid is, essentially, a torque balancing problem. Figure 4.2 shows a simplified model of the dynamic behavior of the platform's electromechanical power system [12, 13]. A flywheel with moment of inertia J represents the aggregated rotating masses of the system. The **GTs** supply mechanical torque T_m to the drive side of the rotating mass. The aggregated electrical loads exert T_e contrary to T_m . The rate in which the ω changes when a torque imbalance occurs is limited by the system's rotational kinetic energy $E_k = J\omega^2/2$. When expressed in terms of power, the balance of the torques in the system becomes:

$$\underbrace{\omega J \frac{d\omega}{dt}}_{\text{Rotating Mass}} = \underbrace{P_m}_{\text{Turbine}} - \underbrace{P_e}_{\text{Loads}}, \quad (4.1)$$

where P_m is the mechanical power delivered by the **GTs** and P_e is the electrical power consumed in the grid.

A common procedure among power system engineers is to normalize equation (4.1). This is performed by dividing both sides of the equation by the

total apparent power of the generators S_n in VA and by re-writing the moment of inertia J in terms of the inertia constant H [12]:

$$H = \frac{E_{kn}}{S_n} = \frac{J\omega_n^2}{2S_n} \quad [\text{s}], \quad (4.2)$$

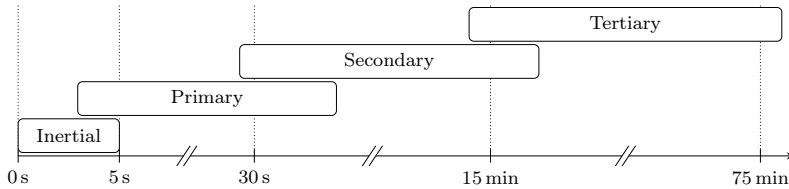
where ω_n is the rated angular frequency of the grid. The constant H is equal to the rated rotating kinetic energy E_{kn} divided by the rated apparent power S_n , which results in a measure of time in seconds. This normalized figure is useful for comparing the relative inertia contribution of different generators.

Replacing gas-powered generation by wind power makes the electrical system of an isolated O&G platform less stable from a frequency control perspective. The reason is that modern WTs are equipped with full scale back-to-back PECs [14–16]. Those do not contribute with mechanical torque T_m to the aggregated rotating mass of the model shown in figure 4.2. Indeed, the power produced by a WT can be modeled as a negative load. In other words, a higher percentage of wind generation means lower electrical torque T_e , not higher T_m . Furthermore, the WTs do not contribute to the aggregated J of the model either [17]. Therefore, every GT that is replaced results in a smaller aggregated kinetic energy buffer E_k . The lower the value of this buffer, the faster the remaining GTs shall respond during disturbances to the power system. However, restrictions in ramping rates and delays of actuators in GT governors limit how fast they can contribute to frequency control. A more in-depth analysis of these limitations and the different strategies and time scales of frequency control are presented in the following section.

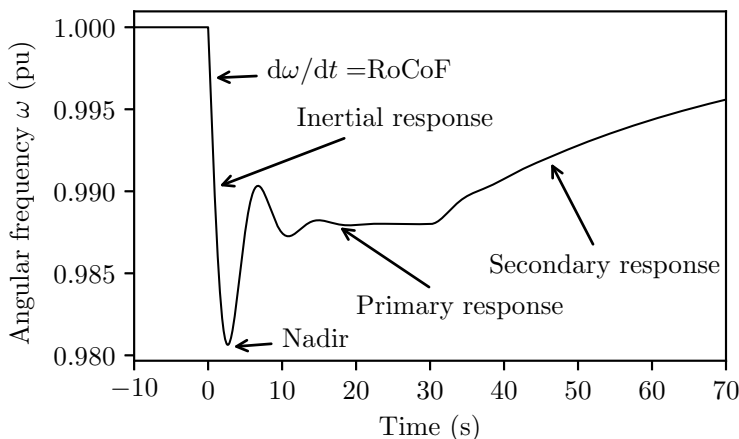
4.2.1 Phases of the Frequency Control

Governors continuously adjust the mechanical power output of GTs to maintain the frequency at its rated value. Figure 4.3 illustrates the typical phases of the frequency control after a sudden large power imbalance with excess load. The inertial response phase begins at time $t = 0$ s with the drop in ω at a given rate of change of frequency (RoCoF). The primary phase starts when the governors are able to react to the frequency change. They respond by increasing the power generation which stops the frequency fall. The minimum value reached by ω is known as nadir. During the primary phase, the frequency is raised to a level closer to the rated value. Subsequently, the frequency increases slowly back to the rated value during the secondary response phase. After that, a PMS can decide to slowly replace the power reserves used for frequency control by more efficient measures. This is typically achieved through redispatching of generators and loads in the tertiary response phase. The time scales of the

frequency control phases are typically: a few seconds for the inertial, seconds to few minutes for the primary, minutes for the secondary, and from a quarter to a full hour for tertiary [17, 18].



(a) Time scales of the frequency response phases, adapted from [17].



(b) Initial stages after a power imbalance with excess load, adapted from [17, 18], source model and dataset at [11].

FIGURE 4.3 | Frequency response phases.

In the next sub-sections, the frequency control phases and their relationship to the inertia and governor responses will be further explained. Though, it is important to emphasize that these descriptions assume that the simplified model in [equation \(4.1\)](#) is valid. This model assumes that the electrical frequency and the mechanical angular velocity are equivalent. It also assumes that the electrical frequency is a single, global variable that can be used to measure power imbalance. On one hand, the electrical frequency of a country or continent-wide electrical grid is not a single global variable, as shown by real life measurements of the European system [19]. On the other hand, this is still a good approximation for the isolated O&G platform scenario under study and for the time scales investigated in this paper. Therefore, the mechanical angular velocity of the aggregated mass and the electrical angular frequency across the whole platform are assumed to be described by the single global variable ω .

The validity of this assumption is assessed later in [section 4.4](#). The reader can find a deeper discussion about this issue in [20].

Inertial Response

[Figure 4.4](#) shows the response of two conceptual systems modeled according to [equation \(4.1\)](#). The models and dataset are publicly available at [11]. The systems are identical with a single turbine and generator unit connected to an electrical load, except for the levels of inertia which are $H = 5\text{ s}$ and $H = 10\text{ s}$. All measurements are in per unit (pu). Figures [4.4d](#), [4.4e](#), and [4.4f](#) represent three components of the electrical power supplied by the generator to the load. The inertial component is provided directly by the rotating mass, no controller needed. The primary and secondary powers are provided by the turbine to the generator.

The power consumed by the load is shown on [figure 4.4a](#). The frequency of the system is initially at equilibrium. On [figure 4.4c](#), the total energy stored in the rotating mass of the high and low inertia cases are shown. At instant $t = 10\text{ s}$, the electrical load increases in a step from 0.26 pu to 0.38 pu . Immediately after the step, the rotating mass delivers the totality of the power imbalance, i.e., 0.12 pu of power. This is seen on [figure 4.4d](#). Consequently, the level of energy in the buffer ([figure 4.4c](#)) begins to drop in conjunction with the frequency ([figure 4.4b](#)). Remark that energy is proportional to the square of the frequency.

The inertial response is dominated by the kinetic energy buffer of the rotating masses of the system. This contribution limits the [RoCoF](#). Note that the smaller the buffer, the steeper the [RoCoF](#). Furthermore, the lower the inertia, the lower the nadir.

Primary Response

The primary response to a power imbalance is shown in [figure 4.4e](#). Once the frequency begins to drop, the turbine governor reacts proportionally to the frequency deviation, i.e., proportionally to $\Delta\omega = \omega_n - \omega$, where ω_n is the rated grid frequency. This action is commonly known as frequency droop [21]. The speed in which the power reacts to the frequency deviation is heavily limited by mechanical constraints of governors and turbines, namely ramping rates and delays of actuators [22]. The higher the actuator delay or the lower the ramping rate, the larger will be the overlap between the inertial and primary responses.

In both high and low inertia cases in [figure 4.4](#), the droop is the same. Therefore, despite featuring different nadirs, the primary response brings the frequency back to the same level for $H = 5\text{ s}$ and $H = 10\text{ s}$ ([figure 4.4b](#)). As with any other purely proportional regulator with a non-zero set point, a

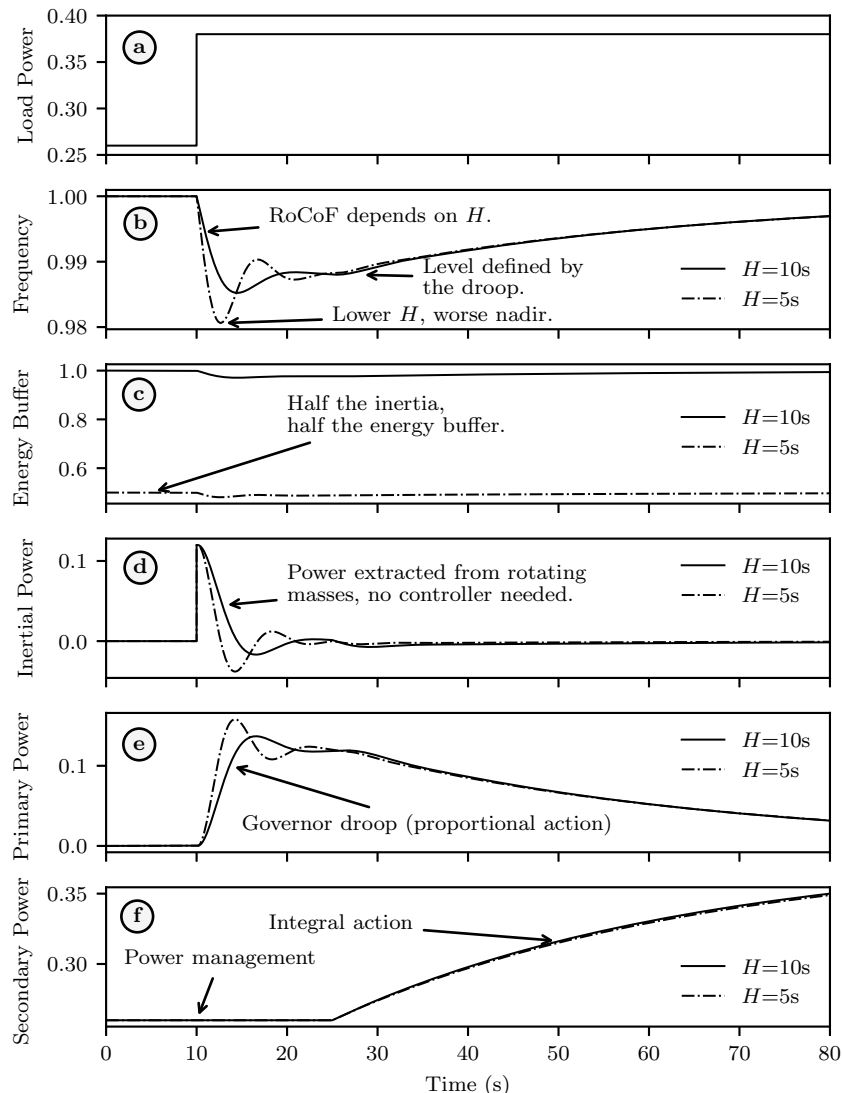


FIGURE 4.4 | Inertia and governor roles in the frequency control, source model and data set [11].

The original figure has been reformatted to fit the page dimensions of this dissertation.

steady-state error between the set point and the controlled variable is always present [23].

Secondary Response

Initially, the turbine and load power were at equilibrium, see figures 4.4a and 4.4f. This was achieved by the action of the PMS on the secondary power. This response is characterized by an integral action. In an isolated O&G platform, the secondary response is typically performed by a PMS which sends commands to the turbine governors. In large electrical systems, this power management receives the name of [automatic generation control \(AGC\)](#) [21]. Nevertheless, if there is only one single generator in the system, the secondary control can be performed directly in the governor by an integral regulator [13].

4.2.2 Other Dynamics

An isolated O&G platform is a power intensive industrial installation with numerous loads as pumps, compressors, and heaters that may or not be interfaced by PECs. A constellation of control loops directly or indirectly connected to each other is necessary to keep the electrical system of a platform in operation. As illustrated by [figure 4.5](#), these controllers operate in different time scales. Traditional voltage regulators and speed governors of synchronous generators work in time scales from 10^{-1} to 10^3 s. The control structures of modern PECs operate in time scales down to 10^{-5} s or lower [18]. On one hand, these faster responses may be beneficial and add new possibilities for frequency control, such as inertia emulation and other forms of fast regulation [22]. On the other hand, detrimental interactions may also be introduced.

For instance, offshore WTs feature low-frequency oscillation modes due to the slow swinging of their tall floating towers [24]. These low-frequency mechanical oscillations, ultimately, are reflected as variations in the power delivered by the WT to grid. In a large WF with several WTs, these low frequency oscillations can be evened out. However, in the scenario under study in this paper with a few WTs, they might not be negligible. Combined with short-term and long-term wind variations, low frequency power oscillations from the WF increase the burden of GTs for controlling the frequency. Therefore, wear and tear of the GTs and their governors can increase.

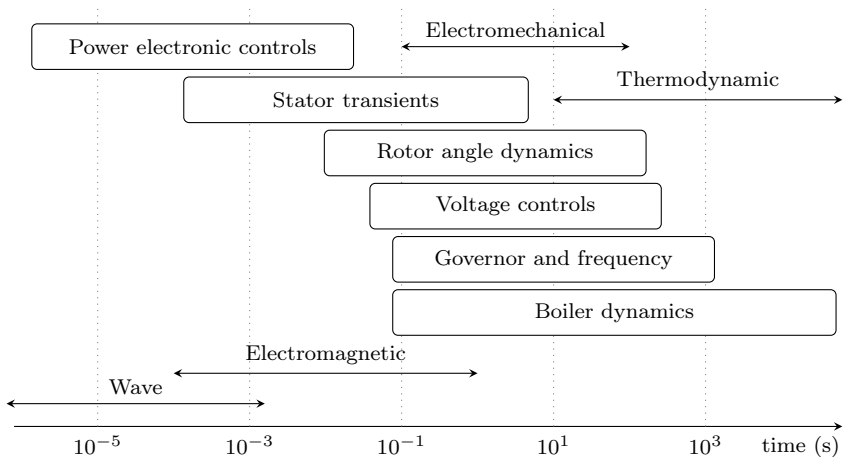


FIGURE 4.5 | Control dynamics in an AC electrical system, adapted from [18].

4.3 HYBRID ENERGY STORAGE SYSTEM

Power and energy demands of the frequency control phases are different. Secondary reserves require the largest energy storage, followed by primary reserves and by inertial support. However, inertial support demands the steepest rates of change of power, followed by primary and the secondary reserves. Today's energy storage solutions vary considerably in peak power capacity, rate of change of power limitations, and energy density. There is no one-size-fits-all **ESD** that is able to store the necessary energy, provide the required peak power, and change the power as fast as required to provide frequency control support during all phases. Therefore, hybrid solutions combining different types of **ESDs** are becoming a preferred choice in transportation and in power system applications [25].

To address the issues caused by wind intermittency and combine the specific characteristics of different **ESDs**, **LowEmission** and **HES-OFF** investigated the implementation of a centralized hybrid **ESS** connected directly to the platform's main **AC** busbar. An example of such system is shown in figure 4.6. Electrolyzer and fuel cell provide secondary reserves for the frequency control. Batteries are employed as a fast **ESD** for the short-term variations supplying inertial support and primary reserves. The **ESDs** operate in **DC** and are interfaced to the grid via a bidirectional **AC-DC** converter. A filter stage and a transformer connect the **ESS** to the platform's main **high-voltage (HV)** busbar.

Sizing the **ESDs** and the **grid converter (GC)** for frequency support in an isolated **AC** power system is an involved and iterative process. A sizing method [9] has been proposed within the frameworks of **LowEmission** and **HES-OFF**. The

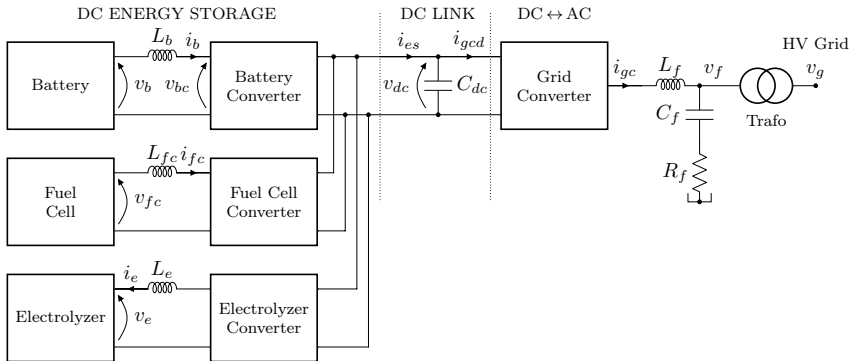


FIGURE 4.6 | Schematic diagram of a hybrid energy storage system.

dataset and models used in this work are available at [10]. Moreover, a hardware-in-the-loop testbed for PECs and ESDs is currently under development for validating the method and for studying the dynamic behavior of a hybrid ESS. Not least, it is worth emphasizing that the proposed method is algebraic and requires the knowledge of a few parameters of the AC power system. Hence, it can be integrated into broader techno-economical optimization algorithms evaluating an installation from a holistic perspective, such as the multi-carrier offshore energy hub approach being developed under LowEmission [26].

4.3.1 Power Balancing Within the ESS

As previously discussed in section 4.2, the frequency control of the platform's AC electric system is a power balancing problem. The power required by the industrial processes and supplied by generators must be continuously equalized. Albeit in a different time scale, the ESS features an analogous power balancing problem.

At the core of the ESS shown in figure 4.6, in the DC link, there is a capacitor bank represented by C_{dc} . Similarly to the rotating masses of the AC grid, the capacitor bank holds an energy buffer $E_e = C_{dc} v_{dc}^2 / 2$. Moreover, variations in the dc-link voltage (v_{dc}) indicate a power imbalance between the ESDs and the AC-DC converter. In other words, if the power supplied by the ESDs and the power transferred from the DC link to the AC grid by the GC are in equilibrium, the voltage at C_{dc} is constant. If the net power supplied to the DC link is positive, v_{dc} increases in conjunction with the energy E_e . Conversely, if the net power is negative, v_{dc} decreases. Assuming that losses on the converters and DC link of the ESS are negligible, the dynamic behavior of v_{dc} described

in terms of the currents i_{es} and i_{gcd} is

$$\underbrace{C_{dc} \frac{dv_{dc}}{dt}}_{\text{Buffer}} = \underbrace{i_{es}}_{\text{From ESDs}} - \underbrace{i_{gcd}}_{\text{To AC side}} . \quad (4.3)$$

Alike a turbine governor controlling the AC grid frequency, the ESS shall contain an internal DC voltage controller acting either on the ESD or GC power flow to constrain v_{dc} variations. Naturally, this DC voltage control happens in a fraction of the time scales for frequency control described in section 4.2. Failure to do so may result in voltage collapse of the ESS or significant power oscillations. Though, note that the larger the capacitance C_{dc} , the larger the energy buffer E_e and the more forgiving the system is to unbalances between the ESDs and GC. Therefore, sizing C_{dc} becomes a techno-economical task that has consequences to the tuning and dynamics of the DC voltage controller. This issue is among the topics discussed in the algebraic method for sizing the ESS proposed in [9].

In this backdrop, a set of structures for the AC frequency support and the internal v_{dc} control have been adopted within the scope of LowEmission and HES-OFF projects. In the next section, these structures are presented.

4.3.2 ESS Control Structure

In this section, the main control structures employed in the battery converter (BC) and GC are presented. The term battery is used for ESDs in general. So, the concepts are also applicable to fuel cells and electrolyzers with only minor adaptations. It is also important to emphasize that an approach based on traditional PID controllers is adopted for the hybrid ESS proposed in this paper. This choice was made because those are well-proven and usually available in commercial products. Moreover, a structure that does not rely on a fast communication link between the different converters of the ESS or with the platform's PMS is chosen. Finally, all PECs of the ESS operate with a pulse-width modulation (PWM) technique, see [27] for more information on this topic. They use cascaded control structures with a fast inner current control loop and a slower outer loop. The outer loops control variables are the grid angular frequency (ω) and the DC-link voltage (v_{dc}) as seen in figure 4.7.

Grid Frequency Control

Figure 4.7a shows the control structure for the AC frequency support provided by the ESS. The dynamic behaviour of this structure will be assessed later in section 4.4.1. Moreover, the structure uses the measurement of the grid

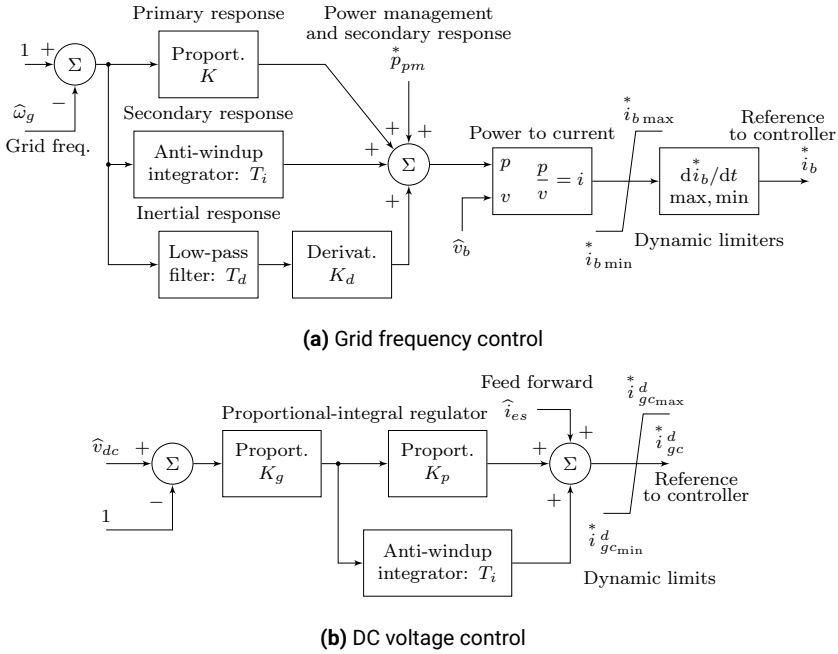


FIGURE 4.7 | Control structures of a hybrid energy storage system.

frequency $\hat{\omega}_g$ to generate the reference i_b^* for the BC inner current control loop. Remark that all measurements (denoted as \hat{x}) in the control structures are assumed to have been properly conditioned, filtered, and scaled. The structure is divided into three branches that correspond to the different phases of the frequency control of AC grids.

- **Primary response:** proportional gain K . It is the equivalent of the inverse of the droop. The higher the gain K , the higher the contribution of the battery for a given grid frequency deviation.
- **Secondary response:** integrator time T_i and input for power reference p_{pm}^* . If the BC is the only device in the system supplying secondary reserves, the integral branch can be enabled. This branch works towards removing the steady-state error left by the droop based control. However, if a GT or another ESD is also a source of secondary reserves, the T_i branch is disabled. Then, the input p_{pm}^* is used by the PMS to coordinate the delivery of reserves between GTs and ESDs. Moreover, p_{pm}^* is also the input for controlling the state of charge (SOC) of the battery.
- **Inertial response:** derivative gain K_d . Contrary to the “real” inertial response provided by rotating masses, the inertia emulation from the

battery relies on a frequency measurement which is inherently noisy. Therefore, a **low-pass filter (LPF)** stage with a time constant T_d is necessary in the derivative branch.

The minimum and maximum values ($i_{b\max}^*$ and $i_{b\min}^*$) in [figure 4.7a](#) provide the means for dynamically limiting the operation based on **SOC**, temperature, or other conditions of the **ESD**. The rate-of-change limiters are not necessarily static nor symmetric. Moreover, the “power to current” block compensates for variations in the battery voltage. This compensation, however, is not yet implemented in the results shown later in [section 4.4](#) as it can be detrimental to the battery health during large charge or discharge power variations. Besides, it adds a non-linearity in the control loop that is known to cause instabilities when the **BC** is heavily loaded [28]. Another method to reach this compensation is implementing a **proportional and integral (PI)** controller for active power control. This alternative adds another layer of control, and consequently reduces the frequency control bandwidth, which might also cause stability problems. Hence, this is a topic currently under investigation in [LowE-mission](#).

DC Voltage Control

The **GC** adopted for the **ESS** is composed of a two-level three-phase **IGBT** bridge. A passive **LCL** filter connects the **GC** to the grid, see [figure 4.6](#). This filter employs a reactor (L_f) and a **capacitive-resistive (CR)** branch (C_f and R_f). The second inductive device is the transformer. See [29] for more information on passive **LCL**-filters.

The **GC** operates as a three-phase voltage source. With the help of **PWM** switching and the **LCL**-filter, the converter is able to synthesize three-phase sinusoidal currents (i_{gc}). The traditional inner current control in a **rotating reference frame (RRF)** is adopted. This strategy relies on the measurement of the phase of the **AC** voltage with a **phase-locked loop (PLL)**. See [30] for a literature review on **PLLs**. A set of mathematical operators is used to transform the measured three-phase voltages and currents to a direct and quadrature reference frame [31]. When the angular frequency of the **RRF** matches the angular frequency of balanced three-phase voltages and currents, the direct and quadrature values become constant. This allows the use of two sets of **PI** regulators for controlling the **AC** current of the converter [32]. Moreover, the **GC** direct-axis current (i_{gc}^d) produces active power. Whereas, the quadrature-axis current (i_{gc}^q) produces reactive power.

[Figure 4.7b](#) shows the **DC** voltage control loop of the **GC**. It has the measurement of the **DC**-link voltage \hat{v}_{dc} as an input. The direct current reference

i_{gc}^d is sent to the converter's fast inner current controller. For improving the DC-voltage dynamics, a feed-forward path (\hat{i}_{es}) is provided for the total current from the ESDs. This, however, does not represent a need for fast communication between the BCs and the GC. If a DC-current measurement transducer is connected at the electrical point marked by i_{es} in figure 4.6 and interfaced with the GC controller, then no direct communication with the different ESDs is necessary.

It is worth mentioning that the performance of current controllers in RRF is affected by unbalanced three-phase loads, i.e., when the loads on each of the phases of the system are considerably different. Within the scope of LowEmission and HES-OFF, a strategy known as dual-sequence current controller has been investigated. This strategy relies on splitting three-phase measurements into two components, one called positive and the other negative sequence. These components are different RRFs with opposite angular speeds. A literature review and a comparison of controllers with two different sequence separation strategies was done in [8]. An improved method for sequence separation was proposed in [33]. Nevertheless, the operation under unbalanced conditions is considered outside the scope of this paper.

4.4 PERSPECTIVES AND POSSIBILITIES WITH A HYBRID ESS

In this section, an analysis of the possibilities provided by a hybrid ESS is presented. Some of the challenges from the perspective of a power system engineer are also discussed. The results of computer simulations are used as illustration. The simulation models used herein have been developed under the frameworks of LowEmission and HES-OFF. The base models [10] were programmed originally in MATLAB R2016a. However, for this paper, these were re-written in DIgSILENT PowerFactory 2020 SP2A. The re-written models are available at [11].

The single line diagram in figure 4.1 represents the test cases. Two gas-powered generators are connected to the platform's main HV busbar. A set of general loads represent the total electrical consumption on the platform. Three type 4 [14] offshore floating WTs are connected to the main busbar via an HV underwater collector system. PowerFactory's detailed model with PWM switching with built-in fast current controllers in the RRF [34] are used for the GCs of the ESS and WTs. A simplified average model of the ESD converters is used. For details on PECs modeling strategies, see [35]. The converters' outer loops from figures 4.7a and 4.7b were manually programmed in PowerFactory. Three cases are used for analysis and discussion in this section:

Case 1 — ESS is connected but does not provide support for frequency con-

trol;

Case 2 — ESS provides primary support;

Case 3 — ESS provides inertial and primary support.

In all cases, two **GTs** and the **WF** are feeding a base load of 46 MW. Each **WT** produces 4 MW. At instant $t = 1$ s, a step load of 4 MW is applied to the platform's **HV** busbar. Both turbine governors run in speed control with a droop of 4.7 %. The rated power of the **ESS GC** is 10 MVA and the rated power of the **ESS BC** is 4 MW. The **ESS fuel cell converter (FCC)** rated power is 6 MW. The **FCC** is set to supply a slow secondary response to frequency variations. This secondary response is, however, not significant within the time scales of the three cases.

4.4.1 Frequency Support Provided by the ESS

Figure 4.8 shows the response to the step load transient. On figure 4.8a, the total electrical load of the platform is shown. The transient causes a sudden dip in the platform's busbar voltage (figure 4.8f). There is room for improvement if an **AC** voltage support control structure were implemented in the **ESS** as discussed in [36]. The power supplied by the generators is shown on figure 4.8e. For **case 1** (no **ESS** support), the two generators supply all the extra power demanded by the step load. When droop and inertial support is provided by the **ESS**, the **BC** assumes part of the load. The next research step within the **LowEmission** project is to investigate scenarios where most of the primary frequency reserve is provided by the **ESS**, not by the **GTs**.

4.4.2 DC Voltage Control within the ESS

Figure 4.9 shows the effect on the **DC** voltage of operating with or without the feed-forward scheme during the transient with **ESS** inertial and primary support (**case 3**). It is clear that the **DC** voltage control becomes worse without the feed-forward scheme. The differences are, however, considerably small. Nevertheless, the lower the capacitance connected to the **DC** link, the higher the **DC** voltage variations will be during transients. Therefore, the improved dynamic provided by the feed-forward can be more suited when a reduction of the capacitance bank is desirable. Reducing the capacitance bank and improving the **DC** voltage regulators are future research paths that might be taken within the scope of **LowEmission** and **HES-OFF**.

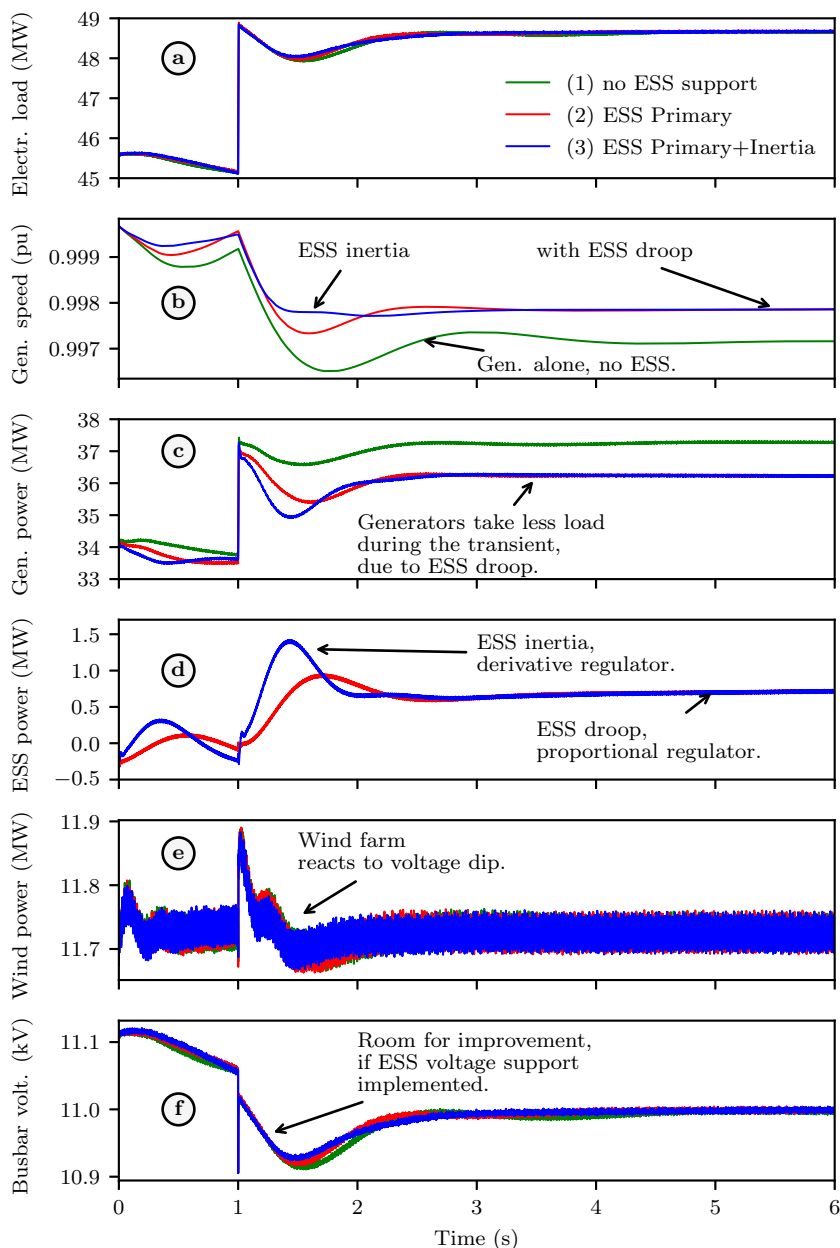


FIGURE 4.8 | ESS providing inertia and primary reserves, source model and dataset at [11].

The original figure has been reformatted to fit the page dimensions of this dissertation.

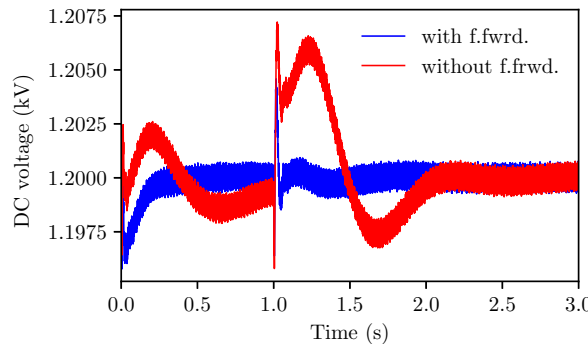


FIGURE 4.9 | Case 3, DC voltage with (blue) and without (red) feed-forward scheme.

4.4.3 Frequency as a Global Variable

In section 4.2, the electrical frequency across the whole platform and the mechanical speed of the GTs are treated as one unique variable. A comparison is made for case 3 to test the validity of the “global variable” assumption. Figure 4.10 shows, in pu, the speed of the GTs and the electrical frequency at the low-voltage (LV)-side of the ESS transformer (ESS 690V) and at the LV-side of the WT3 transformer (WT3 690V). The WT number 3 is the one furthest from the platform. The electrical measurement is performed with PowerFactory’s built-in PLLs [34]. The mechanical speeds of the GTs are almost identical. There is, on the other hand, a noticeable difference between the measured electrical frequencies and the mechanical speeds. Moreover, the sudden change in the voltage profile at the platform’s HV busbar (not shown in the curves) caused by the step load is detected by the PLL at the LV-side of the ESS transformer as a small but sharp frequency dip. For WT3, which is farther from the transient source, the measured electrical frequency features a smoother dip. An ESD with supercapacitors providing inertial support might respond to such dip. Investigating this issue is one of future research paths within the scope of LowEmission.

4.5 FUTURE RESEARCH

A centralized hybrid ESS can be used to alleviate the negative consequences of connecting an intermittent energy source to an isolated electrical system. However, this concept still poses challenges which deserve further investigation. Some of these challenges were identified and discussed in this paper. Among them, the following open topics can be highlighted.

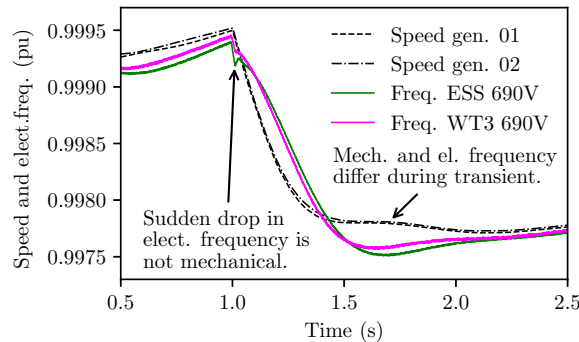


FIGURE 4.10 | Case 3, mechanical speed and electrical frequency.

- **DC voltage:** the feed-forward scheme described in this paper may play an important role in a future optimization of the **DC-link** capacitor bank sizing and, consequently, in the **GC** cost, weight, and space requirements.
- **AC voltage:** the **ESS** is capable of providing reactive power support reducing voltage sags and swells during transients. Nevertheless, fast interactions between the **ESS** converters, other large **PECs** in the platform, and **WTs** shall be further assessed.
- **Primary reserves:** in the scenario analysed in this paper, both the **GTs** and the **ESS** were providing primary reserves. The limitations and techno-economical consequences of increasingly transferring the primary frequency control from the **GTs** to the **ESS** shall be further investigated.
- **Inertial reserves:** electrical transients can produce fast changes in the **AC** frequency that are not representative of mechanical changes in the rotational speed of the **GTs**. These fast changes in the electrical frequency can be detrimental to the performance of **ESDs** providing inertial reserves. Alternative electrical frequency measurement methods and their effects in the dynamics of derivative-based inertial reserves shall be assessed in the future.

4.6 CONCLUSION

This paper analyzed the possibilities provided by a centralized hybrid **ESS** for alleviating the negative consequences of integrating an offshore **WF** to the **AC** grid of an isolated **O&G** platform. It presented a set of structures for

providing inertial, primary, and secondary reserves to frequency control and for controlling the internal DC voltage of the ESS. These structures are based on established PID techniques and do not rely on fast communication links between the different converters of the ESS nor with the platform's PMS. The proposed concept shows promising results when assessed through publicly available models developed under the frameworks of HES-OFF and LowEmission. Notwithstanding, challenges from a power systems perspective remain open. Some of these challenges were highlighted in this paper and must be further investigated.

4.7 REFERENCES

- [1] OED. Norwegian Petroleum Emissions to Air 2020. online Norwegian Ministry of Petroleum and Energy (OED) Oslo, Norway (2022). URL <https://www.norskpetroleum.no/en/environment-and-technology/emissions-to-air/>. Cited on page/s 22.
- [2] OGUK. North Sea Transition Deal. Report NSTD Department for Business, Energy & Industrial Strategy London, United Kingdom (2021). URL https://assets.publishing.service.gov.uk/government/uploads/system/uploads/attachment_data/file/972520/north-sea-transition-deal_A_FINAL.pdf. Cited on page/s 22.
- [3] Adrian Serna Tamez and Stijn Dellaert. Decarbonisation options for the Dutch offshore natural gas industry. Report PBL 416 PBL Netherlands Environmental Assessment Agency and TNO Energy Transition (2020). URL https://www.pbl.nl/sites/default/files/downloads/pbl-2020-decarbonisation-options-for-the-dutch-offshore-natural-gas-industry_4161.pdf. Cited on page/s 22.
- [4] IEA. Offshore Wind Outlook 2019. Report WEO STO 2019 International Energy Agency Paris, France (2019). URL https://iea.blob.core.windows.net/assets/495ab264-4ddf-4b68-b9c0-514295ff40a7/Offshore_Wind_Outlook_2019.pdf. Cited on page/s 22.
- [5] Håvard Devold. Oil and gas production handbook, an introduction to oil and gas production, transport, refining and petrochemical industry. ABB Oil and Gas Oslo, Norway 3.0 edition (2013). ISBN 978-82-997886-3-2. URL https://library.e.abb.com/public/34d5b70e18f7d6c8c1257be500438ac3/Oil%20and%20gas%20production%20handbook%20ed3x0_web.pdf. Cited on page/s 22.
- [6] Magnus Korpås, Leif Warland, Wei He, and John Olav Giæver Tande. A Case-Study on Offshore Wind Power Supply to Oil and Gas Rigs. *Energy Procedia* **24**, 18–26 (2012). ISSN 1876-6102. doi: 10.1016/j_egypro.2012.06.082. URL <http://www.sciencedirect.com/science/article/pii/S1876610212011228>. Cited on page/s 23.
- [7] Luca Riboldi, Erick F. Alves, Marcin Pilarczyk, Elisabetta Tedeschi, and Lars O. Nord. Optimal Design of a Hybrid Energy System for the Supply of Clean and Stable Energy to Offshore Installations. *Frontiers in Energy Research* **8**, 346 (2020). ISSN 2296-598X. doi: 10.3389/fenrg.2020.607284. URL <https://www.frontiersin.org/article/10.3389/fenrg.2020.607284>. Cited on page/s 23.
- [8] Daniel dos Santos Mota and Elisabetta Tedeschi. Understanding the Effects of Exponentially Decaying DC Currents on the Dual dq Control of Power Converters in Systems with High X/R. In *IEEE 15th International Conference on Compatibility, Power Electronics and Power Engineering* pages 1–6 Florence, Italy (2021). IEEE. DOI: [10.1109/CPE-POWERENG50821.2021.9501204](https://doi.org/10.1109/CPE-POWERENG50821.2021.9501204). Cited on page/s 23, 35.
- [9] Erick Fernando Alves, Daniel dos Santos Mota, and Elisabetta Tedeschi. Sizing of Hy-

- brid Energy Storage Systems for Inertial and Primary Frequency Control. *Frontiers in Energy Research* **9**, 206 (2021). ISSN 2296-598X. DOI [10.3389/fenrg.2021.649200](https://doi.org/10.3389/fenrg.2021.649200). Cited on page/s 23, 30, 32.
- [10] Erick Fernando Alves. Hybrid ESS design repository - data set and simulation files. Zenodo (2021). DOI [10.5281/zenodo.4384697](https://doi.org/10.5281/zenodo.4384697). Cited on page/s 23, 31, 35.
- [11] Daniel dos Santos Mota. Data repository of the manuscript Offshore Wind Farms and Isolated Oil and Gas Platforms. Zenodo (2021). DOI [10.5281/zenodo.6095756](https://doi.org/10.5281/zenodo.6095756). Cited on page/s 23, 26, 27, 28, 35, 37.
- [12] P. Kundur, N. J. Balu, and M. G. Lauby. Power System Stability and Control. EPRI Power System Engineering Series. McGraw-Hill New York, USA (1994). ISBN 978-0-07-035958-1. Cited on page/s 24, 25.
- [13] Jan Machowski. Power system dynamics: Stability and control. Wiley Chichester, U.K. 2nd edition (2008). ISBN 978-1-119-96505-3. Cited on page/s 24, 29.
- [14] IEC. Wind turbines - part 27-1: Electrical simulation models. IEC Standard 61400-27-1:2015 International Electrotechnical Commission Geneva, Switzerland (2015). URL <https://webstore.iec.ch/publication/21811>. Cited on page/s 25, 35.
- [15] Siemens. The top-performing wind converter Trusted technology for maximum power yield – SINAMICS W180. Brochure PDLD-B10099-00-7600 Siemens AG Munich, Germany (2017). URL https://assets.new.siemens.com/siemens/assets/api/uuid:26ef63b7cae9657fae9e98618212ba874f3fd729/455_170680_ws_sinamicsw180us.pdf. Cited on page/s 25.
- [16] ABB. ACS880-77LC/-87LC/-87CC wind turbine converters. System Description 3AXD50000022022 Rev C ABB Zurich, Switzerland (2020). URL <https://search.abb.com/library/Download.aspx?DocumentID=3AXD50000022022&LanguageCode=en&DocumentPartId=1&Action=Launch>. Cited on page/s 25.
- [17] Federico Milano, Florian Dörfler, Gabriela Hug, David J. Hill, and Gregor Verbic. Foundations and Challenges of Low-Inertia Systems (Invited Paper). pages 1–25 Dublin, Ireland (2018). IEEE. DOI [10.23919/PSCC.2018.8450880](https://doi.org/10.23919/PSCC.2018.8450880). Cited on page/s 25, 26.
- [18] Nikos Hatziargyriou, et al. Definition and Classification of Power System Stability – Revisited & Extended. *IEEE Transactions on Power Systems* **36** (4), 3271–3281 (2021). ISSN 1558-0679. doi: [10.1109/TPWRS.2020.3041774](https://doi.org/10.1109/TPWRS.2020.3041774). URL <https://doi.org/10.1109/TPWRS.2020.3041774>. Cited on page/s 26, 29, 30.
- [19] Swissgrid. Current grid key figures - Frequency (2022). URL <https://www.swissgrid.ch/en/home/operation/grid-data/current-data.html>. Cited on page/s 26.
- [20] Sina Y. Caliskan and Paulo Tabuada. Uses and abuses of the swing equation model. In *2015 54th IEEE Conference on Decision and Control (CDC)* pages 6662–6667 Osaka, Japan (2015). IEEE. ISBN 978-1-4799-7886-1. DOI [10.1109/CDC.2015.7403268](https://doi.org/10.1109/CDC.2015.7403268). Cited on page/s 27.
- [21] IEEE Task Force on Turbine-Governor Modeling. Dynamic Models for Turbine-Governors in Power System Studies. Report PES-TR1 IEEE Power & Energy Society (2013). URL https://site.ieee.org/fw-pes/files/2013/01/PES_TR1.pdf. Cited on page/s 27, 29.
- [22] ENTSO-E. Fast Frequency Reserve – Solution to the Nordic inertia challenge. Report FFR ENTSO-E / Danske Energinet Denmark (2019). URL <https://energinet.dk/-/media/762E225FFB894177A37B75A7CF4C894C.PDF>. Cited on page/s 27, 29.
- [23] Katsuhiko Ogata. Modern control engineering. Prentice-Hall Boston, USA 5th edition (2010). ISBN 978-0-13-615673-4. Cited on page/s 29.
- [24] T J Larsen and T D Hanson. A method to avoid negative damped low frequent tower vibrations for a floating, pitch controlled wind turbine. *Journal of Physics: Conference Series* **75**, 012073 (2007). ISSN 1742-6596. URL <https://iopscience.iop.org/article/10.1088/1742-6596/75/1/012073>. Cited on page/s 29.

- [25] Reza Hemmati and Hedayat Saboori. Emergence of hybrid energy storage systems in renewable energy and transport applications – A review. *Renewable and Sustainable Energy Reviews* **65**, 11–23 (2016). ISSN 1364-0321. URL <https://www.sciencedirect.com/science/article/pii/S1364032116302374>. Cited on page/s 30.
- [26] Hongyu Zhang, Asgeir Tomasdard, Brage Rugstad Knudsen, Harald G. Svendsen, Steffen J. Bakker, and Ignacio E. Grossmann. Modelling and analysis of offshore energy hubs. *Cornell University arXiv:2110.05868 [cs, eess, math]* (2021). URL <https://arxiv.org/abs/2110.05868>. Cited on page/s 31.
- [27] Ned Mohan, Tore M. Undeland, and William P. Robbins. Power electronics: Converters, applications, and design. Wiley New York, USA 2nd ed edition (1995). ISBN 978-0-471-58408-7. Cited on page/s 32.
- [28] Federico Martin Ibanez, Fernando Martin, Joshua Eletu, and Jose Martin Echeverria. Input Voltage Feedforward Control Technique for DC/DC Converters to Avoid Instability in DC Grids. *IEEE Journal of Emerging and Selected Topics in Power Electronics* **9** (5), 6099–6112 (2021). ISSN 2168-6777, 2168-6785. doi: \href{https://doi.org/10.1109/JESTPE.2021.3058850}{https://doi.org/10.1109/JESTPE.2021.3058850}. Cited on page/s 34.
- [29] Henrik Brantsæter, Lukasz Kocwiak, Elisabetta Tedeschi, and Atle Rygg Årdal. Passive Filter Design and Offshore Wind Turbine Modelling for System Level Harmonic Studies. *Energy Procedia* **80**, 401–410 (2015). ISSN 1876-6102. URL <https://ntuopen.ntnu.no/ntnu-xmlui/handle/11250/2381992>. Cited on page/s 34.
- [30] Saeed Golestan, Josep M. Guerrero, and Juan C. Vasquez. Three-Phase PLLs: A Review of Recent Advances. *IEEE Transactions on Power Electronics* **32** (3), 1894–1907 (2017). ISSN 1941-0107. URL <https://doi.org/10.1109/TPEL.2016.2565642>. Cited on page/s 34.
- [31] C. J. O'Rourke, M. M. Qasim, M. R. Overlin, and J. L. Kirtley. A Geometric Interpretation of Reference Frames and Transformations: Dq0, Clarke, and Park. *IEEE Transactions on Energy Conversion* **34** (4), 2070–2083 (2019). ISSN 1558-0059. URL <https://doi.org/10.1109/TEC.2019.2941175>. Cited on page/s 34.
- [32] F. Blaabjerg, R. Teodorescu, M. Liserre, and A.V. Timbus. Overview of Control and Grid Synchronization for Distributed Power Generation Systems. *IEEE Transactions on Industrial Electronics* **53** (5), 1398–1409 (2006). ISSN 1557-9948. URL <https://doi.org/10.1109/TIE.2006.881997>. Cited on page/s 34.
- [33] Daniel dos Santos Mota, Erick Fernando Alves, and Elisabetta Tedeschi. Dual Sequence Controller with Delayed Signal Cancellation in the Rotating Reference Frame. In *IEEE 22nd Workshop on Control and Modelling of Power Electronics* pages 1–8 Cartagena, Colombia (2021). DOI [10.1109/COMPEL52922.2021.9646023](https://doi.org/10.1109/COMPEL52922.2021.9646023). Cited on page/s 35.
- [34] DIgSILENT. PowerFactory 2020, Technical Reference. Overview PF2020 DIgSILENT GmbH (2021). URL <https://www.digsilent.de>. Cited on page/s 35, 38.
- [35] Seddik Bacha, Iulian Munteanu, and Antoneta Iuliana Bratcu. Power Electronic Converters Modelling and Control with Case Studies. Advanced Textbooks in Control and Signal Processing. Springer London, England (2013). ISBN 978-1-4471-5478-5. URL <https://link.springer.com/book/10.1007/978-1-4471-5478-5>. Cited on page/s 35.
- [36] Erick Alves, Santiago Sanchez, Danilo Brandao, and Elisabetta Tedeschi. Smart Load Management with Energy Storage for Power Quality Enhancement in Wind-Powered Oil and Gas Applications. *Energies* **12** (15), 2985 (2019). ISSN 1996-1073. doi: [10.3390/en12152985](https://doi.org/10.3390/en12152985). Cited on page/s 36.

CHAPTER 5

Sizing of Hybrid Energy Storage Systems for Inertial and Primary Frequency Control

Erick Fernando Alves^{1,*}, Daniel dos Santos Mota^{1,*}, Elisabetta Tedeschi^{1,2}

*These authors contributed equally to this study.

First published in: *Frontiers in Energy Research*, vol. 9, 2021.

DOI: [10.3389/fenrg.2021.649200](https://doi.org/10.3389/fenrg.2021.649200)



Open Access This article is licensed under a Creative Commons Attribution 4.0 International License. It means that unrestricted use, sharing, adaptation, distribution, and reproduction in any medium or format are allowed, as long as the original author(s) and the source are appropriately credited, a link to the Creative Commons license is provided, and any changes made are indicated. To view a copy of this license, please visit <http://creativecommons.org/licenses/by/4.0/>.

© Alves, Mota, Tedeschi, 2021.

Contributions

EA and ET conceptualized the idea. EA and DM developed the software and performed the formal analysis and investigation. EA developed the methodology, validated the results, curated the data, wrote the original draft, and produced figures and tables. ET acquired the funding, supervised and administrated the project. DM and ET reviewed and edited this paper.

¹[NTNU](#), Trondheim, Norway. ²University of Trento, Trento, Italy.

ABSTRACT

The exponential rise of renewable energy sources and microgrids brings about the challenge of guaranteeing frequency stability in low-inertia grids through the use of energy storage systems. This paper reviews the frequency response of ac power systems, highlighting its different time scales and control actions. Moreover, it pinpoints main distinctions among high-inertia interconnected systems relying on synchronous machines and low-inertia systems with high penetration of converter-interfaced generation. Grounded on these concepts and with a set of assumptions, it derives algebraic equations to rate an energy storage system providing inertial and primary control. The equations rely on parameters typically defined by system operators, industry standards or network codes, are independent from the energy storage technology and robust to system nonlinearities. Using these results, the authors provide a step-by-step procedure to size the main components of a converter-interfaced hybrid energy storage system. Finally, a case study of a wind-powered oil and gas platform in the North Sea demonstrates with numerical examples how the proposed methodology: 1) can be applied in a practical problem; 2) allows the system designer to take advantage of different technologies and set specific requirements for each storage device and converter according to the type of frequency control provided.

5.1 INTRODUCTION

Planning, design and operation of [AC power systems \(ACPSs\)](#) are becoming more involved. For instance, conversion from primary sources and storage is performed using not only [synchronous machines \(SMs\)](#) but also [Converter-interfaced generators \(CIGs\)](#). Moreover, groups of interconnected loads and distributed energy resources, also known as [microgrids \(MGs\)](#) [1, 2], can form islands and operate independently from the interconnected power system.

From this perspective, [ESSs](#) can help to balance demand and supply, and control frequency, voltage and power flows in isolated power systems or [MGs](#) operating in islanded mode. These features increase not only the stability and security of the system, but also its efficiency and assets utilization [3, 4]. Nonetheless, these desired features can be achieved only with the proper sizing of [ESSs](#).

In particular, sizing the components of a converter-interfaced [ESS](#) is one of the main challenges in [MGs](#) and large [ACPSs](#) with high penetration of [CIGs](#). The main reason being the trade-off among key technical characteristics in

storage solutions, where no single technology stands out [5–7]. For instance, ultracapacitors and flywheels are appropriate for inertia simulation as they offer high power density and efficiency. However, their low energy density and high cost per kWh make them unsuitable for primary and secondary control. Further examples are the several types of batteries and fuel cell technologies. These solutions are well-suited for secondary control because they offer reasonable power and energy densities and cost per kWh. Nevertheless, their life time can be extremely reduced if applied in inertia simulation and primary control due to the abrupt current changes and number of charge and discharge cycles required. In summary, there is no one-size-fits-all technology for ESSs, so hybrid solutions are currently becoming the preferred choice not only in transportation, but also in ACPSs applications [8].

When considering all that, sizing an ESS to provide inertial and primary frequency control becomes an intricate task. Many researchers have been devoting time to untangle this problem. For MGs, Aghamohammadi and Abdolahinia [9] optimally size a battery ESS for primary frequency control considering overloading characteristics and limitation of the state of charge. For that, the authors propose an iterative procedure based on time-domain simulations that considers the battery permissible overload coefficient and duration. In [10, 11], the authors present a control-based approach applying the Hamiltonian Surface Shaping and Power Flow Control to size the ESS and to address how communication and controller bandwidth can affect the sizing and filtering requirements. For large ACPSs with high penetration of CIGs, Knap *et al.* [12] introduce a methodology to size ESSs for the provision of inertial response and primary frequency regulation. In this work, a linearized version of the swing equation is applied to determine the ESS rated power and energy capacity and it is shown that this converter-interfaced system can achieve similar performance to a conventional peak power plant. In [13], the authors focus on primary control and propose a more broad three-stage methodology, that evaluates not only the battery dynamic response and provision of frequency reserves, but also its lifetime and economic assessment.

From a system operator or developer point of view, the main limitations in these previous works are: 1) the extensive use of time-domain simulations to support their sizing methodology; 2) the assumption that the required ESS technology and model parameters are well-known beforehand; 3) the linearization of the swing equation to study the frequency control problem.

For the first limitation, it must be noted that defining the rated active power and energy capacity of an ESS is a multi-stage process involving a technoeconomical evaluation as emphasized by Sandelic *et al.* [13], Riboldi *et al.* [14]. Hence, the analysis of the ESS dynamic response is only one step of the problem, which requires integration into a broad optimization involving several

time scales. Nonetheless, an inspection of recent literature reviews on ac MG planning [15, 16] reveals that conditions for frequency stability are largely overlooked in the problem formulation and most optimization algorithms consider that matching power demand with generation is the only required dynamic constraint, without imposing minimum requirements on system damping or frequency reserves. This is typically justified by the argument that frequency stability analysis in ACPS requires computationally demanding simulation models that can turn the optimization into an intractable problem. Therefore, ESS sizing models should be efficient and, if possible, algebraic to be directly incorporated as constraints in larger optimization algorithms.

For the second limitation, system operators of ACPSs are fundamentally interested in specifying the minimum equivalent inertia, damping, deadband and time delay of equipment supplying inertial response and primary frequency regulation [17]. Indeed, in many regulated ACPS, such as transmission and distribution grids, system operators avoid requiring specific technologies and prefer to limit specifications to functionalities to be provided [18]. For instance, Chang *et al.* [19] solved the unit commitment problem for an islanded ACPS with high penetration of CIGs including constraints on frequency reserves using mixed-integer linear programming. For that, the authors determined the minimum system damping empirically relying on the load-frequency sensitivity index. Moreover, frequency stability constraints have also been proposed in planning and operation studies of large ACPSs, such as optimal power flow problems, by Wen *et al.* [20], Abhyankar *et al.* [21], Geng *et al.* [22], Nguyen *et al.* [23].

For the third limitation, it is reported in the literature that the linearized swing equation may underestimate frequency variations during transients [24] and, as consequence, the required damping of an ACPS [25]. Accordingly, a certain level of robustness must be considered when sizing an ESS to account for nonlinear effects, especially in low-inertia systems.

Considering this context, the contributions of this work are threefold: 1) it offers an updated literature review of the frequency response of ACPSs, highlighting the different time scales of the frequency control problem and the main distinctions among traditional systems, large systems with high penetration of CIG and MGs; 2) based on the type of frequency control being supplied by a converter-interfaced ESS, it proposes an algebraic method to calculate the rated energy of its ESDs and the rated power of its converters. The proposed method is robust to system nonlinearities and based on parameters typically defined by system operators, industry standards or network codes; 3) it provides a step-by-step systematic procedure to size the main components of hybrid ESSs independently from the technologies used in the ESDs and requiring knowledge of few ACPS parameters.

5.2 MATERIALS AND METHODS

5.2.1 Frequency Control in AC power systems

The principles of frequency control in ACPSs can be understood by analysing a simplified model of a flywheel spinning at a rated angular frequency ω_s [rad s⁻¹]. The rotating masses of all synchronous generators and motors connected to the ACPS are represented by an equivalent moment of inertia J . On the driving end of the shaft, all generators deliver energy to the flywheel via a torque T_G , whereas the consumers remove energy through T_L . The natural and controlled damping of the system are represented by a coefficient B .

Equation (5.1) is obtained by applying Newton's second law of motion to this simplified flywheel model. The moment of inertia $J(t, \omega)$ is in [kg m²], the damping coefficient $B(t, \omega)$ is in [N m s rad⁻¹], the average (center of inertia) angular speed ω is in [rad s⁻¹], and the equivalent torques $T_G(t, \omega)$ and $T_L(t, \omega)$ are the in [N m].

$$J(t, \omega)\dot{\omega} = T_G(t, \omega) - T_L(t, \omega) - B(t, \omega)(\omega - \omega_s) \quad (5.1)$$

The representation of an ACPS as an equivalent rotating mass and equation (5.1), also referred as the Swing Equation, was already applied in the inter-war period by Doherty and Nickle [26] and reported in many classical power systems books such as Concordia [27], Grainger and Stevenson [28], Kimbark [29], Kundur *et al.* [30], Machowski [31]. Moreover, limitations of this model have been discussed in the last 40 years [24, 32]. Mainly, a proper transient analysis of an ACPS must include voltage dynamics, which requires very detailed models and knowledge of the network topology and characteristics, time delays of controllers and so on [33]. This level of detail is often not available during the planning phases of ACPSs and the Swing Equation model is still today an useful concept to evaluate the frequency response in the early design of a project [34–36] or in operation planning [19, 20, 37].

It is convenient to normalize and express the balance of torques in equation (5.1) as a balance of power. The normalization starts by dividing equation (5.1) by the rated apparent power of the system S_b [VA], whereas the balance of power requires a multiplication by the angular frequency ω , as shown in equation (5.2).

$$\frac{\omega}{S_b} J(t, \omega)\dot{\omega} = \frac{P_G(t, \omega)}{S_b} - \frac{P_L(t, \omega)}{S_b} - \frac{\omega}{S_b} B(t, \omega)(\omega - \omega_s). \quad (5.2)$$

[Equation \(5.2\)](#) contains two variables that are not yet normalized, namely ω and $\dot{\omega}$. The normalization can be performed by introducing an equivalent inertia constant $M(t, \omega) = \frac{J(t, \omega)\omega_s^2}{S_b}$ in [s] and a damping coefficient $D(t, \omega) = \frac{B(t, \omega)\omega_s^2}{S_b}$ in [pu]. Furthermore, one can obtain a state-space representation by defining the state $x = \frac{\omega}{\omega_s}$, as in [equation \(5.3\)](#), where $u(t, x)$ and $w(t, x)$ are the normalized power generation $\frac{P_G}{S_b}$ and power consumption $\frac{P_L}{S_b}$ from [equation \(5.2\)](#).

$$xM(t, x)\dot{x} = u(t, x) - w(t, x) - xD(t, x)(x - 1) \quad (5.3)$$

The dynamics from [equation \(5.3\)](#) is better understood when rearranging it and defining a state centered at the rated angular frequency, i.e. $\tilde{x} = x - 1$, which results in [equation \(5.4\)](#).

$$\dot{\tilde{x}} = -\frac{D(t, \tilde{x})}{M(t, \tilde{x})}\tilde{x} + \frac{u(t, \tilde{x}) - w(t, \tilde{x})}{(\tilde{x} + 1)M(t, \tilde{x})} \quad (5.4)$$

When inspecting [equation \(5.4\)](#) and assuming that $D(t, \tilde{x}) > 0$ and $M(t, \tilde{x}) > 0$, it becomes clear that $\tilde{x} = 0$ (i.e. $\omega = \omega_s$) is an equilibrium point of the system whenever there is balance between power generation and consumption (i.e. $u(t, \tilde{x}) = w(t, \tilde{x})$). Moreover, the dynamics of \tilde{x} are governed by three terms: $M(t, \tilde{x})$, $D(t, \tilde{x})$, and $u(t, \tilde{x}) - w(t, \tilde{x})$. Each of them is affected by the strategies for frequency control in [ACPSs](#), namely: inertial, primary and secondary control.

In traditional interconnected [ACPSs](#) with high inertia ($M > 10$ s) and centralized power generation and dispatch, these control strategies are implemented as following:

- **Inertial control** is physically embedded in [SMs](#), because their rotors are flywheels providing the inertial effect required to oppose frequency variations. In other words, $M(t, \tilde{x})$ increases whenever a [SM](#) is directly connected to the power system. Conversely, it reduces if a [SM](#) is disconnected. The inertial control is offered by both generators and motors with a practically instantaneous reaction time, as the rotor of a [SM](#) is electromagnetically coupled to the [ACPS](#).
- **Primary control** is offered by generators or loads sensing frequency deviations from the rated value and automatically adjusting their active power accordingly. This control scheme is known as frequency-droop control [1] or [frequency sensitivity mode \(FSM\)](#) [38]. The slope of the [FSM](#) curve (solid black line) shown in [figure 5.1](#) represents the value of $D(t, \tilde{x})$. Note that, for a specific generator, the damping coefficient

$D(t, \tilde{x})$ is equal to zero within the dead band (solid orange line), if the power reaches the maximum level (solid teal line), or if it reaches a minimum level (solid violet line). The primary control reaction time is in the order of seconds, and it is directly connected to the actuation delay of turbines and their governors [18, 39]. In Europe, the set of generators and loads offering primary control is called **frequency containment reserves (FCR)** [40].

- **Secondary control** is provided by a central controller typically in a dispatch center and requires communication infrastructure. When a frequency deviation is detected in the system and after a pre-defined time delay, this controller remotely changes the active power setpoint of generators or loads to match the power demand, i.e. make $u(t, \tilde{x}) = w(t, \tilde{x})$. This process can be done by an automatic controller or manually by an operator. In general, the secondary control reaction time is in the order of minutes. In Europe, the set of generators and loads offering secondary control is called **fast restoration reserves (FRR)** [40].

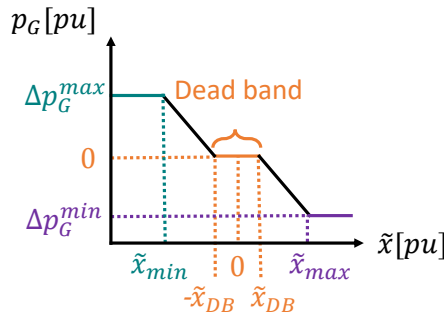


FIGURE 5.1 | Frequency-droop, the main mechanism for primary frequency control.

In MGs and ACPSs with high penetration of CIGs, where inertia may be low ($M < 5$ s) and power generation is typically more distributed, the alternatives are the following:

- **Inertial control** is usually implemented in grid-forming units [41] using virtual inertia emulation [42, 43]. In this case, the value of $M(t, \tilde{x})$ is a parameter of the inertia emulator. The inertial control reaction time is not instantaneous and will depend heavily on the frequency measurement algorithm and filtering techniques applied [44]. Furthermore, it may consume part of the FCR when activated, as grid-forming units typically provide primary control [18]. In Europe, the set of CIGs offering inertial control is called **fast frequency reserves (FFR)** [18].

- **Primary control** is provided by grid-forming and grid-following units using the frequency-droop mechanism [41] akin to interconnected ACPSs. However, the reaction time is a fraction of a second, because the bandwidth of a CIG controller is at least one order of magnitude larger than traditional turbine governors and motor drives [43].
- **Secondary control** is provided by grid-following units [41]. Considering that a MG may contain a large number of small units, manual operation can become unfeasible and automatic dispatch coordinated by a central unit, such as a MG controller, may be necessary. The reaction time of secondary control is typically faster than in traditional ACPSs, from a couple of minutes in a large system with high penetration of CIGs [18], to a couple of seconds in a MG [45, 46].

The dynamic behavior of the average system frequency after an active power imbalance is similar for high- and low-inertia ACPSs, despite their differences, and can be divided in three periods [39]:

1. **Arrest:** it starts immediately after the imbalance occurs. If there is lack of generation ($u < w$), the frequency will decrease until it reaches its minimum value (nadir). If there is excess of generation ($u > w$), the frequency will increase until it reaches its maximum value (zenith). At first, most of the balancing power P_a required to stabilize the system is provided by the inertial control. Then, primary controllers gradually take over P_a as the frequency deviation \tilde{x} increases. Important metrics of this period are the RoCoF and the total time required to reach the nadir/zenith t_a .
2. **Rebound:** it starts immediately after the nadir/zenith is reached. During this period, the primary control is fully activated, and will bring the frequency to a new equilibrium condition. This settling point is below the rated value when $u < w$ and above the rated value when $u > w$. In general, the balancing power P_a is provided only by the primary control. However, the inertial control may work against the frequency restoration, as the sign of the frequency derivative can be inverted. In SMs, this negative effect is counteracted by adding damper windings in the rotor [30]. The same result can be obtained in CIGs by applying adaptive virtual inertia emulation [43]. One of the important metrics of this period is the settling time t_b , i.e. the total time required to reach the settling point.
3. **Recovery:** it starts after the settling point is reached and secondary control is activated. Primary control does not have the capacity to restore

the frequency to its rated value after an imbalance. Hence, the system frequency remains at the settling point until the secondary control is activated. In traditional high-inertia systems, the frequency is often restored to its rated value slowly due to practical limitations and to avoid counteraction of inertial control. Although, when secondary control is fast, the rebound period can be considerably shortened and even eliminated (i.e. $t_a = t_b$ and $\tilde{x}(t_a) = \tilde{x}(t_b)$). In the recovery period, the primary control is still active, but the secondary control gradually takes over the balancing power P_a , until the balance $u(t) = w(t)$ is restored. One of the important metrics of this period is the recovery time t_c , i.e. the total time required to reestablish the rated frequency.

Figure 5.2 illustrates the three control actions and the three periods following a perturbation caused by lack of generation. Even though the three periods following an active power imbalance are similar for both high- and low-inertia ACPSs, their energy management strategies for frequency control may differ considerably.

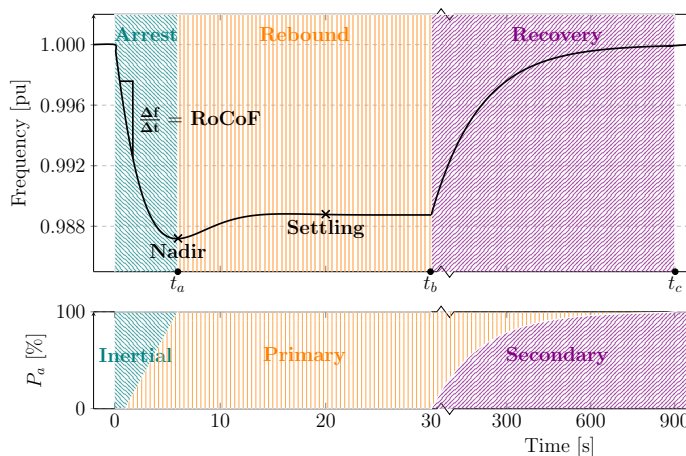


FIGURE 5.2 | The three periods of frequency variation (arrest, rebound and recovery) and the control actions (inertial, primary and secondary) following a perturbation caused by lack of generation.

During the arrest period, a high-inertia system relies on the rotating masses of SMs as its main energy buffer. In other words, kinetic energy is drained from or stored into the rotor of SMs limiting the RoCoF and bounding the nadir or zenith. This energy exchange happens “automatically” without any dedicated power or control equipment, because the rotor of a SM is electromagnetically coupled to its stator and hence the ACPS. For low-inertia systems, on the other hand, the energy buffer formed by rotating masses may not be large enough to guarantee the stable operation after a large power imbalance.

In such cases, **CIGs** must participate as **FFR** and support the system by either supplying or absorbing energy during the arrest period. The dc-link capacitor of **CIGs** could be considered an obvious candidate for storing the additional **FFR** energy. However, for power systems applications in the MW range, the required capacitance or voltage values become so high, that this solution becomes unfeasible with current technology. Therefore, an additional **ESS** must be sized specifically for this purpose [47].

As mentioned earlier, primary reserves are responsible for bringing the frequency from its extreme values to an acceptable settling point during the rebound phase. In traditional high-inertia systems, some generators are selected to operate with spare up- and down power capacity and form the **FCR**. Commonly, those are dispatchable and fast-acting generating units, such as those in gas and hydro plants, and have a large energy buffer in the form of chemical or potential energy. However, low-inertia systems may not have the necessary power or energy reserves for primary frequency control. This is because **CIGs** are typically connected to renewable energy sources operating in maximum power point tracking. Those have no available power up capacity and have limited down capacity. Moreover, as is the case with **FFR**, the dc-link capacitor of **CIGs** is not designed to store the energy amount required by **FCR**. In summary, an **ESS** must be sized to provide the energy and power capacity demanded by **FCR** in low-inertia systems.

The main goal of this paper is, thus, establishing a procedure for sizing an **ESS** power and energy capacities according to its expected use (inertial control or **FFR**, primary control or **FCR**, or both) based on parameters that are:

1. typically defined by system operators, industry standards or network codes;
2. independent from the energy storage technology;
3. robust to system nonlinearities.

It is worth mentioning, though, that sizing the **ESS** for secondary control or **FRR** is outside the scope of this paper. Also, the procedure presented in the following sections assumes that a thorough stability analysis was carried out beforehand in the **ACPS** where the **ESS** will perform frequency control. This stability analysis must include measurement and actuation time delays, nonlinearities and, as result, select or at least restrict the possible values of M and D . This type of assessment is typically a task of the Transmission System Operator in large and regulated **ACPSs**. However, this responsibility might be debatable in smaller and unregulated systems such as **MGs**. A detailed discussion about this topic is outside the scope of this paper, but it is worth highlighting that if $\epsilon_{max} < \frac{M}{D}$, where ϵ_{max} is the maximum time delay of all active power sources

in an ACPS, then this system can be frequency stable in the presence of time delays. For details and proofs, refer to appendix B of [25] and [33]. Though, this single criterion does not guarantee global stability of the ACPS, and other aspects such as voltage, load-angle and phase-locked loop stability must be carefully investigated.

Additional information about frequency control in high-inertia ACPSs is discussed by Kundur *et al.* [30], Machowski [31], Sauer *et al.* [48]. The main characteristics and challenges of low-inertia systems can be reviewed in Eto *et al.* [39], Vandoorn *et al.* [41], Fang *et al.* [43], dos Santos Alonso *et al.* [45], Milano *et al.* [47], Brandao *et al.* [49].

Lastly, tertiary control and generator rescheduling are further alternatives for frequency control. They are long-term, slow-response strategies based on communication infrastructure and/or electricity markets that are outside the scope of this paper. A throughout description of the European approach to these strategies is given by EU Comission Regulation [50], while the North-American approach is summarized by Eto *et al.* [39].

5.2.2 Sizing of the Converter-Interfaced ESS Elements

This section includes the proposed procedure to size the energy capacity of the ESD and the rated power of an **energy storage (ES)** converter providing inertial or primary frequency control. Based on this initial estimation and selected references from the literature, it describes a methodology to dimension the remaining **ESS** power unit components.

Figure 5.3 presents an overview of the main elements of a converter-interfaced ESS, namely the power and control units. In general terms, the power unit can be further subdivided in: the ESD and its converter, the dc link, the grid converter and its **inductive-capacitive (LC) filter**.

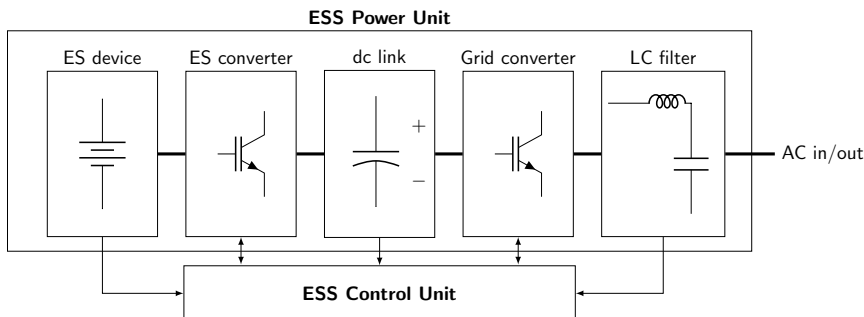


FIGURE 5.3 | Elements of a converter-interfaced ESS.

The ES Device and its Converter

This section proposes a method to calculate the **ES** converter rated power P_{es} [W] and the **ESD** storage capacity E_{es} [J] according to the type of frequency control being provided. These variables are chosen as the starting point of the sizing procedure because they are the key drivers for the **ESS** equipment cost [51].

The calculation of P_{es} , E_{es} starts by categorizing the terms of [equation \(5.3\)](#) in three sub-components according to the type of frequency control required to keep the power balance in the **ACPS**, as in [equation \(5.5\)](#), where p_{iner} , p_{pri} and p_{sec} are respectively the amount of power in pu required for inertial, primary and secondary control.

$$\underbrace{(\tilde{x} + 1)M(t, \tilde{x})\dot{\tilde{x}}}_{p_{iner}} = \underbrace{u(t, \tilde{x}) - w(t, \tilde{x})}_{-p_{sec}} - \underbrace{(\tilde{x} + 1)D(t, \tilde{x})\tilde{x}}_{p_{pri}} \quad (5.5)$$

Using this framework, algebraic expressions for P_{es} and E_{es} can be obtained with the following assumptions.

Assumption 1 — Constant inertia and damping during the interval $0 \leq t < t_c$:
 $M(t, \tilde{x})$ and $D(t, \tilde{x})$ are constant throughout the power imbalance.

Assumption 2 — Primary control linearly takes over the inertial control during the interval $0 \leq t < t_a$: during the arrest period, the primary control linearly takes over the balancing power from the inertial control and the contributions of the secondary control are minimal compared to the overall balancing power required. Possible time delays of controllers are ignored for the energy calculations. In addition, the **RoCoF** upper bound during this period can be approximated by $\dot{\tilde{x}}_{0a} = \frac{\tilde{x}(t_a)}{t_a}$.

Assumption 3 — Frequency nadir or zenith are bounded: the frequency nadir and zenith are enforced either by a proper combination of inertia, damping and primary control delays or the actuation of extreme control actions such as automatic generation curtailment or load shedding [39, 40].

In this case, the normalized angular speed error $\tilde{x}(t_a)$ is upper and lower bounded by \tilde{x}_{tr}^{max} and \tilde{x}_{tr}^{min} respectively. In other words, if $u < w$, then the frequency nadir is greater than \tilde{x}_{tr}^{min} . Conversely, if $u > w$, then the frequency zenith is lower than \tilde{x}_{tr}^{max} . Hence, if the transient frequency limit is defined as $r_{tr} = \max(\tilde{x}_{tr}^{max}, \tilde{x}_{tr}^{min})$, then $\|\tilde{x}(t_a)\| \leq r_{tr}$.

Assumption 4 — Only primary control is active during the interval $t_a \leq t < t_b$: during the rebound period, only the primary control is active and the

contributions of the inertial control and secondary control are minimal compared to the overall balancing power required. Moreover, the RoCoF lower bound during this period can be approximated by $\tilde{x}_{ab} = \frac{\tilde{x}(t_b) - \tilde{x}(t_a)}{t_b - t_a}$.

Assumption 5 — *The settling point is bounded:* after a power imbalance, the primary control is capable of driving the angular frequency back from the frequency zenith or nadir to within an acceptable steady-state frequency deviation r_{ss} .

The normalized angular speed error at the settling point $\tilde{x}(t_b)$ is upper and lower bounded by \tilde{x}_{ss}^{max} and \tilde{x}_{ss}^{min} respectively. In other words, if $u < w$, then $\tilde{x}(t_b) > \tilde{x}_{ss}^{min}$. Conversely, if $u > w$, then $\tilde{x}(t_b) < \tilde{x}_{ss}^{max}$. Hence, if the steady-state frequency limit is defined as $r_{ss} = \max(\tilde{x}_{ss}^{max}, \tilde{x}_{ss}^{min})$, then $\|\tilde{x}(t_b)\| \leq r_{ss}$.

Assumption 6 — *Secondary control linearly takes over during the interval $t_b \leq t < t_c$:* during the recovery period, the secondary control linearly takes over the balancing power from the primary control and the contributions of the inertial control are minimal. In addition, the RoCoF lower bound during this period can be approximated by $\dot{x}_{bc} = \frac{x(t_c) - x(t_b)}{t_c - t_b}$.

Using [assumption 2](#), P_{es} can be defined as the maximum between the components p_{iner} and p_{pri} in [equation \(5.5\)](#), as presented in [equation \(5.6\)](#). Using [assumption 3](#), the bounds for p_{iner} are given by [equation \(5.7\)](#). However, obtaining a bound to p_{pri} requires an involved mathematical analysis, which is described in [25], and [equation \(5.8\)](#) presents only the main result of this analysis.

$$P_{es} = S_b \max(p_{es}^{iner}, p_{es}^{pri}) \quad (5.6)$$

$$P_{es}^{iner} = S_b \|(\tilde{x} + 1)M\dot{\tilde{x}}\| \leq S_b(1 + r_{tr})M\|\dot{\tilde{x}}\| \quad (5.7)$$

$$P_{es}^{pri} \leq S_b D r_{ss} (1 - r_{tr}) \quad (5.8)$$

The energy required by the inertial control E_{iner} and the primary control E_{pri} can be calculated as the time integral of their power components defined in [equation \(5.2\)](#), as seen in [equations \(5.9\)](#) and [\(5.10\)](#). To solve these integrals analytically, it is necessary to:

1. remember that $\dot{\tilde{x}} = \dot{x} = \frac{dx}{dt}$;
2. use [assumptions 2, 4](#) and [6](#).

In [equations \(5.10\)](#) to [\(5.13\)](#), the terms E_{pri}^{arr} , E_{pri}^{reb} and E_{pri}^{rec} are respectively the energy required by the primary control during the arrest, rebound and recovery periods.

$$\begin{aligned} E_{iner} &= S_b \int_0^{t_a} (\tilde{x} + 1) M \dot{\tilde{x}} dt \\ &= S_b \int_{\tilde{x}(0)}^{\tilde{x}(t_a)} (\tilde{x} + 1) M d\tilde{x} \\ &= S_b M \left[\frac{\tilde{x}^2(t_a)}{2} + \tilde{x}(t_a) \right] \end{aligned} \quad (5.9)$$

$$E_{pri} = \underbrace{\frac{S_b}{2} \int_0^{t_a} (\tilde{x} + 1) D \tilde{x} dt}_{E_{pri}^{arr}} + \underbrace{S_b \int_{t_a}^{t_b} (\tilde{x} + 1) D \tilde{x} dt}_{E_{pri}^{reb}} + \underbrace{\frac{S_b}{2} \int_{t_b}^{t_c} (\tilde{x} + 1) D \tilde{x} dt}_{E_{pri}^{rec}} \quad (5.10)$$

$$\begin{aligned} E_{pri}^{arr} &= \frac{S_b D}{2 \dot{\tilde{x}}_{0a}} \left(\frac{\tilde{x}^3}{3} + \frac{\tilde{x}^2}{2} \right) \Big|_0^{t_a} \\ &= \frac{S_b D}{2} (t_a - t_0) \left[\frac{\tilde{x}^2(t_a)}{3} + \frac{\tilde{x}(t_a)}{2} \right] \end{aligned} \quad (5.11)$$

$$\begin{aligned} E_{pri}^{reb} &= \frac{S_b D}{\dot{\tilde{x}}_{ab}} \left(\frac{\tilde{x}^3}{3} + \frac{\tilde{x}^2}{2} \right) \Big|_{t_a}^{t_b} \\ &= S_b D \left[\frac{t_b - t_a}{\tilde{x}(t_b) - \tilde{x}(t_a)} \right] \left[\frac{\tilde{x}^3(t_b) - \tilde{x}^3(t_a)}{3} + \frac{\tilde{x}^2(t_b) - \tilde{x}^2(t_a)}{2} \right] \end{aligned} \quad (5.12)$$

$$\begin{aligned} E_{pri}^{rec} &= \frac{S_b D}{2 \dot{\tilde{x}}_{bc}} \left(\frac{\tilde{x}^3}{3} + \frac{\tilde{x}^2}{2} \right) \Big|_{t_b}^{t_c} \\ &= \frac{S_b D}{2} (t_c - t_b) \left[\frac{\tilde{x}^2(t_b)}{3} + \frac{\tilde{x}(t_b)}{2} \right] \end{aligned} \quad (5.13)$$

To define the worst-case value for E_{es} , the bounds defined in [assumptions 3](#) and [5](#) can be applied in [equations \(5.9\)](#) and [\(5.11\)](#) to [\(5.13\)](#), leading to [equations \(5.14\)](#) to [\(5.19\)](#).

$$E_{es} \geq E_{es}^{iner} + E_{es}^{pri} \quad (5.14)$$

$$E_{es}^{iner} \leq \frac{S_b M}{2} r_{tr} (r_{tr} + 2) \quad (5.15)$$

$$E_{es}^{pri} \leq E_{pri}^{arr} + E_{pri}^{reb} + E_{pri}^{rec} \quad (5.16)$$

$$E_{pri}^{arr} \leq \frac{S_b D}{12} (t_a - t_0) (2r_{tr}^2 + 3r_{tr}) \quad (5.17)$$

$$E_{pri}^{reb} \leq \frac{S_b D}{6} (t_b - t_a) \left(\frac{2r_{tr}^3 + 3r_{tr}^2 - 2r_{ss}^3 - 3r_{ss}^2}{r_{tr} - r_{ss}} \right) \quad (5.18)$$

$$E_{pri}^{rec} \leq \frac{S_b D}{12} (t_c - t_b) (2r_{ss}^2 + 3r_{ss}) \quad (5.19)$$

In short, a bound for P_{es} and the rated power of the **ES** converter can be obtained with [equations \(5.6\)](#) to [\(5.8\)](#), whereas [equations \(5.14\)](#) to [\(5.19\)](#) can be employed for bounding E_{es} and calculating the rated capacity of the **ESD**.

Notice that r_{tr} , r_{ss} , t_a , t_b , t_c are typically defined in industry standards and network codes such as [1, 38]. Likewise, boundaries for M , $\|\dot{x}\|$, and D can be specified based on system operator requirements or power system stability and protection coordination studies. The latter can also be used to define less conservative values of $\tilde{x}(t_a)$ and $\tilde{x}(t_b)$. In doing so, [equations \(5.9\)](#) and [\(5.10\)](#) can be applied to calculate E_{es} . Not least, the use of normalized terms M , D allows system operators to specify inertia and damping requirements on a system level without knowing the installed power of a specific subsystem or installation.

The DC Link

The main goal of this section is to define the rated capacitance C_{dc} [F] of the **DC** link. The **DC** link capacitor is a required energy source that provides balance between the **ES** converter and the grid converter, allowing them to be decoupled and controlled independently. Its capacitance is defined by [equation \(5.20\)](#) [52] where U_{dc} [V] is the **DC**-link rated voltage and ΔU_{dc}^{max} is its maximum tolerable variation [V]; T_r [s] represents the total time delay of the U_{dc} controller; ΔP_{dc}^{max} is the maximum power variation in the **DC** link [W].

$$C_{dc} \geq \frac{T_r \Delta P_{dc}^{max}}{2U_{dc} \Delta U_{dc}^{max}} \quad (5.20)$$

Typically, U_{dc} , ΔU_{dc}^{max} are parameters associated with:

1. the capacitor material and technology [53];
2. the voltage class of the power switch [54];
3. network codes and requirements, because variations in U_{dc} will influence the maximum voltage that can be delivered by the grid converter.

The value of T_r will be affected by the parameters of the U_{dc} controller. If the latter is modeled as a transport-delay, an estimate is given by [equation \(5.21\)](#) where T_m , T_c , T_a are the U_{dc} measurement, the controller, and the actuator (i.e. the **ES** converter) delays, respectively.

$$T_r = T_m + T_c + T_a \quad (5.21)$$

Finally, ΔP_{dc}^{max} can be approximated by the active power step applied immediately after the inertial or primary controllers leave their deadband zones, as seen in [equations \(5.23\)](#) and [\(5.24\)](#), where x_{DB}^{iner} , x_{DB}^{pri} [pu] are the dead band bounds of the inertial and primary control, respectively.

$$\Delta P_{dc}^{max} = \max(P_{iner}^{DB}, P_{pri}^{DB}) \quad (5.22)$$

$$P_{iner}^{DB} = 2S_b\tilde{x}_{DB}^{iner}M\dot{\tilde{x}} \quad (5.23)$$

$$P_{pri}^{DB} = 2S_bD\tilde{x}_{DB}^{pri} \quad (5.24)$$

In the approximation of [equations \(5.22\)](#) to [\(5.24\)](#), it is assumed that \tilde{x} is a smooth function. Though, this assumption will not hold in an **ACPS** where *all* generators and loads are interfaced by converters because $M \rightarrow 0$ in [equation \(5.4\)](#) and the model and analysis presented in [section 5.2.2](#) will no longer be valid.

The Grid Converter and its LC Filter

This section discusses briefly the sizing of the grid converter and recommends references for the design of the **LC** filter. [Figure 5.4](#) shows a schematic representation of the grid converter, the **DC** link and the **LC** filter.

Contractual and grid code requirements have to be taken into consideration when defining the rated apparent power of the grid converter. Among those requirements, one can mention minimum reactive power injection capacity, short-term overload, and low-voltage ride through capability [1, 38]. However, a relative simple and common practice in the industry is adopted in this paper. It uses a defined or required power factor λ . The rated apparent power of the converter, S_{gc} [VA], is then calculated as in [equation \(5.25\)](#).

$$S_{gc} = \frac{P_{gc}}{\lambda} \quad (5.25)$$

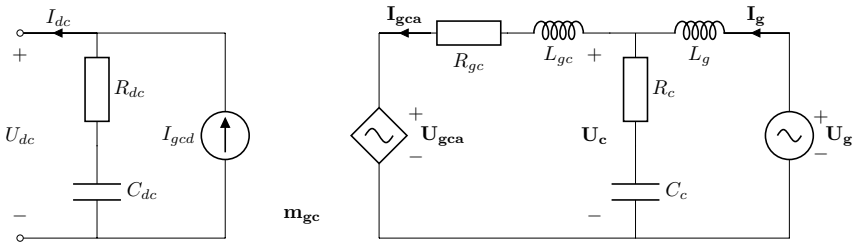


FIGURE 5.4 | Schematic representation of the DC link, the grid converter and its LC filter.

This practice generally limits the equipment size and cost. Nevertheless, it does not necessarily guarantee unsaturated operation for systems with high penetration of CIGs and MG applications. In such cases, the grid converter sizing may have to consider the compensation of harmonic distortions and the definition of S_{gc} will become more involved. More information about this topic can be obtained in [55].

Once S_{gc} is defined, the design of the grid converter LC filter can start. For grid-connected converters, the LCL configuration is preferred as it limits the influence of the switching frequency harmonics in other equipment and reduces the filter size and cost [56]. Typically, the second inductance of the LCL configuration is provided by the series inductance of a step-up transformer between the ESS and the grid. The design of an LCL filter is an iterative procedure well documented in the literature, see [56–59]. It can be summarized in the following steps.

1. Calculate the converter side inductance L_{gc} based on the desired maximum current ripple ΔI_{gca} on the ac side of the converter, its switching frequency f_{sw} and dc link voltage V_{dc} .
2. Choose the step-up transformer series inductance L_g upper-bounding the total inductance $L_T = L_{gc} + L_g$ to avoid excessive voltage drop across the inductors. Note that L_g is usually higher than 0.04 pu for medium-voltage transformers [60, 61]. When $5 \text{ kHz} \leq f_{sw} \leq 10 \text{ kHz}$, it is usually possible to adopt $L_T \leq 0.1 \text{ pu}$. On the contrary, a lower f_{sw} may demand a higher L_T .
3. Select the filter capacitance C_c upper-bounding its value to 0.05 pu (with converter rated power and voltage as base).
4. Check if the filter resonance frequency f_{res} lies between 0.2 and 0.5 times f_{sw} .
5. Calculate the filter damping resistance R_c based on the optimal quality factor Q and maximum power losses, limiting it to $R_c^{min} = \frac{1}{10\pi f_{res} C_c}$

to avoid instabilities.

For that, the following equations can be used as guidelines:

$$L_{gc} = \frac{U_{dc}}{24 * f_{sw} * \Delta I_{gca}} \quad (5.26)$$

$$L_g = 0.1 * L_b - L_{gc} \quad (5.27)$$

$$C_c = \frac{L_{gc}}{Z_b^2} \quad (5.28)$$

$$f_{res} = \frac{Z_b}{2\pi L_{gc}} \sqrt{\frac{L_T}{L_g}} \quad (5.29)$$

$$R_c = Q \sqrt{\frac{L_{gc} L_g}{L_T C_c}} \quad (5.30)$$

where $L_b = \frac{Z_b}{\omega_s}$, $Z_b = \frac{U_{2n}^2}{S_{gc}}$ are the base inductance and impedance of the grid-side converter, U_{2n} is the rated line voltage on the low-voltage side of the step-up transformer.

It is worth emphasizing that the design of an **LCL** filter is iterative. Failure to comply with requirements implies restarting the whole process and changing the initial assumptions, i.e. ΔI_{gca} , f_{sw} , and U_{dc} . Moreover, additional optimization objectives and constraints may require the use of high-order filters or active damping. These topics are outside the scope of this paper, but can be further explored in [62–67].

Finally, alternative topologies to the one presented in [figure 5.3](#) and [figure 5.4](#) are possible. Nonetheless, the principles discussed earlier in this section can also be applied to more complex solutions. For instance, **ESDs** using different technologies may be connected in parallel, such as ultracapacitors and batteries. The hybridization is possible because the requirements for each type of frequency control (inertial and primary) are set independently, as discussed in [section 5.2.2](#). This also allows control strategies to operate in parallel and **ES** converters to share the same **DC** link, grid converter and **LC** filter in a hybrid solution, which may help to reduce equipment costs, volume and weight [68]. Not least, **ESSs** may require more complex and robust configurations for the grid converter and consider aspects such as operating costs, efficiency, reliability, power quality and others, as discussed in [69]. However, note that these considerations will not affect the rated energy of **ESDs** nor the rated power of their converters, which are the variables being focused in the procedure presented in this paper.

5.3 RESULTS

This section presents a case study with numerical examples demonstrating how the method and equations presented in the previous section are applied to size the main components of a hybrid, converter-interfaced ESS supplying primary and secondary frequency control to an ACPS, supported by inertial control of traditional synchronous generators.

5.3.1 Case study: a wind-powered offshore platform in the North Sea

The system used as reference is depicted in figure 5.5 and represents an isolated ACPS of an offshore oil and gas platform in the North Sea.

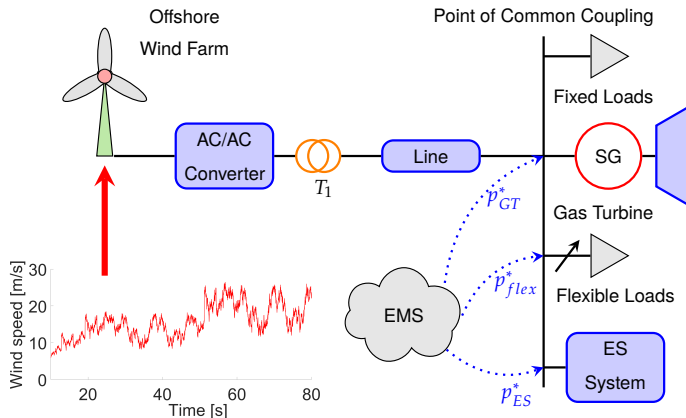


FIGURE 5.5 | Schematic representation of the case study ACPS.

This installation operates at 60 Hz ($\omega_s = 377 \text{ rad s}^{-1}$) and is equipped with two turbo-generators composed of a LM2500+ gas turbine from GE and an AMS 1250LG synchronous generator from ABB. Their combined active power is 70 MW, which is the value adopted for S_b . The normalized moment of inertia for these turbo-generators M_{GT} is equal to 5.1 s. This offshore installation must comply with IEC 61892:2019 [70] which requires equipment to withstand frequency variations of up 5% continuously. However, it is a goal to keep frequency variations below 2% to limit excessive overheating of electrical machines and transformers. Therefore, $r_{ss} = 0.02 \text{ pu}$ and $r_{tr} = 0.05 \text{ pu}$.

An initial techno-economical study of this installation [36] suggests that a reduction of up to 30% of its annual CO₂ emissions is possible when connecting it to a 12 MW offshore wind farm and employing an ESS based on 4 MW of proton exchange membrane (PEM) fuel cells and 6 MW of PEM electrolyzers.

The main goal of this hydrogen-based ESS is to stabilize the wind farm output, allowing turbo-generators to operate with optimized setpoints and, hence, attaining higher efficiencies and lower emissions. From a frequency control perspective, the turbo-generators provide inertial control and the ESS is responsible for primary and secondary control in normal operational conditions. To limit the size of the ESS, the turbo-generators contribute with additional primary and secondary control when the ESS saturates during occasional large frequency excursions.

Nevertheless, high number of start-stop and load-change cycles are known to be the main drivers for PEM devices deterioration and performance decay [71]. To avoid that, PEM fuel cells and electrolyzers are assigned to secondary control only and their load ramp rate is restricted to 0 to 100% in 120 s. The latter is also the value assumed for the recovery period ($t_c - t_b$). Hence, an additional ESD must be considered to provide primary frequency control and to allow operation of the PEM fuell cells and electrolyzers in more favorable conditions.

Further on the topic primary control, it is important to mention that electric loads of this platform are divided in two groups: fixed ($P_{fix} = 37$ MW) and flexible ($P_{flex} = 7.6$ MW). The first group represents equipment that cannot be influenced by the energy management system (EMS), because changes in their set point are not possible or would affect negatively the oil and gas extraction and processing. Meanwhile, the second group represents loads whose set point can be temporarily raised or lowered by the EMS or primary control. An example of flexible load is the water injection system, which is responsible to maintain overall and hydrostatic reservoir pressures and force the oil toward the production wells [72]. This type of load is flexible because reservoir pressures can vary within a certain range without considerable impacts to production. In addition, this system time constant is large (minutes) when compared to the electrical system dynamics (seconds). This concept is explored in detail by DNV-GL [73], Sanchez *et al.* [74], Alves *et al.* [75].

Hence, the water injection system can also be considered a short-term ESS that is capable of offering primary frequency control to the ACPS. When assuming that 20% of the installed flexible load can be used for primary frequency control, the following damping coefficient is obtained:

$$\begin{aligned} D_{flex} &= \frac{P_{flex}^{pri}}{S_{br_{ss}}} \\ &= \frac{0.2 \times 7.6}{70 \times 0.02} = 1.09 \text{ pu} \end{aligned}$$

Finally, the load demand was obtained from the platform's supervisory control and data acquisition (SCADA) system for one representative week with

a sampling period of one second. Figure 5.6 presents the histogram of this data set, which is fit by a normal distribution when ignoring outliers below 0.6 pu. The distribution gives a load variation of 0.0428 pu or 3 MW in normal operational conditions with 99.9% of probability, which should be covered by primary control. Using equation (5.8):

$$\begin{aligned} D_{min} &\geq \frac{p_{es}^{pri}}{r_{ss}(1 - r_{tr})} \\ &\geq \frac{0.0428}{0.02 \times (1 - 0.05)} = 2.25 \text{ pu} \end{aligned}$$

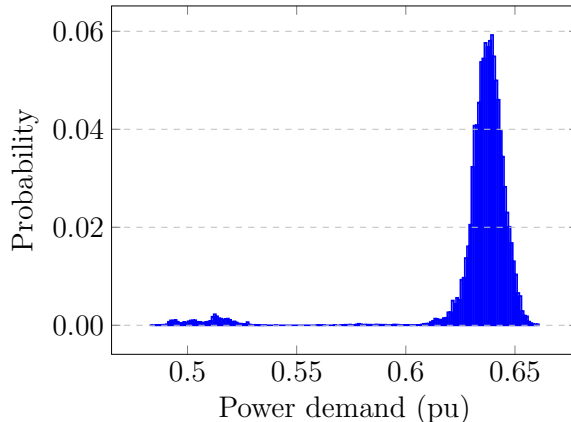


FIGURE 5.6 | Histogram of the platform active power demand showing an average load of 0.6377 pu and maximum variation of 0.0428 pu with 99.9% of probability when outliers below 0.6 pu are ignored.

Thus, the ESD responsible for primary control should provide the following additional damping: $D_{es} = D_{min} - D_{flex} = 1.16$ pu. With these parameters, initial simulations of the case study installation for a 3 MW load perturbations gives an arrest period $(t_a - t_0) = 25$ s and a rebound period $(t_b - t_a) = 15$ s.

Table 5.1 presents a summary of the installation parameters and the ESS requirements listed above.

5.3.2 Sizing of the Energy Storage System

Applying equations (5.8) and (5.16) using the values from table 5.1, the rated power P_{es1} and energy capacity E_{es1} of the ESD providing primary control can be defined as $P_{es1} = 1.54$ MW and $E_{es1} = 113.6$ MJ or 31.56 kWh. Note though that the primary control must be bidirectional, i.e. it must compensate

TABLE 5.1 | Parameters of the **ACPS** of an offshore oil and gas platform in the **NCS** and the requirements for its converter-interfaced **ESS**.

| Param. | Value | Param. | Value |
|---------------|---------|---------------|--------------------------|
| S_b | 70 MW | ω_s | 377 rad s^{-1} |
| r_{tr} | 0.05 pu | r_{ss} | 0.02 pu |
| M_{GT} | 5.1 s | D_{min} | 2.25 pu |
| D_{flex} | 1.09 pu | D_{es} | 1.16 pu |
| P_{ELY} | 6 MW | P_{FC} | 4 MW |
| $(t_a - t_0)$ | 25 s | $(t_b - t_a)$ | 15 s |
| $(t_c - t_b)$ | 120 s | | |

either lack or excess of power in the system. Therefore, a 50% state of charge for the **ESS** in normal operation should be considered. Hence, $E_{es1} = \frac{113.6}{0.5} = 227.2 \text{ MJ}$ or 63.12 kWh .

The most suitable **ESD** is chosen based on the calculated P_{es1} and E_{es1} , on the parameters in **table 5.1**, and on a techno-economical evaluation. The latter is not covered in this paper. It is assumed, however, that a commercial lithium-ion system such as Saft Intensium Max+ 20P [76] is selected. This system incorporates **ESD** and converter in one assembly with two regulated dc output voltages of $771 \pm 96 \text{ V}$ that can be connected in series or parallel and losses of about 25 kW at rated conditions. Considering the requirements of commercial grid converters such as Siemens SINACON PV [77], the **ESD** is assumed to have its two outputs connected in series and the following characteristics: $U_{dc} = 1500 \text{ V}$, $\Delta U_{dc}^{max} = 150 \text{ V}$, $P_{losses}^{es1} = 25 \text{ kW}$, and $T_r = 2.1 \text{ ms}$ (one eighth of a grid cycle).

To define ΔP_{dc}^{max} , the value $x_{DB}^{pri} = 0.0025 \text{ pu}$ or 150 mHz is obtained from industry standards or grid codes such as [1, 38]. Then, $\Delta P_{dc}^{max} = 360.5 \text{ kW}$ is attained when applying **equations (5.22)** and **(5.24)**. With these values defined, the **DC**-link capacitor is calculated using **equation (5.20)** and $C_{dc} \geq 1.7 \text{ mF}$ is retrieved.

The next step in the procedure is defining S_{gc} . Assuming that all **ESDs** share the same **DC** link and that fuel cell and electrolyzer do not operate simultaneously, the active power bound will be defined by $P_{ELY} + P_{es1} + P_{losses}^{es1} = 7.57 \text{ MW}$, where P_{ELY} denotes the electrolyzer rated power. To have a buffer for the grid converter and **LC** filter losses, a safety margin of 2% is added to this value resulting in $P_{gc} = 7.72 \text{ MW}$. Additionally, $\lambda = 0.8$ is adopted to limit the size of the grid converter. It then follows that $S_{gc} = 9.65 \text{ MVA}$.

The final step is calculating the components of the **LC** filter. For the sake of brevity, this design is not presented in this paper. The recommended procedure and references are listed in **section 5.2.2**. Nonetheless, the algorithm for calculating the **LC** filter is available for the reader in [78]. The grid con-

verter switching frequency is adopted as $f_{sw} = 5.4 \text{ kHz}$ and its maximum current ripple as $\Delta I_{gca} = 0.25 \text{ pu}$. This results in the following values for the filter components: $L_{gc} = 5.61 \mu\text{H}$, $L_g = 6.92 \mu\text{H}$, $C_c = 2.5 \text{ mF}$, and $R_c = 0.189 \text{ m}\Omega$. Refer to figure 5.4 for the placement of each filter element. It is worth mentioning that R_c yields an over-damped characteristic at the filter's resonance frequency, which is $f_{res} = 1.80 \text{ kHz}$ or 0.334 times f_{sw} .

5.3.3 Sizing validation

To validate the calculations presented in section 5.3.2, a surrogate model of the case study installation was implemented in MATLAB Simulink R2018a. It has the level of details required to represent the frequency dynamics of the installation and to validate the proposed sizing of the ESD responsible for primary frequency control. It includes all main elements represented in figure 5.5, namely: the turbo-generators, the fixed and flexible loads, the wind farm and its transmission line, the ESS and the EMS. Figure 5.7 gives an overview of these elements in Simulink.

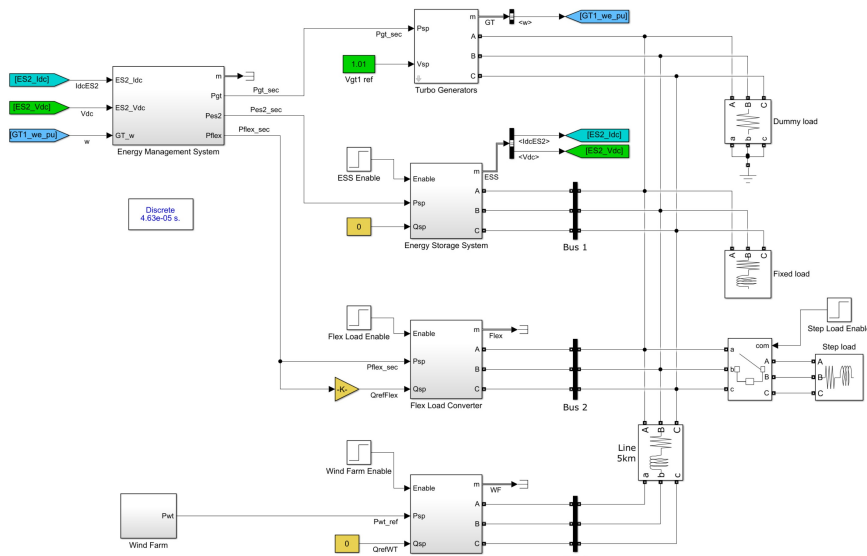


FIGURE 5.7 | Overview of the MATLAB Simulink model used to validate the proposed sizing of the energy storage device responsible for primary control in the case study.

The model was implemented using blocks of the Simscape Electrical Specialized Power Systems Toolbox complemented by an open library developed by the authors [79]. The latter includes a generalized nonlinear droop controller that is presented in figure 5.8. This block is used as the main primary

frequency controller in the turbo-generators, **ESS** and flexible load subsystems with their parameters as presented in [table 5.2](#). Moreover, the secondary control is implemented in the **EMS** subsystem using a nonlinear integral controller from the open library with anti-windup and hold functionalities. To minimize CO₂ emissions, the **EMS** gives priority for changes in the **ESS** setpoint when the secondary control is active. The re-dispatch of turbo-generators happens only when the limits of fuel cell or electrolyzers are reached and those may be considered a supplementary **FRR**.

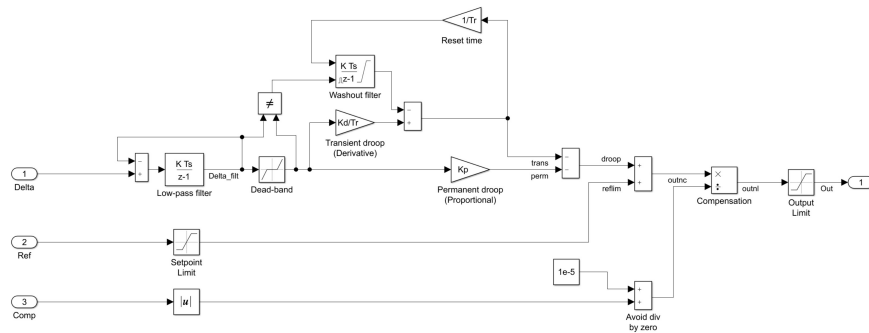


FIGURE 5.8 | Generalized nonlinear droop controller with deadband, permanent droop (proportional gain), transient droop (derivative gain), output compensation, setpoint and output limitation.

TABLE 5.2 | Parameters of the primary controllers used during the validation.

| Parameter [Unit] | Turbo-gen | ESS | Flex |
|---|-----------------------|------------------|--------------------|
| Permanent droop [pu] | | | |
| Case 1 – 3 MW load step without ESS | $\frac{0.0214}{0.02}$ | 0 | $\frac{0.2}{0.02}$ |
| Case 2 – 3 MW load step with ESS | $\frac{0.1714}{0.02}$ | $\frac{1}{0.02}$ | $\frac{0.2}{0.02}$ |
| Case 3 – 12 MW load step without ESS | $\frac{0.0857}{0.02}$ | 0 | $\frac{0.2}{0.02}$ |
| Case 4 – 12 MW load step with ESS | $\frac{0.1714}{0.02}$ | $\frac{1}{0.02}$ | $\frac{0.2}{0.02}$ |
| Transient droop [pu] | 0 | 0 | 0 |
| Reset time [s] | 0.1 | 0.1 | 0.1 |
| Low-pass frequency [Hz] | 10 | 450 | 30 |
| Deadband [pu] | 0.025 | 0.0025 | 0.0025 |

It should be emphasized that it is not the goal of this model to validate the design of the grid converter, its controllers or its **LC** filter, nor to evaluate harmonics or possible power quality problems. Moreover, the validation of

the fuel cell and electrolyzer stacks size, and their required H_2 storage is presented by Riboldi *et al.* [14]. For the sake of brevity, the validation model is not described further in this section. However, the interested reader can inspect it and find all necessary details, parameters and simulation files to reproduce the results presented below in [78].

To create the power imbalance required for checking the ESS sizing, a load of 3 MW (Step Load) is connected to the system at $t_0 = 2$ s. As presented earlier in section 5.3.1, this is the expected maximum load variation under normal operational conditions with 99.9% of probability. Figure 5.9 shows the results of two simulations of the case study behavior during a load increase of 3 MW: Case 1 does not include the ESS in the installation, while Case 2 does include it.

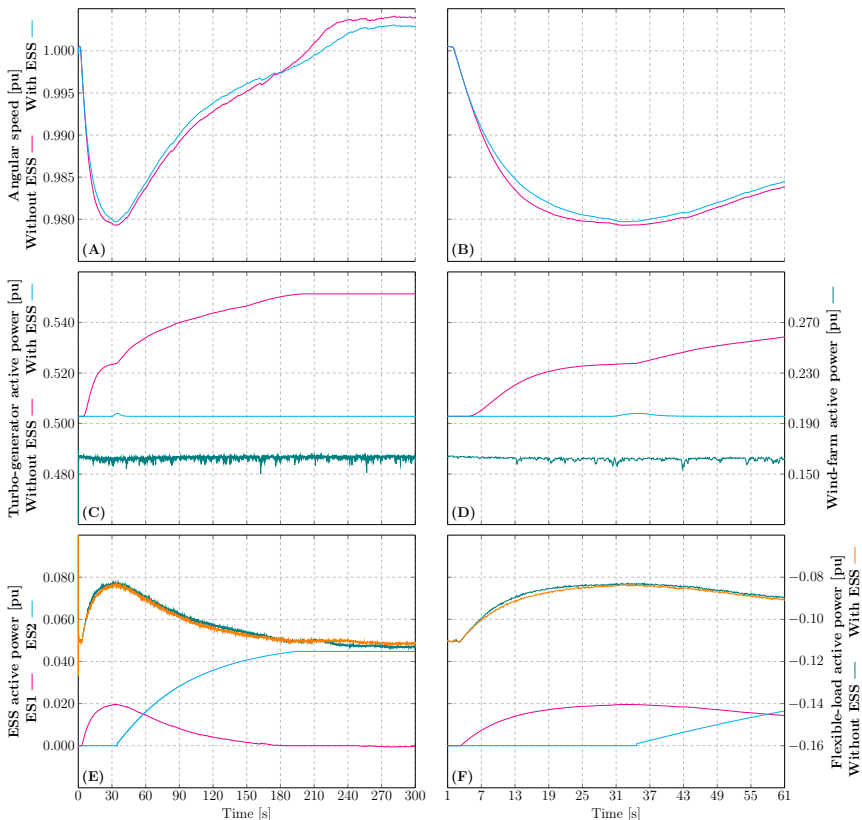


FIGURE 5.9 | Case-study behavior during a load increase of 3 MW with and without the proposed ESS: Normalized angular speed (A) during the whole transient and (B) detail of the first minute; Turbo-generator and wind-farm active power in pu (C) during the whole transient and (D) detail of the first minute; Active power of the ES devices responsible for primary control (ES1) and secondary control (ES2) (E) during the whole transient and (F) detail of the first minute

From a frequency-control standpoint, a closer look at figure 5.9-(A) and (B) reveals that the angular speed behaves similarly in both cases, i.e. with and without **ESS**. The minor deviations among the cases are explained by the different deadbands and actuation delays of the turbo-generator and the **ESS**. Indeed, the smaller deadband and actuation delay of the converter-interfaced **ESS** makes its performance slightly superior, achieving a higher nadir (0.9797 pu) than the turbine governor (0.9793 pu) and a smaller steady-state error (0.29% versus 0.39%) after secondary control is deactivated. This better performance is reflected in the results seen in figure 5.9-(E) and (F), which show a marginal reduction of the flexible-load active power deviation from its original setpoint while the primary control is active. Foremost, figure 5.9-(C) and (D) corroborate the idea proposed in section 5.3.2, i.e. a properly sized battery **ESS** would allow turbo-generators to operate at a constant setpoint when a 3 MW load variation happens suddenly, while respecting the load ramp-rate limit of the **PEM** fuel cell, as shown in figure 5.9-(E) and (F).

From a sizing perspective, the **ESD** responsible for primary control (battery system) delivered a peak active power of 0.0196 pu or 1.37 MW and consumed 29.2 kW h of energy. The latter was calculated by trapezoidal numerical integration of the curve ES1 in figure 5.9-(E) using a step of 100 ms. When compared to the calculated values (1.54 kW h and 31.56 kW h) from section 5.3.2, the proposed procedure oversized the battery system's active power by 13% and its energy by 8%. Nonetheless, as opposed to the simulation model used for validation, the proposed procedure 1) requires knowledge of very few **ACPS** parameters; 2) relies only on algebraic equations, which are easy to integrate in optimization algorithms typically necessary for techno-economical evaluation of **ESSs**.

At this point, it is important to recap that the energy of the **ESD** responsible for primary control is dependent on: 1) the damping D_{es} provided, 2) the frequency limits r_{ss} and r_{tr} , 3) the duration of the arrest ($t_a - t_0$), rebound ($t_b - t_a$) and recovery ($t_c - t_b$) periods, as seen in equations (5.17) to (5.19). Thus, when defining these variables, it is critical to evaluate if the **ESS** must provide frequency control uninterruptedly during high-impact, low-probability events. A complete disconnection of the wind farm under full production (12 MW) is an example of such event for the case study presented. Figure 5.10 presents the results of two simulations of the case study behavior during this condition: **Case 3** does not include the **ESS** in the installation, while **Case 4** does. It is important to highlight that, for **Case 3**, the turbo-generator permanent droop must be increased to guarantee frequency stability and display the same dynamics of **Case 4**, as seen in table 5.2.

From a frequency-control point of view, figure 5.10-(B) suggests that the angular speed behaves similarly with and without the **ESS** during the arrest

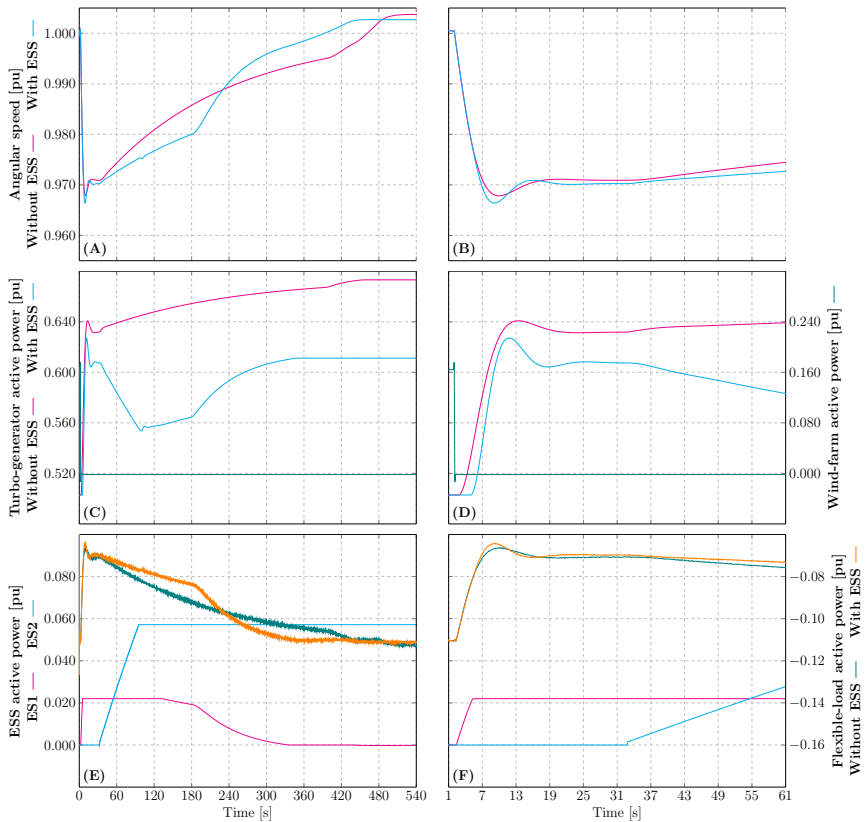


FIGURE 5.10 | Case-study behavior during the wind farm disconnection under full production (12 MW) with and without the proposed ESS: Normalized angular speed (A) during the whole transient and (B) detail of the first minute; Turbo-generator and wind-farm active power in pu (C) during the whole transient and (D) detail of the first minute; Active power of the ES devices responsible for primary control (ES1) and secondary control (ES2) (E) during the whole transient and (F) detail of the first minute

and rebound period. However, a closer look at figure 5.10-(A) reveals that the dynamics of the recovery period in Cases 3 and 4 are distinct. This happens because the secondary controller acts differently in these two simulations.

In Case 3, the turbo-generator is the sole contributor to the FRR and, as seen in figure 5.10-(C), its active power increases exponentially in the recovery period. As consequence, the angular speed deviation decreases exponentially, until it reaches the deadband of the droop controller.

In Case 4, there are two sources for the FRR: the hydrogen-based ESS (preferential) and the turbo-generator (supplementary). Hence, the secondary controller ramps up the PEM fuel cell (ES2) until it reaches its rated power, as seen in figure 5.10-(E). At the same time, the angular speed deviation decreases and, as consequence, the droop controller reduces the turbo-generator active

power, as shown in [figure 5.10](#)-(A) and (C). When the ES2 limit is hit, the secondary controller starts increasing the turbo-generator active power. However, the latter is also reduced by its droop controller, because the angular speed is still decreasing. These adversarial contributions continue until the deadband of the turbo-generator droop controller is reached. After that, only the secondary controller is active and the angular speed deviation decreases exponentially, until it reaches the deadband of the ES2 droop controller.

From a sizing frame of reference, the peak active power delivered by the battery system was 1.54 MW and the energy supplied was 95.8 kWh. The peak active power was limited by the nonlinear droop controller and matches the value defined in [section 5.3.2](#). On the other hand, the energy obtained in the simulation is more than 3 times larger the calculated value. Naturally, this happens because the parameters of the 3 MW and 12 MW load-increase events are disparate.

By inspection of [figure 5.10](#)-(A), one will note that the frequency limits $r_{ss} = 0.02$ and $r_{tr} = 0.05$ were obeyed. However, the duration of the arrest, rebound and recovery periods were approximately 8 s, 120 s and 165 s. When substituting these new values in [equations \(5.17\)](#) to [\(5.19\)](#), the energy obtained is 113.3 kWh, i.e. the proposed procedure oversizes the battery system energy by about 18% when compared to the simulation results. This shows that the proposed procedure can produce correct upper-bounds for the [ESS](#) power and energy even when large disturbances and nonlinearities are considered.

5.4 CONCLUSIONS

This paper reviewed the frequency response theory in ac power systems, highlighting the different time periods (arrest, rebound, recovery) and control actions (inertial, primary, secondary) of the frequency control problem. It also highlighted the main distinctions among traditional high-inertia systems relying on synchronous machines, and low-inertia systems such as those with high penetration of converter-interfaced generation and microgrids. Grounded on these concepts and some assumptions, it derived analytical equations to rate the energy capacity and active power required by an energy storage system for providing inertial and primary control to an ac power system. The proposed equations rely on parameters typically defined by system operators, industry standards or network codes, namely the steady-state and transient frequency ranges, the maximum rate of change of frequency, the desired equivalent moment of inertia and damping coefficient. Note that these parameters are independent from the technologies or topologies used in the energy storage devices and converters.

Using these results, this work also provided a step-by-step systematic procedure to initially size the remaining components of a converter-interfaced hybrid energy storage system connected to three-phase ac systems, i.e. the shared DC link, the grid converter and its LC filter. Finally, a case study of a wind-powered oil and gas platform in the North Sea was presented. It demonstrated with numerical examples how the proposed equations and the step-by-step procedure can be applied in a practical problem, where simulations in MATLAB Simulink validated the algebraic calculations and showed they slightly oversize energy storage devices. Not least, the case study demonstrated that the proposed method allows the system designer to take advantage of different energy storage technologies and set specific requirements for each storage device and converter in a hybrid system according to the type of frequency control action being provided and requirements set by industry standards and grid codes.

CONFLICT OF INTEREST STATEMENT

The authors declare that the research was conducted in the absence of any commercial or financial relationships that could be construed as a potential conflict of interest.

FUNDING

This research was funded by the Research Council of Norway under the program PETROMAKS2, grant number 281986, project [Innovative Hybrid Energy System for Stable Power and Heat Supply in Offshore O&G Installation Project](#), and through the PETROENTER scheme, under the [LowEmission Research Centre](#), grant number 296207.

DATA AVAILABILITY STATEMENT

The datasets generated and analyzed for this study can be found at [\[78\]](#).

5.5 REFERENCES

- [1] IEEE 1547-2018. IEEE Standard for Interconnection and Interoperability of Distributed Energy Resources with Associated Electric Power Systems Interfaces. IEEE New York, NY (2018). ISBN 978-1-5044-4639-6. Cited on page/s [44, 48, 57, 58, 64](#).
- [2] IEEE 2030.8-2018. IEEE Standard for the Testing of Microgrid Controllers. IEEE New York, NY (2018). ISBN 978-1-5044-5050-8. Cited on page/s [44](#).

- [3] Qiang Fu, Ahmad Hamidi, Adel Nasiri, Vijay Bhavaraju, Slobodan Bob Krstic, and Peter Theisen. The Role of Energy Storage in a Microgrid Concept: Examining the opportunities and promise of microgrids. *IEEE Electrific. Mag.* **1** (2), 21–29 (12 2013). ISSN 2325-5897, 2325-5889. DOI [10.1109/MELE.2013.2294736](https://doi.org/10.1109/MELE.2013.2294736). Cited on page/s [44](#).
- [4] Goran Strbac, Nikos Hatziargyriou, Joao Pecas Lopes, Carlos Moreira, Aris Dimeas, and Dimitrios Papadaskalopoulos. Microgrids: Enhancing the Resilience of the European Megagrid. *IEEE Power and Energy Magazine* **13** (3), 35–43 (5 2015). ISSN 1540-7977. DOI [10.1109/MPE.2015.2397336](https://doi.org/10.1109/MPE.2015.2397336). Cited on page/s [44](#).
- [5] Sam Koohi-Kamali, V.V. Tyagi, N.A. Rahim, N.L. Panwar, and H. Mokhlis. Emergence of energy storage technologies as the solution for reliable operation of smart power systems: A review. *Renewable and Sustainable Energy Reviews* **25**, 135–165 (9 2013). ISSN 13640321. DOI [10.1016/j.rser.2013.03.056](https://doi.org/10.1016/j.rser.2013.03.056). Cited on page/s [45](#).
- [6] A.B. Gallo, J.R. Simões-Moreira, H.K.M. Costa, M.M. Santos, and E. Moutinho dos Santos. Energy storage in the energy transition context: A technology review. *Renewable and Sustainable Energy Reviews* **65**, 800–822 (11 2016). ISSN 13640321. DOI [10.1016/j.rser.2016.07.028](https://doi.org/10.1016/j.rser.2016.07.028). Cited on page/s [45](#).
- [7] Mustafa Farhadi and Osama Mohammed. Energy Storage Technologies for High-Power Applications. *IEEE Trans. on Ind. Applicat.* **52** (3), 1953–1961 (2016). ISSN 0093-9994, 1939-9367. DOI [10.1109/TIA.2015.2511096](https://doi.org/10.1109/TIA.2015.2511096). Cited on page/s [45](#).
- [8] Reza Hemmati and Hedayat Saboori. Emergence of hybrid energy storage systems in renewable energy and transport applications – A review. *Renewable and Sustainable Energy Reviews* **65**, 11–23 (2016). ISSN 1364-0321. URL <https://www.sciencedirect.com/science/article/pii/S1364032116302374>. Cited on page/s [45](#).
- [9] Mohammad Reza Aghamohammadi and Hajar Abdolahinia. A new approach for optimal sizing of battery energy storage system for primary frequency control of islanded Microgrid. *Int. J. Electr. Power Energy Syst.* **54**, 325–333 (1 2014). ISSN 01420615. DOI [10.1016/j.ijepes.2013.07.005](https://doi.org/10.1016/j.ijepes.2013.07.005). Cited on page/s [45](#).
- [10] Mehrzad M. Bijaei, Wayne W. Weaver, and Rush D. Robinett. Energy Storage Power and Energy Sizing and Specification Using HSSPFC. *Electronics* **9** (4), 638 (4 2020). ISSN 2079-9292. DOI [10.3390/electronics9040638](https://doi.org/10.3390/electronics9040638). Cited on page/s [45](#).
- [11] Mehrzad Mohammadi Bijaei, Wayne W. Weaver, and Rush D. Robinett. Energy Storage Requirements for Inverter-Based Microgrids Under Droop Control in d-q Coordinates. *IEEE Trans. Energy Convers.* **35** (2), 611–620 (6 2020). ISSN 0885-8969, 1558-0059. DOI [10.1109/TEC.2019.2959189](https://doi.org/10.1109/TEC.2019.2959189). Cited on page/s [45](#).
- [12] Vaclav Knap, Sanjay K. Chaudhary, Daniel-Ioan Stroe, Maciej Swierczynski, Bogdan-Ionut Craciun, and Remus Teodorescu. Sizing of an Energy Storage System for Grid Inertial Response and Primary Frequency Reserve. *IEEE Trans. Power Syst.* **31** (5), 3447–3456 (2016). ISSN 0885-8950, 1558-0679. DOI [10.1109/TPWRS.2015.2503565](https://doi.org/10.1109/TPWRS.2015.2503565). Cited on page/s [45](#).
- [13] Monika Sandelic, Daniel-Ioan Stroe, and Florin Iov. Battery Storage-Based Frequency Containment Reserves in Large Wind Penetrated Scenarios: A Practical Approach to Sizing. *Energies* **11** (11), 3065 (11 2018). ISSN 1996-1073. DOI [10.3390/en11113065](https://doi.org/10.3390/en11113065). Cited on page/s [45](#).
- [14] Luca Riboldi, Erick F. Alves, Marcin Pilarczyk, Elisabetta Tedeschi, and Lars O. Nord. Optimal design of a hybrid energy system for the supply of clean and stable energy to offshore installations. *Frontiers in Energy Research* (1 2021). DOI [10.3389/fenrg.2020.607284](https://doi.org/10.3389/fenrg.2020.607284). Cited on page/s [45, 67](#).
- [15] Carlos Gamarra and Josep M. Guerrero. Computational optimization techniques applied to microgrids planning: A review. *Renew. Sustain. Energy Rev.* **48**, 413–424 (8 2015). ISSN 13640321. DOI [10.1016/j.rser.2015.04.025](https://doi.org/10.1016/j.rser.2015.04.025). Cited on page/s [46](#).
- [16] Mohammad A.A. Al-Jaafreh and Geev Mokryani. Planning and operation of LV distribution

- networks: A comprehensive review. *IET Energy Syst. Integ.* **1** (3), 133–146 (9 2019). ISSN 2516-8401. DOI [10.1049/iet-esi.2019.0013](https://doi.org/10.1049/iet-esi.2019.0013). Cited on page/s [46](#).
- [17] Daniel Duckwitz. Power System Inertia: Derivation of Requirements and Comparison of Inertia Emulation Methods for Converter-based Power Plants. *PhD thesis*. University of Kassel Kassel, Germany (3 2019). DOI [10.17170/kobra-20190510451](https://doi.org/10.17170/kobra-20190510451). Cited on page/s [46](#).
 - [18] ENTSO-E. Fast Frequency Reserve – Solution to the Nordic inertia challenge. Technical report ENTSO-E (December 2019). Cited on page/s [46, 49, 50](#).
 - [19] Gary W. Chang, Ching-Sheng Chuang, Tai-Ken Lu, and Ching-Chung Wu. Frequency-regulating reserve constrained unit commitment for an isolated power system. *IEEE Trans. Power Syst.* **28** (2), 578–586 (5 2013). ISSN 0885-8950, 1558-0679. DOI [10.1109/TPWRS.2012.2208126](https://doi.org/10.1109/TPWRS.2012.2208126). Cited on page/s [46, 47](#).
 - [20] Yunfeng Wen, Wenyuan Li, Gang Huang, and Xuan Liu. Frequency Dynamics Constrained Unit Commitment With Battery Energy Storage. *IEEE Trans. Power Syst.* **31** (6), 5115–5125 (11 2016). ISSN 0885-8950, 1558-0679. DOI [10.1109/TPWRS.2016.2521882](https://doi.org/10.1109/TPWRS.2016.2521882). Cited on page/s [46, 47](#).
 - [21] Shrirang Abhyankar, Guangchao Geng, Mihai Anitescu, Xiaoyu Wang, and Venkata Dinavahi. Solution techniques for transient stability-constrained optimal power flow – Part I. *IET Gener. Transm. Distrib* **11** (12), 3177–3185 (8 2017). ISSN 1751-8687, 1751-8695. DOI [10.1049/iet-gtd.2017.0345](https://doi.org/10.1049/iet-gtd.2017.0345). Cited on page/s [46](#).
 - [22] Guangchao Geng, Shrirang Abhyankar, Xiaoyu Wang, and Venkata Dinavahi. Solution techniques for transient stability-constrained optimal power flow – Part II. *IET Gener. Transm. Distrib* **11** (12), 3186–3193 (8 2017). ISSN 1751-8687, 1751-8695. DOI [10.1049/iet-gtd.2017.0346](https://doi.org/10.1049/iet-gtd.2017.0346). Cited on page/s [46](#).
 - [23] Nga Nguyen, Saleh Almasabi, Atri Bera, and Joydeep Mitra. Optimal Power Flow Incorporating Frequency Security Constraint. *IEEE Trans. Ind. Appl.* **55** (6), 6508–6516 (11 2019). ISSN 0093-9994, 1939-9367. DOI [10.1109/TIA.2019.2938918](https://doi.org/10.1109/TIA.2019.2938918). Cited on page/s [46](#).
 - [24] Sina Y. Caliskan and Paulo Tabuada. Uses and abuses of the swing equation model. In *2015 54th IEEE Conference on Decision and Control (CDC)* pages 6662–6667 Osaka, Japan (2015). IEEE. ISBN 978-1-4799-7886-1. DOI [10.1109/CDC.2015.7403268](https://doi.org/10.1109/CDC.2015.7403268). Cited on page/s [46, 47](#).
 - [25] Erick Fernando Alves, Gilbert Bergna, Danilo Iglesias Brandao, and Elisabetta Tedeschi. Sufficient Conditions for Robust Frequency Stability of AC Power Systems. *IEEE Trans. Power Syst.* pages 1–1 (2020). ISSN 0885-8950, 1558-0679. DOI [10.1109/TPWRS.2020.3039832](https://doi.org/10.1109/TPWRS.2020.3039832). Cited on page/s [46, 53, 55](#).
 - [26] R. E. Doherty and C. A. Nickle. Synchronous Machines III - Torque-Angle Characteristics Under Transient Conditions. *Trans. AIEE XLVI*, 1–18 (1 1927). ISSN 0096-3860. DOI [10.1109/T-AIEE.1927.5061336](https://doi.org/10.1109/T-AIEE.1927.5061336). Cited on page/s [47](#).
 - [27] Charles Concordia. Synchronous machines, theory and performance. Number viii, 224 p. in General Electric Series. Wiley New York (1951). Cited on page/s [47](#).
 - [28] John J. Grainger and William D. Stevenson. Power system analysis. McGraw-Hill Series in Electrical and Computer Engineering. McGraw-Hill New York (1994). ISBN 978-0-07-061293-8. Cited on page/s [47](#).
 - [29] Edward Wilson Kimbark. Power system stability. IEEE Press Power Systems Engineering Series. IEEE Press New York (1995). ISBN 978-0-7803-1135-0. Cited on page/s [47](#).
 - [30] P. Kundur, N. J. Balu, and M. G. Lauby. Power System Stability and Control. EPRI Power System Engineering Series. McGraw-Hill New York, USA (1994). ISBN 978-0-07-035958-1. Cited on page/s [47, 50, 53](#).
 - [31] Jan Machowski. Power system dynamics: Stability and control. Wiley Chichester, U.K. 2nd edition (2008). ISBN 978-1-119-96505-3. Cited on page/s [47, 53](#).

- [32] Carlos Tavora and Otto M. Smith. Characterization of Equilibrium and Stability in Power Systems. *IEEE Trans. on Power Apparatus and Syst.* **PAS-91** (3), 1127–1130 (5 1972). ISSN 0018-9510. DOI [10.1109/TPAS.1972.293468](https://doi.org/10.1109/TPAS.1972.293468). Cited on page/s [47](#).
- [33] Florian Dörfler and Francesco Bullo. Synchronization and Transient Stability in Power Networks and Nonuniform Kuramoto Oscillators. *SIAM Journal on Control and Optimization* **50** (3), 1616–1642 (1 2012). ISSN 0363-0129, 1095-7138. DOI [10.1137/110851584](https://doi.org/10.1137/110851584). Cited on page/s [47, 53](#).
- [34] Gauthier Delille, Bruno Francois, and Gilles Malarange. Dynamic Frequency Control Support by Energy Storage to Reduce the Impact of Wind and Solar Generation on Isolated Power System's Inertia. *IEEE Trans. Sustain. Energy* **3** (4), 931–939 (10 2012). ISSN 1949-3029, 1949-3037. DOI [10.1109/TSTE.2012.2205025](https://doi.org/10.1109/TSTE.2012.2205025). Cited on page/s [47](#).
- [35] I. Egido, L. Sigrist, E. Lobato, L. Rouco, and A. Barrado. An ultra-capacitor for frequency stability enhancement in small-isolated power systems: Models, simulation and field tests. *Applied Energy* **137**, 670–676 (1 2015). ISSN 03062619. DOI [10.1016/j.apenergy.2014.08.041](https://doi.org/10.1016/j.apenergy.2014.08.041). Cited on page/s [47](#).
- [36] Luca Riboldi, Erick F Alves, Marcin Pilarczyk, Elisabetta Tedeschi, and Lars O. Nord. Innovative hybrid energy system for stable power and heat supply in offshore oil & gas installation (HES-OFF): System design and grid stability. In *30th European Symposium on Computer Aided Process Engineering (ESCAPE30)* page 8 Milano, Italy (9 2020). Elsevier. Cited on page/s [47, 61](#).
- [37] Hamed Ahmadi and Hassan Ghasemi. Security-Constrained Unit Commitment With Linearized System Frequency Limit Constraints. *IEEE Trans. Power Syst.* **29** (4), 1536–1545 (7 2014). ISSN 0885-8950, 1558-0679. doi: [10.1109/TPWRS.2014.2297997](https://doi.org/10.1109/TPWRS.2014.2297997). Cited on page/s [47](#).
- [38] EU Commission Regulation. Network code on requirements for grid connection of generators. EU 2016/631. Technical report European Union (2016). eur-lex.europa.eu/eli/reg/2016/631/oj. Accessed 2020-07-17. Cited on page/s [48, 57, 58, 64](#).
- [39] Joseph H Eto, John Undrill, Ciaran Roberts, Peter Mackin, and Jeffrey Ellis. Frequency Control Requirements for Reliable Interconnection Frequency Response. Technical Report LBNL-2001103 Lawrence Berkeley National Laboratory Berkley, CA (2 2018). Cited on page/s [49, 50, 53, 54](#).
- [40] EU Comission Regulation. Guideline on electricity transmission system operation. EU 2017/1485. Technical report European Union (2017). eur-lex.europa.eu/eli/reg/2017/1485/oj. Accessed 2020-07-17. Cited on page/s [49, 54](#).
- [41] Tine L. Vandoorn, Juan C. Vasquez, Jeroen De Kooning, Josep M. Guerrero, and Lieven Vandervelde. Microgrids: Hierarchical Control and an Overview of the Control and Reserve Management Strategies. *IEEE Ind. Electron. Mag.* **7** (4), 42–55 (12 2013). ISSN 1932-4529. DOI [10.1109/MIE.2013.2279306](https://doi.org/10.1109/MIE.2013.2279306). Cited on page/s [49, 50, 53](#).
- [42] Salvatore D'Arco and Jon Are Suul. Virtual synchronous machines — Classification of implementations and analysis of equivalence to droop controllers for microgrids. In *PowerTech* pages 1–7 Grenoble, France (6 2013). IEEE. ISBN 978-1-4673-5669-5. DOI [10.1109/PTC.2013.6652456](https://doi.org/10.1109/PTC.2013.6652456). Cited on page/s [49](#).
- [43] Jingyang Fang, Hongchang Li, Yi Tang, and Frede Blaabjerg. On the Inertia of Future More-Electronics Power Systems. *IEEE J. Emerg. Sel. Topics Power Electron.* **7** (4), 2130–2146 (12 2019). ISSN 2168-6777, 2168-6785. DOI [10.1109/JESTPE.2018.2877766](https://doi.org/10.1109/JESTPE.2018.2877766). Cited on page/s [49, 50, 53](#).
- [44] Jürgen Marchgraber, Christian Alács, Yi Guo, Wolfgang Gawlik, Adolfo Anta, Alexander Stimmer, Martin Lenz, Manuel Froschauer, and Michaela Leonhardt. Comparison of Control Strategies to Realize Synthetic Inertia in Converters. *Energies* **13** (13), 3491 (7 2020). ISSN 1996-1073. DOI [10.3390/en13133491](https://doi.org/10.3390/en13133491). Cited on page/s [49](#).

- [45] Augusto Matheus dos Santos Alonso, Leonardo Carlos Afonso, Danilo Iglesias Brandao, Elisabetta Tedeschi, and Fernando Pinhabel Marafao. Considerations on Communication Infrastructures for Cooperative Operation of Smart Inverters. In *2019 IEEE 15th Brazilian Power Electronics Conference and 5th IEEE Southern Power Electronics Conference (COBEP/SPEC)* pages 1–6 Santos, Brazil (12 2019). IEEE. ISBN 978-1-72814-180-0. DOI [10.1109/COBEP/SPEC44138.2019.9065382](https://doi.org/10.1109/COBEP/SPEC44138.2019.9065382). Cited on page/s [50, 53](#).
- [46] Danilo I. Brandao, Lucas S. Araujo, Augusto M. S. Alonso, Geovane L. dos Reis, Eduardo V. Liberado, and Fernando P. Marafao. Coordinated Control of Distributed Three- and Single-phase Inverters Connected to Three-Phase Three-Wire Microgrids. *IEEE J. Emerg. Sel. Topics Power Electron.* pages 1–1 (2019). ISSN 2168-6777, 2168-6785. DOI [10.1109/JESTPE.2019.2931122](https://doi.org/10.1109/JESTPE.2019.2931122). Cited on page/s [50](#).
- [47] Federico Milano, Florian Dörfler, Gabriela Hug, David J. Hill, and Gregor Verbić. Foundations and Challenges of Low-Inertia Systems (Invited Paper). pages 1–25 Dublin, Ireland (2018). IEEE. DOI [10.23919/PSCC.2018.8450880](https://doi.org/10.23919/PSCC.2018.8450880). Cited on page/s [52, 53](#).
- [48] Peter W. Sauer, M. A. Pai, and J. H. Chow. Power system dynamics and stability: With synchrophasor measurement and power system toolbox. Wiley Hoboken, NJ, USA second edition edition (2017). ISBN 978-1-119-35577-9. Cited on page/s [53](#).
- [49] Danilo I. Brandao, Willian M. Ferreira, Augusto M. S. Alonso, Elisabetta Tedeschi, and Fernando P. Marafao. Optimal Multiobjective Control of Low-Voltage AC Microgrids: Power Flow Regulation and Compensation of Reactive Power and Unbalance. *IEEE Trans. Smart Grid* **11** (2), 1239–1252 (3 2020). ISSN 1949-3053, 1949-3061. DOI [10.1109/TSG.2019.2933790](https://doi.org/10.1109/TSG.2019.2933790). Cited on page/s [53](#).
- [50] EU Commission Regulation. Guideline on capacity allocation and congestion management. EU 2015/1222. Technical report European Union (2015). eur-lex.europa.eu/eli/reg/2015/1222/oj. Accessed 2020-07-17. Cited on page/s [53](#).
- [51] Abbas A Akhil, Georgianne Huff, Aileen B Currier, Benjamin C Kaun, Dan M Rastler, Stella Bingqing Chen, Andrew L Cotter, Dale T Bradshaw, and William D Gauntlett. DOE/EPRI Electricity Storage Handbook in Collaboration with NRECA. Technical Report SAND2015-1002 Sandia National Laboratories Albuquerque, NM (1 2015). Cited on page/s [54](#).
- [52] L. Malesani, L. Rossetto, P. Tenti, and P. Tomasin. AC/DC/AC PWM converter with reduced energy storage in the DC link. *IEEE Trans. on Ind. Applicat.* **31** (2), 287–292 (3-4 1995). ISSN 00939994. DOI [10.1109/28.370275](https://doi.org/10.1109/28.370275). Cited on page/s [57](#).
- [53] W.J. Sarjeant, I.W. Clelland, and R.A. Price. Capacitive components for power electronics. *Proceedings of the IEEE* **89** (6), 846–855 (6 2001). ISSN 00189219. DOI [10.1109/5.931475](https://doi.org/10.1109/5.931475). Cited on page/s [58](#).
- [54] Infineon Technologies. Power and Sensing Selection Guide 2020. Technical report Infineon Technologies Austria AG (4 2020). Cited on page/s [58](#).
- [55] Paolo Tenti, Alessandro Costabeber, Paolo Mattavelli, Fernando Pinhabel Marafao, and Helmo K. M. Paredes. Load Characterization and Revenue Metering Under Non-Sinusoidal and Asymmetrical Operation. *IEEE Trans. Instrum. Meas.* **63** (2), 422–431 (2 2014). ISSN 0018-9456, 1557-9662. DOI [10.1109/TIM.2013.2280480](https://doi.org/10.1109/TIM.2013.2280480). Cited on page/s [59](#).
- [56] Remus Narcis Beres, Xiongfei Wang, Marco Liserre, Frede Blaabjerg, and Claus Leth Bak. A Review of Passive Power Filters for Three-Phase Grid-Connected Voltage-Source Converters. *IEEE J. Emerg. Sel. Topics Power Electron.* **4** (1), 54–69 (3 2016). ISSN 2168-6777, 2168-6785. DOI [10.1109/JESTPE.2015.2507203](https://doi.org/10.1109/JESTPE.2015.2507203). Cited on page/s [59](#).
- [57] Robert W Erickson and Dragan Maksimović. Fundamentals of Power Electronics. Springer 2 edition (2001). ISBN 978-0-306-48048-5. Cited on page/s [59](#).
- [58] Marco Liserre, Frede Blaabjerg, and Antonio Dell'Aquila. Step-by-step design procedure for a grid-connected three-phase PWM voltage source converter. *International*

- Journal of Electronics* **91** (8), 445–460 (8 2004). ISSN 0020-7217, 1362-3060. DOI [10.1080/00207210412331306186](https://doi.org/10.1080/00207210412331306186). Cited on page/s [59](#).
- [59] R. Peña-Alzola, M. Liserre, F. Blaabjerg, R. Sebastián, J. Dannehl, and F. W. Fuchs. Analysis of the Passive Damping Losses in LCL-Filter-Based Grid Converters. *IEEE Trans. Power Electron.* **28** (6), 2642–2646 (6 2013). ISSN 0885-8993, 1941-0107. doi: [10.1109/TPEL.2012.2222931](https://doi.org/10.1109/TPEL.2012.2222931). Cited on page/s [59](#).
 - [60] ABB. Technical data for vacuum cast coil dry-type transformers. Technical Report ILES100021-ZD ABB Zaragoza, Spain (2016). Cited on page/s [59](#).
 - [61] Siemens. The GEAFOL Neo: The optimum foundation for power distribution. Technical Report EMTR-B10021-00-7600 Siemens AG Erlangen, Germany (2017). Cited on page/s [59](#).
 - [62] K. Jalili and S. Bernet. Design of lcl Filters of Active-Front-End Two-Level Voltage-Source Converters. *IEEE Trans. Ind. Electron.* **56** (5), 1674–1689 (5 2009). ISSN 0278-0046. DOI [10.1109/TIE.2008.2011251](https://doi.org/10.1109/TIE.2008.2011251). Cited on page/s [60](#).
 - [63] Parikshith Channegowda and Vinod John. Filter Optimization for Grid Interactive Voltage Source Inverters. *IEEE Trans. Ind. Electron.* **57** (12), 4106–4114 (12 2010). ISSN 0278-0046, 1557-9948. DOI [10.1109/TIE.2010.2042421](https://doi.org/10.1109/TIE.2010.2042421). Cited on page/s [60](#).
 - [64] A. A. Rockhill, Marco Liserre, Remus Teodorescu, and Pedro Rodriguez. Grid-Filter Design for a Multimegawatt Medium-Voltage Voltage-Source Inverter. *IEEE Trans. Ind. Electron.* **58** (4), 1205–1217 (4 2011). ISSN 0278-0046, 1557-9948. DOI [10.1109/TIE.2010.2087293](https://doi.org/10.1109/TIE.2010.2087293). Cited on page/s [60](#).
 - [65] Jonas Muhlethaler, Mario Schweizer, Robert Blattmann, Johann W. Kolar, and Andreas Ecklebe. Optimal Design of LCL Harmonic Filters for Three-Phase PFC Rectifiers. *IEEE Trans. Power Electron.* **28** (7), 3114–3125 (7 2013). ISSN 0885-8993, 1941-0107. DOI [10.1109/TPEL.2012.2225641](https://doi.org/10.1109/TPEL.2012.2225641). Cited on page/s [60](#).
 - [66] Remus Narcis Beres, Xiongfei Wang, Frede Blaabjerg, Marco Liserre, and Claus Leth Bak. Optimal Design of High-Order Passive-Damped Filters for Grid-Connected Applications. *IEEE Trans. Power Electron.* **31** (3), 2083–2098 (3 2016). ISSN 0885-8993, 1941-0107. DOI [10.1109/TPEL.2015.2441299](https://doi.org/10.1109/TPEL.2015.2441299). Cited on page/s [60](#).
 - [67] Jinming Xu and Shaojun Xie. LCL-resonance damping strategies for grid-connected inverters with LCL filters: A comprehensive review. *J. Mod. Power Syst. Clean Energy* **6** (2), 292–305 (3 2018). ISSN 2196-5625, 2196-5420. doi: [10.1007/s40565-017-0319-7](https://doi.org/10.1007/s40565-017-0319-7). Cited on page/s [60](#).
 - [68] Joan Rocabert, Ruben Capo-Misut, Raul Santiago Munoz-Aguilar, Jose Ignacio Candela, and Pedro Rodriguez. Control of Energy Storage System Integrating Electrochemical Batteries and Supercapacitors for Grid-Connected Applications. *IEEE Trans. on Ind. Applicat.* **55** (2), 1853–1862 (3 2019). ISSN 0093-9994, 1939-9367. DOI [10.1109/TIA.2018.2873534](https://doi.org/10.1109/TIA.2018.2873534). Cited on page/s [60](#).
 - [69] Lucas S. Xavier, William C. S. Amorim, Allan F. Cupertino, Victor F. Mendes, Wallace C. do Boaventura, and Heverton A. Pereira. Power converters for battery energy storage systems connected to medium voltage systems: A comprehensive review. *BMC Energy* **1** (1), 7 (12 2019). ISSN 2524-4469. DOI [10.1186/s42500-019-0006-5](https://doi.org/10.1186/s42500-019-0006-5). Cited on page/s [60](#).
 - [70] IEC 61892:2019. Mobile and fixed offshore units - Electrical installations. IEC Geneva, Switzerland 4.0 edition (4 2019). Cited on page/s [61](#).
 - [71] P Pei, Q Chang, and T Tang. A quick evaluating method for automotive fuel cell lifetime. *International Journal of Hydrogen Energy* **33** (14), 3829–3836 (7 2008). ISSN 03603199. DOI [10.1016/j.ijhydene.2008.04.048](https://doi.org/10.1016/j.ijhydene.2008.04.048). Cited on page/s [62](#).
 - [72] Håvard Devold. Oil and gas production handbook, an introduction to oil and gas production, transport, refining and petrochemical industry. ABB Oil and Gas Oslo, Norway 3.0 edition (2013). ISBN 978-82-997886-3-2. URL

- https://library.e.abb.com/public/34d5b70e18f7d6c8c1257be500438ac3/Oil%20and%20gas%20production%20handbook%20ed3x0_web.pdf. Cited on page/s 62.
- [73] DNV-GL. Joint Industry Project: Wind-powered water injection. Technical report DNV-GL Høvik, Norway (4 2016). URL <https://www.dnvg.com/research/power-and-renewables/pr-win-win.html>. Cited on page/s 62.
- [74] Santiago Sanchez, Elisabetta Tedeschi, Jesus Silva, Muhammad Jafar, and Alexandra Marichalar. Smart load management of water injection systems in offshore oil and gas platforms integrating wind power. *IET Renewable Power Generation* **11** (9), 1153–1162 (7 2017). ISSN 1752-1416, 1752-1424. DOI [10.1049/iet-rpg.2016.0989](https://doi.org/10.1049/iet-rpg.2016.0989). Cited on page/s 62.
- [75] Erick Alves, Santiago Sanchez, Danilo Brandao, and Elisabetta Tedeschi. Smart Load Management with Energy Storage for Power Quality Enhancement in Wind-Powered Oil and Gas Applications. *Energies* **12** (15), 2985 (2019). ISSN 1996-1073. doi: 10.3390/en12152985. Cited on page/s 62.
- [76] Saft. Intensium Max+ 20P product datasheet. Technical report Saft (3 2017). Cited on page/s 64.
- [77] Siemens. Sinacon pv photovoltaic central inverter: Technical data. Technical Report SIDS-B10020-00-7600 Siemens AG Erlangen, Germany (2020). URL <https://assets.new.siemens.com/siemens/assets/api/uuid:cb65b0d3-6425-48f5-92cb-cc217d2d5285/sinacon-pv-technical-data-en.pdf>. Cited on page/s 64.
- [78] Erick F. Alves. Efantnu/hybrid-ess-design: Review 1 release (version v1.1). Zenodo (3 2021). URL <https://zenodo.org/record/4601067>. DOI [10.5281/zenodo.4601067](https://doi.org/10.5281/zenodo.4601067). Cited on page/s 64, 67, 71.
- [79] Erick F. Alves. Efantnu/pwrsys-matlab: Initial release. Zenodo (12 2020). URL <https://zenodo.org/record/4384758>. DOI [10.5281/zenodo.4384758](https://doi.org/10.5281/zenodo.4384758). Cited on page/s 65.

CHAPTER 6

Title of the chapter 6 displayed in the page

Author 1^{1,*}, Author 2^{1,2,*}, Author 3³, Author 4¹, Author 5¹, Author 6¹, Author 7^{2,4,#} and Author 8^{1,#}

First published in: *Scientific Reports* **10**, 853 (2020).

DOI: [10.1038/s41598-019-55424-z](https://doi.org/10.1038/s41598-019-55424-z)



Open Access This article is licensed under a Creative Commons Attribution 4.0 International License. It means that unrestricted use, sharing, adaptation, distribution, and reproduction in any medium or format are allowed, as long as the original author(s) and the source are appropriately credited, a link to the Creative Commons license is provided, and any changes made are indicated. To view a copy of this license, please visit <http://creativecommons.org/licenses/by/4.0/>.

© Liudi Mulyo *et al.*, 2020.

Contributions

Nam dui ligula, fringilla a, euismod sodales, sollicitudin vel, wisi. Morbi auctor lorem non justo. Nam lacus libero, pretium at, lobortis vitae, ultricies et, tellus. Donec aliquet, tortor sed accumsan bibendum, erat ligula aliquet magna, vitae ornare odio metus a mi. Morbi ac orci et nisl hendrerit mollis. Suspendisse ut massa. Cras nec ante. Pellentesque a nulla. Cum sociis natoque penatibus et magnis dis parturient montes, nascetur ridiculus mus. Aliquam tincidunt urna. Nulla ullamcorper vestibulum turpis. Pellentesque cursus luctus mauris.

¹Department X, University 1, City A, Country B. ²Department Y, University 2, City C, Country D.

³Institute E, City F, Country G. ⁴Research Center H, University I, City J, Country K. [#]e-mail: author7@university2.ac.countryD and author8@universityl.countryK

ABSTRACT

Lorem ipsum dolor sit amet, consectetuer adipiscing elit. Ut purus elit, vestibulum ut, placerat ac, adipiscing vitae, felis. Curabitur dictum gravida mauris. Nam arcu libero, nonummy eget, consectetuer id, vulputate a, magna. Donec vehicula augue eu neque. Pellentesque habitant morbi tristique senectus et netus et malesuada fames ac turpis egestas. Mauris ut leo. Cras viverra metus rhoncus sem. Nulla et lectus vestibulum urna fringilla ultrices. Phasellus eu tellus sit amet tortor gravida placerat. Integer sapien est, iaculis in, pretium quis, viverra ac, nunc. Praesent eget sem vel leo ultrices bibendum. Aenean faucibus. Morbi dolor nulla, malesuada eu, pulvinar at, mollis ac, nulla. Curabitur auctor semper nulla. Donec varius orci eget risus. Duis nibh mi, congue eu, accumsan eleifend, sagittis quis, diam. Duis eget orci sit amet orci dignissim rutrum.

As in [??](#). Lorem ipsum dolor sit amet, consectetuer adipiscing elit [1]. Ut purus elit, vestibulum ut, placerat ac, adipiscing vitae, felis [1](#). Curabitur dictum gravida mauris. Nam arcu libero, nonummy eget, consectetuer id, vulputate a, magna. Donec vehicula augue eu neque [\[2\]](#). Pellentesque habitant morbi tristique senectus et netus et malesuada fames ac turpis egestas [2](#). Mauris ut leo. Cras viverra metus rhoncus sem [\[3\]](#). Nulla et lectus vestibulum urna fringilla ultrices. Phasellus eu tellus sit amet tortor gravida placerat [3](#). Integer sapien est, iaculis in, pretium quis, viverra ac, nunc. Praesent eget sem vel leo ultrices bibendum [\[4\]](#). Aenean faucibus. Morbi dolor nulla, malesuada eu, pulvinar at [\(6.1\)](#), mollis ac, nulla. Curabitur auctor semper nulla [4](#). Donec varius orci eget risus. Duis nibh mi, congue eu, accumsan eleifend, sagittis quis, diam. Duis eget orci sit amet orci dignissim rutrum [\[1–6\]](#).

6.1 SECTION 1 IN CHAPTER 6

Nam dui ligula, fringilla a, euismod sodales, sollicitudin vel, wisi. Morbi auctor lorem non justo. Nam lacus libero, pretium at, lobortis vitae, ultricies et, tellus. Donec aliquet, tortor sed accumsan bibendum, erat ligula aliquet magna, vitae ornare odio metus a mi. Morbi ac orci et nisl hendrerit mollis. Suspendisse ut massa. Cras nec ante. Pellentesque a nulla. Cum sociis natoque penatibus et magnis dis parturient montes, nascetur ridiculus mus. Aliquam tincidunt urna. Nulla ullamcorper vestibulum turpis. Pellentesque cursus luctus mauris.

Nulla malesuada porttitor diam. Donec felis erat, congue non, volutpat at, tincidunt tristique, libero. Vivamus viverra fermentum felis. Donec nonummy pellentesque ante. Phasellus adipiscing semper elit. Proin fermentum massa ac quam. Sed diam turpis, molestie vitae, placerat a, molestie nec, leo. Maecenas

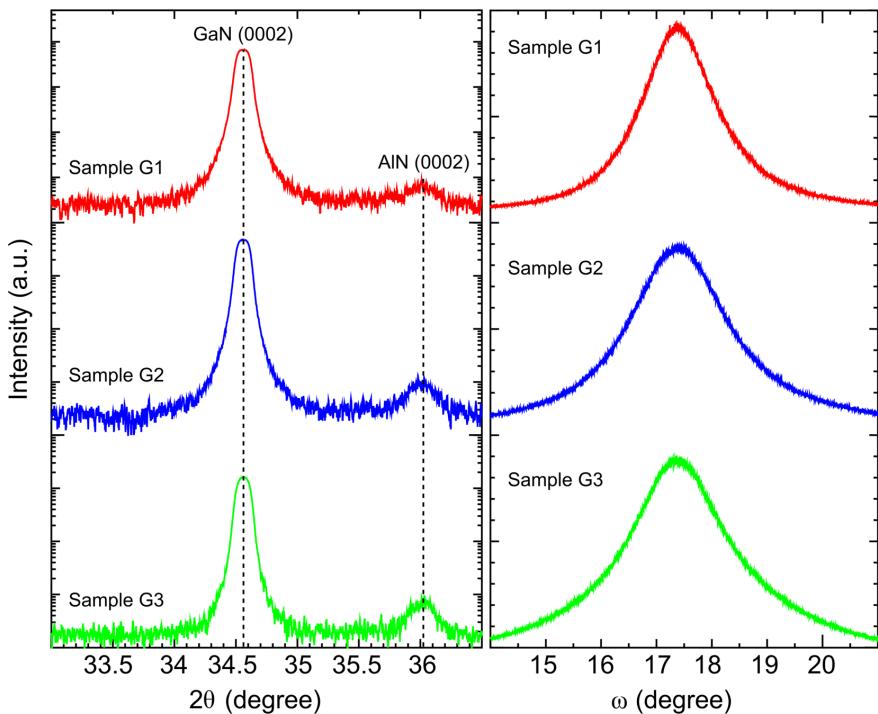


FIGURE 6.1 | HRXRD measurements of the nanocolumns. (a) 2θ - ω scanning curve and (b) ω scanning curve of samples G1, G2 and G3 (adapted with permission from ref. 4 © Liudi Mulyo et al, 2020).

lacinia. Nam ipsum ligula, eleifend at, accumsan nec, suscipit a, ipsum. Morbi blandit ligula feugiat magna. Nunc eleifend consequat lorem. Sed lacinia nulla vitae enim. Pellentesque tincidunt purus vel magna. Integer non enim. Praesent euismod nunc eu purus. Donec bibendum quam in tellus. Nullam cursus pulvinar lectus. Donec et mi. Nam vulputate metus eu enim. Vestibulum pellentesque felis eu massa.

Quisque ullamcorper placerat ipsum. Cras nibh. Morbi vel justo vitae lacus tincidunt ultrices. Lorem ipsum dolor sit amet, consectetur adipiscing elit. In hac habitasse platea dictumst. Integer tempus convallis augue. Etiam facilisis. Nunc elementum fermentum wisi. Aenean placerat. Ut imperdiet, enim sed gravida sollicitudin, felis odio placerat quam, ac pulvinar elit purus eget enim. Nunc vitae tortor. Proin tempus nibh sit amet nisl. Vivamus quis tortor vitae risus porta vehicula.

6.1.1 *Subsection 6.1 of section 1 in chapter 6*

Fusce mauris. Vestibulum luctus nibh at lectus. Sed bibendum, nulla a faucibus semper, leo velit ultricies tellus, ac venenatis arcu wisi vel nisl. Vestibulum diam. Aliquam pellentesque, augue quis sagittis posuere, turpis lacus congue quam, in hendrerit risus eros eget felis. Maecenas eget erat in sapien mattis porttitor. Vestibulum porttitor. Nulla facilisi. Sed a turpis eu lacus commodo facilisis. Morbi fringilla, wisi in dignissim interdum, justo lectus sagittis dui, et vehicula libero dui cursus dui. Mauris tempor ligula sed lacus. Duis cursus enim ut augue. Cras ac magna. Cras nulla. Nulla egestas. Curabitur a leo. Quisque egestas wisi eget nunc. Nam feugiat lacus vel est. Curabitur consectetur.

Suspendisse vel felis. Ut lorem lorem, interdum eu, tincidunt sit amet, laoreet vitae, arcu. Aenean faucibus pede eu ante. Praesent enim elit, rutrum at, molestie non, nonummy vel, nisl. Ut lectus eros, malesuada sit amet, fermentum eu, sodales cursus, magna. Donec eu purus. Quisque vehicula, urna sed ultricies auctor, pede lorem egestas dui, et convallis elit erat sed nulla. Donec luctus. Curabitur et nunc. Aliquam dolor odio, commodo pretium, ultricies non, pharetra in, velit. Integer arcu est, nonummy in, fermentum faucibus, egestas vel, odio.

Sed commodo posuere pede. Mauris ut est. Ut quis purus. Sed ac odio. Sed vehicula hendrerit sem. Duis non odio. Morbi ut dui. Sed accumsan risus eget odio. In hac habitasse platea dictumst. Pellentesque non elit. Fusce sed justo eu urna porta tincidunt. Mauris felis odio, sollicitudin sed, volutpat a, ornare ac, erat. Morbi quis dolor. Donec pellentesque, erat ac sagittis semper, nunc dui lobortis purus, quis congue purus metus ultricies tellus. Proin et quam. Class aptent taciti sociosqu ad litora torquent per conubia nostra, per inceptos

hymenaeos. Praesent sapien turpis, fermentum vel, eleifend faucibus, vehicula eu, lacus.

6.1.2 Subsection 6.2 of section 1 in chapter 6

Pellentesque habitant morbi tristique senectus et netus et malesuada fames ac turpis egestas. Donec odio elit, dictum in, hendrerit sit amet, egestas sed, leo. Praesent feugiat sapien aliquet odio. Integer vitae justo. Aliquam vestibulum fringilla lorem. Sed neque lectus, consectetur at, consectetur sed, eleifend ac, lectus. Nulla facilisi. Pellentesque eget lectus. Proin eu metus. Sed porttitor. In hac habitasse platea dictumst. Suspendisse eu lectus. Ut mi mi, lacinia sit amet, placerat et, mollis vitae, dui. Sed ante tellus, tristique ut, iaculis eu, malesuada ac, dui. Mauris nibh leo, facilisis non, adipiscimus quis, ultrices a, dui.

Morbi luctus, wisi viverra faucibus pretium, nibh est placerat odio, nec commodo wisi enim eget quam. Quisque libero justo, consectetur a, feugiat vitae, porttitor eu, libero. Suspendisse sed mauris vitae elit sollicitudin malesuada. Maecenas ultricies eros sit amet ante. Ut venenatis velit. Maecenas sed mi eget dui varius euismod. Phasellus aliquet volutpat odio. Vestibulum ante ipsum primis in faucibus orci luctus et ultrices posuere cubilia Curae; Pellentesque sit amet pede ac sem eleifend consectetur. Nullam elementum, urna vel imperdiet sodales, elit ipsum pharetra ligula, ac pretium ante justo a nulla. Curabitur tristique arcu eu metus. Vestibulum lectus. Proin mauris. Proin eu nunc eu urna hendrerit faucibus. Aliquam auctor, pede consequat laoreet varius, eros tellus scelerisque quam, pellentesque hendrerit ipsum dolor sed augue. Nulla nec lacus.

Suspendisse vitae elit. Aliquam arcu neque, ornare in, ullamcorper quis, commodo eu, libero. Fusce sagittis erat at erat tristique mollis. Maecenas sapien libero, molestie et, lobortis in, sodales eget, dui. Morbi ultrices rutrum lorem. Nam elementum ullamcorper leo. Morbi dui. Aliquam sagittis. Nunc placerat. Pellentesque tristique sodales est. Maecenas imperdiet lacinia velit. Cras non urna. Morbi eros pede, suscipit ac, varius vel, egestas non, eros. Praesent malesuada, diam id pretium elementum, eros sem dictum tortor, vel consectetur odio sem sed wisi.

Sed feugiat. Cum sociis natoque penatibus et magnis dis parturient montes, nascetur ridiculus mus. Ut pellentesque augue sed urna. Vestibulum diam eros, fringilla et, consectetur eu, nonummy id, sapien. Nullam at lectus. In sagittis ultrices mauris. Curabitur malesuada erat sit amet massa. Fusce blandit. Aliquam erat volutpat. Aliquam euismod. Aenean vel lectus. Nunc imperdiet justo nec dolor.

6.2 SHORT SECTION TITLE IN THE CHAPTER

Sed feugiat. Cum sociis natoque penatibus et magnis dis parturient montes, nascetur ridiculus mus. Ut pellentesque augue sed urna. Vestibulum diam eros, fringilla et, consectetur eu, nonummy id, sapien. Nullam at lectus. In sagittis ultrices mauris. Curabitur malesuada erat sit amet massa. Fusce blandit. Aliquam erat volutpat. Aliquam euismod. Aenean vel lectus. Nunc imperdiet justo nec dolor.

Etiam euismod. Fusce facilisis lacinia dui. Suspendisse potenti. In mi erat, cursus id, nonummy sed, ullamcorper eget, sapien. Praesent pretium, magna in eleifend egestas, pede pede pretium lorem, quis consectetur tortor sapien facilisis magna. Mauris quis magna varius nulla scelerisque imperdiet. Aliquam non quam. Aliquam porttitor quam a lacus. Praesent vel arcu ut tortor cursus volutpat. In vitae pede quis diam bibendum placerat. Fusce elementum convallis neque. Sed dolor orci, scelerisque ac, dapibus nec, ultricies ut, mi. Duis nec dui quis leo sagittis commodo.

Aliquam lectus. Vivamus leo. Quisque ornare tellus ullamcorper nulla. Mauris porttitor pharetra tortor. Sed fringilla justo sed mauris. Mauris tellus. Sed non leo. Nullam elementum, magna in cursus sodales, augue est scelerisque sapien, venenatis congue nulla arcu et pede. Ut suscipit enim vel sapien. Donec congue. Maecenas urna mi, suscipit in, placerat ut, vestibulum ut, massa. Fusce ultrices nulla et nisl.

Etiam ac leo a risus tristique nonummy. Donec dignissim tincidunt nulla. Vestibulum rhoncus molestie odio. Sed lobortis, justo et pretium lobortis, mauris turpis condimentum augue, nec ultricies nibh arcu pretium enim. Nunc purus neque, placerat id, imperdiet sed, pellentesque nec, nisl. Vestibulum imperdiet neque non sem accumsan laoreet. In hac habitasse platea dictumst. Etiam condimentum facilisis libero. Suspendisse in elit quis nisl aliquam dapibus. Pellentesque auctor sapien. Sed egestas sapien nec lectus. Pellentesque vel dui vel neque bibendum viverra. Aliquam porttitor nisl nec pede. Proin mattis libero vel turpis. Donec rutrum mauris et libero. Proin euismod porta felis. Nam lobortis, metus quis elementum commodo, nunc lectus elementum mauris, eget vulputate ligula tellus eu neque. Vivamus eu dolor.

Nulla in ipsum. Praesent eros nulla, congue vitae, euismod ut, commodo a, wisi. Pellentesque habitant morbi tristique senectus et netus et malesuada fames ac turpis egestas. Aenean nonummy magna non leo. Sed felis erat, ullamcorper in, dictum non, ultricies ut, lectus. Proin vel arcu a odio lobortis euismod. Vestibulum ante ipsum primis in faucibus orci luctus et ultrices posuere cubilia Curae; Proin ut est. Aliquam odio. Pellentesque massa turpis, cursus eu, euismod nec, tempor congue, nulla. Duis viverra gravida mauris. Cras tincidunt. Curabitur eros ligula, varius ut, pulvinar in, cursus faucibus,

augue.

Nulla mattis luctus nulla. Duis commodo velit at leo. Aliquam vulputate magna et leo. Nam vestibulum ullamcorper leo. Vestibulum condimentum rutrum mauris. Donec id mauris. Morbi molestie justo et pede. Vivamus eget turpis sed nisl cursus tempor. Curabitur mollis sapien condimentum nunc. In wisi nisl, malesuada at, dignissim sit amet, lobortis in, odio. Aenean consequat arcu a ante. Pellentesque porta elit sit amet orci. Etiam at turpis nec elit ultricies imperdier. Nulla facilisi. In hac habitasse platea dictumst. Suspendisse viverra aliquam risus. Nullam pede justo, molestie nonummy, scelerisque eu, facilisis vel, arcu.

Curabitur tellus magna, porttitor a, commodo a, commodo in, tortor. Donec interdum. Praesent scelerisque. Maecenas posuere sodales odio. Vivamus metus lacus, varius quis, imperdier quis, rhoncus a, turpis. Etiam ligula arcu, elementum a, venenatis quis, sollicitudin sed, metus. Donec nunc pede, tincidunt in, venenatis vitae, faucibus vel, nibh. Pellentesque wisi. Nullam malesuada. Morbi ut tellus ut pede tincidunt porta. Lorem ipsum dolor sit amet, consectetur adipiscing elit. Etiam congue neque id dolor.

Donec et nisl at wisi luctus bibendum. Nam interdum tellus ac libero. Sed sem justo, laoreet vitae, fringilla at, adipiscing ut, nibh. Maecenas non sem quis tortor eleifend fermentum. Etiam id tortor ac mauris porta vulputate. Integer porta neque vitae massa. Maecenas tempus libero a libero posuere dictum. Vestibulum ante ipsum primis in faucibus orci luctus et ultrices posuere cubilia Curae; Aenean quis mauris sed elit commodo placerat. Class aptent taciti sociosqu ad litora torquent per conubia nostra, per inceptos hymenaeos. Vivamus rhoncus tincidunt libero. Etiam elementum pretium justo. Vivamus est. Morbi a tellus eget pede tristique commodo. Nulla nisl. Vestibulum sed nisl eu sapien cursus rutrum. See [6.1](#)

TABLE 6.1 | Al-content of each axial nanocolumn segment for the vertical GaN/AlGaN nanocolumn ensemble (top to bottom) obtained from fitting the simulation model to the HRXRD 2θ-ω scan data

| Segment | Thickness (nm) | Al bottom (%) | Al top (%) |
|--------------------------|----------------|---------------|------------|
| p-GaN | 1 | 2 | 3 |
| p-AlGaN (linear grading) | 4 | 5 | 6 |
| i-GaN quantum disk | 7 | 8 | 9 |
| n-AlGaN (linear grading) | 10 | 11 | 12 |
| n-GaN | 13 | 14 | 15 |
| n-AlN buffer layer | 16 | 17 | 18 |

6.2.1 Subsection 6.2 of section 2 in chapter 6

Aliquam lectus. Vivamus leo. Quisque ornare tellus ullamcorper nulla. Mauris porttitor pharetra tortor. Sed fringilla justo sed mauris. Mauris tellus. Sed non leo. Nullam elementum, magna in cursus sodales, augue est scelerisque sapien, venenatis congue nulla arcu et pede. Ut suscipit enim vel sapien. Donec congue. Maecenas urna mi, suscipit in, placerat ut, vestibulum ut, massa. Fusce ultrices nulla et nisl.

Etiam ac leo a risus tristique nonummy. Donec dignissim tincidunt nulla. Vestibulum rhoncus molestie odio. Sed lobortis, justo et pretium lobortis, mauris turpis condimentum augue, nec ultricies nibh arcu pretium enim. Nunc purus neque, placerat id, imperdiet sed, pellentesque nec, nisl. Vestibulum imperdiet neque non sem accumsan laoreet. In hac habitasse platea dictumst. Etiam condimentum facilisis libero. Suspendisse in elit quis nisl aliquam dapibus. Pellentesque auctor sapien. Sed egestas sapien nec lectus. Pellentesque vel dui vel neque bibendum viverra. Aliquam porttitor nisl nec pede. Proin mattis libero vel turpis. Donec rutrum mauris et libero. Proin euismod porta felis. Nam lobortis, metus quis elementum commodo, nunc lectus elementum mauris, eget vulputate ligula tellus eu neque. Vivamus eu dolor. See [Appendix C](#) for the reffig:figures/paper-iv/fig-7 and reffig:figures/paper-iv/fig-8.

6.3 REFERENCES

- [1] A. Liudi Mulyo, Y. Konno, J. S. Nilsen, A. T. J. van Helvoort, B.-O. Fimland, H. Weman, and K. Kishino. [Growth study of self-assembled GaN nanocolumns on silica glass by plasma assisted molecular beam epitaxy](#). *Journal of Crystal Growth* **480**, 67–73 (2017). Cited on page/s 80.
- [2] A. Liudi Mulyo, M. K. Rajpalke, H. Kuroe, P.-E. Vullum, H. Weman, B.-O. Fimland, and K. Kishino. [Vertical GaN nanocolumns grown on graphene intermediated with a thin AlN buffer layer](#). *Nanotechnology* **30** (1), 015604 (2018). Cited on page/s 80.
- [3] I. M. Höiaas, A. Liudi Mulyo, P. E. Vullum, D.-C. Kim, L. Ahtapodov, B.-O. Fimland, K. Kishino, and H. Weman. [GaN/AlGaN Nanocolumn Ultraviolet Light-Emitting Diode Using Double-Layer Graphene as Substrate and Transparent Electrode](#). *Nano Letters* **19** (3), 1649–1658 (2019). Cited on page/s 80.
- [4] A. Liudi Mulyo, M. K. Rajpalke, P. E. Vullum, H. Weman, K. Kishino, and B.-O. Fimland. [The influence of AlN buffer layer on the growth of self-assembled GaN nanocolumns on graphene](#). *Scientific Reports* **10** (1), 853 (2020). Cited on page/s 80, 81.
- [5] A. Liudi Mulyo *et al.* [The Influence of AlN Buffer Layer on the Growth of Self-Assembled GaN Nanocolumns on Graphene](#). *Unpublished* (n.d.). Cited on page/s 80.
- [6] A. Liudi Mulyo *et al.* [Utilization of Graphene as Substrate and Bottom Electrode for High-Density and Vertically-Aligned GaN/AlGaN Nanocolumns](#). *Unpublished* (n.d.). Cited on page/s 80.

Part III

EPILOGUE

CHAPTER 7

Conclusion

Lorem ipsum dolor sit amet, consectetuer adipiscing elit [1]. Ut purus elit, vestibulum ut, placerat ac, adipiscing vitae, felis 1. Curabitur dictum gravida mauris. Nam arcu libero, nonummy eget, consectetuer id, vulputate a, magna. Donec vehicula augue eu neque [2]. Pellentesque habitant morbi tristique senectus et netus et malesuada fames ac turpis egestas 2. Mauris ut leo. Cras viverra metus rhoncus sem [3]. Nulla et lectus vestibulum urna fringilla ultrices. Phasellus eu tellus sit amet tortor gravida placerat 3. Integer sapien est, iaculis in, pretium quis, viverra ac, nunc. Praesent eget sem vel leo ultrices bibendum [4]. Aenean faucibus. Morbi dolor nulla, malesuada eu, pulvinar at (1.1), mollis ac, nulla. Curabitur auctor semper nulla 4. Donec varius orci eget risus. Duis nibh mi, congue eu, accumsan eleifend, sagittis quis, diam. Duis eget orci sit amet orci dignissim rutrum [1–6]. For ?? and ??, as well as [Chapter 6](#)

7.1 SECTION 1 IN CHAPTER 7

Nam dui ligula, fringilla a, euismod sodales, sollicitudin vel, wisi. Morbi auctor lorem non justo. Nam lacus libero, pretium at, lobortis vitae, ultricies et, tellus. Donec aliquet, tortor sed accumsan bibendum, erat ligula aliquet magna, vitae ornare odio metus a mi. Morbi ac orci et nisl hendrerit mollis. Suspendisse ut massa. Cras nec ante. Pellentesque a nulla. Cum sociis natoque penatibus et magnis dis parturient montes, nascetur ridiculus mus. Aliquam tincidunt urna. Nulla ullamcorper vestibulum turpis. Pellentesque cursus luctus mauris.

Nulla malesuada porttitor diam. Donec felis erat, congue non, volutpat at, tincidunt tristique, libero. Vivamus viverra fermentum felis. Donec nonummy pellentesque ante. Phasellus adipiscing semper elit. Proin fermentum massa ac quam. Sed diam turpis, molestie vitae, placerat a, molestie nec, leo. Maecenas lacinia. Nam ipsum ligula, eleifend at, accumsan nec, suscipit a, ipsum. Morbi blandit ligula feugiat magna. Nunc eleifend consequat lorem. Sed lacinia nulla vitae enim. Pellentesque tincidunt purus vel magna. Integer non enim. Praesent euismod nunc eu purus. Donec bibendum quam in tellus. Nullam cursus pulvinar lectus. Donec et mi. Nam vulputate metus eu enim. Vestibulum

pellentesque felis eu massa.

Quisque ullamcorper placerat ipsum. Cras nibh. Morbi vel justo vitae lacus tincidunt ultrices. Lorem ipsum dolor sit amet, consectetur adipiscing elit. In hac habitasse platea dictumst. Integer tempus convallis augue. Etiam facilisis. Nunc elementum fermentum wisi. Aenean placerat. Ut imperdiet, enim sed gravida sollicitudin, felis odio placerat quam, ac pulvinar elit purus eget enim. Nunc vitae tortor. Proin tempus nibh sit amet nisl. Vivamus quis tortor vitae risus porta vehicula.

7.1.1 *Subsection 7.1 of section 1 in chapter 7*

Fusce mauris. Vestibulum luctus nibh at lectus. Sed bibendum, nulla a faucibus semper, leo velit ultricies tellus, ac venenatis arcu wisi vel nisl. Vestibulum diam. Aliquam pellentesque, augue quis sagittis posuere, turpis lacus congue quam, in hendrerit risus eros eget felis. Maecenas eget erat in sapien mattis porttitor. Vestibulum porttitor. Nulla facilisi. Sed a turpis eu lacus commodo facilisis. Morbi fringilla, wisi in dignissim interdum, justo lectus sagittis dui, et vehicula libero dui cursus dui. Mauris tempor ligula sed lacus. Duis cursus enim ut augue. Cras ac magna. Cras nulla. Nulla egestas. Curabitur a leo. Quisque egestas wisi eget nunc. Nam feugiat lacus vel est. Curabitur consectetur.

Suspendisse vel felis. Ut lorem lorem, interdum eu, tincidunt sit amet, laoreet vitae, arcu. Aenean faucibus pede eu ante. Praesent enim elit, rutrum at, molestie non, nonummy vel, nisl. Ut lectus eros, malesuada sit amet, fermentum eu, sodales cursus, magna. Donec eu purus. Quisque vehicula, urna sed ultricies auctor, pede lorem egestas dui, et convallis elit erat sed nulla. Donec luctus. Curabitur et nunc. Aliquam dolor odio, commodo pretium, ultricies non, pharetra in, velit. Integer arcu est, nonummy in, fermentum faucibus, egestas vel, odio.

Sed commodo posuere pede. Mauris ut est. Ut quis purus. Sed ac odio. Sed vehicula hendrerit sem. Duis non odio. Morbi ut dui. Sed accumsan risus eget odio. In hac habitasse platea dictumst. Pellentesque non elit. Fusce sed justo eu urna porta tincidunt. Mauris felis odio, sollicitudin sed, volutpat a, ornare ac, erat. Morbi quis dolor. Donec pellentesque, erat ac sagittis semper, nunc dui lobortis purus, quis congue purus metus ultricies tellus. Proin et quam. Class aptent taciti sociosqu ad litora torquent per conubia nostra, per inceptos hymenaeos. Praesent sapien turpis, fermentum vel, eleifend faucibus, vehicula eu, lacus.

7.1.2 Subsection 7.2 of section 1 in chapter 7

Pellentesque habitant morbi tristique senectus et netus et malesuada fames ac turpis egestas. Donec odio elit, dictum in, hendrerit sit amet, egestas sed, leo. Praesent feugiat sapien aliquet odio. Integer vitae justo. Aliquam vestibulum fringilla lorem. Sed neque lectus, consectetur at, consectetur sed, eleifend ac, lectus. Nulla facilisi. Pellentesque eget lectus. Proin eu metus. Sed porttitor. In hac habitasse platea dictumst. Suspendisse eu lectus. Ut mi mi, lacinia sit amet, placerat et, mollis vitae, dui. Sed ante tellus, tristique ut, iaculis eu, malesuada ac, dui. Mauris nibh leo, facilisis non, adipiscing quis, ultrices a, dui.

Morbi luctus, wisi viverra faucibus pretium, nibh est placerat odio, nec commodo wisi enim eget quam. Quisque libero justo, consectetur a, feugiat vitae, porttitor eu, libero. Suspendisse sed mauris vitae elit sollicitudin malesuada. Maecenas ultricies eros sit amet ante. Ut venenatis velit. Maecenas sed mi eget dui varius euismod. Phasellus aliquet volutpat odio. Vestibulum ante ipsum primis in faucibus orci luctus et ultrices posuere cubilia Curae; Pellentesque sit amet pede ac sem eleifend consectetur. Nullam elementum, urna vel imperdiet sodales, elit ipsum pharetra ligula, ac pretium ante justo a nulla. Curabitur tristique arcu eu metus. Vestibulum lectus. Proin mauris. Proin eu nunc eu urna hendrerit faucibus. Aliquam auctor, pede consequat laoreet varius, eros tellus scelerisque quam, pellentesque hendrerit ipsum dolor sed augue. Nulla nec lacus.

Suspendisse vitae elit. Aliquam arcu neque, ornare in, ullamcorper quis, commodo eu, libero. Fusce sagittis erat at erat tristique mollis. Maecenas sapien libero, molestie et, lobortis in, sodales eget, dui. Morbi ultrices rutrum lorem. Nam elementum ullamcorper leo. Morbi dui. Aliquam sagittis. Nunc placerat. Pellentesque tristique sodales est. Maecenas imperdiet lacinia velit. Cras non urna. Morbi eros pede, suscipit ac, varius vel, egestas non, eros. Praesent malesuada, diam id pretium elementum, eros sem dictum tortor, vel consectetur odio sem sed wisi.

Sed feugiat. Cum sociis natoque penatibus et magnis dis parturient montes, nascetur ridiculus mus. Ut pellentesque augue sed urna. Vestibulum diam eros, fringilla et, consectetur eu, nonummy id, sapien. Nullam at lectus. In sagittis ultrices mauris. Curabitur malesuada erat sit amet massa. Fusce blandit. Aliquam erat volutpat. Aliquam euismod. Aenean vel lectus. Nunc imperdiet justo nec dolor.

7.2 SHORT SECTION TITLE IN THE CHAPTER

Sed feugiat. Cum sociis natoque penatibus et magnis dis parturient montes, nascetur ridiculus mus. Ut pellentesque augue sed urna. Vestibulum diam eros, fringilla et, consectetur eu, nonummy id, sapien. Nullam at lectus. In sagittis ultrices mauris. Curabitur malesuada erat sit amet massa. Fusce blandit. Aliquam erat volutpat. Aliquam euismod. Aenean vel lectus. Nunc imperdiet justo nec dolor.

Etiam euismod. Fusce facilisis lacinia dui. Suspendisse potenti. In mi erat, cursus id, nonummy sed, ullamcorper eget, sapien. Praesent pretium, magna in eleifend egestas, pede pede pretium lorem, quis consectetur tortor sapien facilisis magna. Mauris quis magna varius nulla scelerisque imperdiet. Aliquam non quam. Aliquam porttitor quam a lacus. Praesent vel arcu ut tortor cursus volutpat. In vitae pede quis diam bibendum placerat. Fusce elementum convallis neque. Sed dolor orci, scelerisque ac, dapibus nec, ultricies ut, mi. Duis nec dui quis leo sagittis commodo.

Aliquam lectus. Vivamus leo. Quisque ornare tellus ullamcorper nulla. Mauris porttitor pharetra tortor. Sed fringilla justo sed mauris. Mauris tellus. Sed non leo. Nullam elementum, magna in cursus sodales, augue est scelerisque sapien, venenatis congue nulla arcu et pede. Ut suscipit enim vel sapien. Donec congue. Maecenas urna mi, suscipit in, placerat ut, vestibulum ut, massa. Fusce ultrices nulla et nisl.

Etiam ac leo a risus tristique nonummy. Donec dignissim tincidunt nulla. Vestibulum rhoncus molestie odio. Sed lobortis, justo et pretium lobortis, mauris turpis condimentum augue, nec ultricies nibh arcu pretium enim. Nunc purus neque, placerat id, imperdiet sed, pellentesque nec, nisl. Vestibulum imperdiet neque non sem accumsan laoreet. In hac habitasse platea dictumst. Etiam condimentum facilisis libero. Suspendisse in elit quis nisl aliquam dapibus. Pellentesque auctor sapien. Sed egestas sapien nec lectus. Pellentesque vel dui vel neque bibendum viverra. Aliquam porttitor nisl nec pede. Proin mattis libero vel turpis. Donec rutrum mauris et libero. Proin euismod porta felis. Nam lobortis, metus quis elementum commodo, nunc lectus elementum mauris, eget vulputate ligula tellus eu neque. Vivamus eu dolor.

Nulla in ipsum. Praesent eros nulla, congue vitae, euismod ut, commodo a, wisi. Pellentesque habitant morbi tristique senectus et netus et malesuada fames ac turpis egestas. Aenean nonummy magna non leo. Sed felis erat, ullamcorper in, dictum non, ultricies ut, lectus. Proin vel arcu a odio lobortis euismod. Vestibulum ante ipsum primis in faucibus orci luctus et ultrices posuere cubilia Curae; Proin ut est. Aliquam odio. Pellentesque massa turpis, cursus eu, euismod nec, tempor congue, nulla. Duis viverra gravida mauris. Cras tincidunt. Curabitur eros ligula, varius ut, pulvinar in, cursus faucibus,

augue.

Nulla mattis luctus nulla. Duis commodo velit at leo. Aliquam vulputate magna et leo. Nam vestibulum ullamcorper leo. Vestibulum condimentum rutrum mauris. Donec id mauris. Morbi molestie justo et pede. Vivamus eget turpis sed nisl cursus tempor. Curabitur mollis sapien condimentum nunc. In wisi nisl, malesuada at, dignissim sit amet, lobortis in, odio. Aenean consequat arcu a ante. Pellentesque porta elit sit amet orci. Etiam at turpis nec elit ultricies imperdiet. Nulla facilisi. In hac habitasse platea dictumst. Suspendisse viverra aliquam risus. Nullam pede justo, molestie nonummy, scelerisque eu, facilisis vel, arcu.

Curabitur tellus magna, porttitor a, commodo a, commodo in, tortor. Donec interdum. Praesent scelerisque. Maecenas posuere sodales odio. Vivamus metus lacus, varius quis, imperdiet quis, rhoncus a, turpis. Etiam ligula arcu, elementum a, venenatis quis, sollicitudin sed, metus. Donec nunc pede, tincidunt in, venenatis vitae, faucibus vel, nibh. Pellentesque wisi. Nullam malesuada. Morbi ut tellus ut pede tincidunt porta. Lorem ipsum dolor sit amet, consectetur adipiscing elit. Etiam congue neque id dolor.

Donec et nisl at wisi luctus bibendum. Nam interdum tellus ac libero. Sed sem justo, laoreet vitae, fringilla at, adipiscing ut, nibh. Maecenas non sem quis tortor eleifend fermentum. Etiam id tortor ac mauris porta vulputate. Integer porta neque vitae massa. Maecenas tempus libero a libero posuere dictum. Vestibulum ante ipsum primis in faucibus orci luctus et ultrices posuere cubilia Curae; Aenean quis mauris sed elit commodo placerat. Class aptent taciti sociosqu ad litora torquent per conubia nostra, per inceptos hymenaeos. Vivamus rhoncus tincidunt libero. Etiam elementum pretium justo. Vivamus est. Morbi a tellus eget pede tristique commodo. Nulla nisl. Vestibulum sed nisl eu sapien cursus rutrum.

Nulla non mauris vitae wisi posuere convallis. Sed eu nulla nec eros scelesque pharetra. Nullam varius. Etiam dignissim elementum metus. Vestibulum faucibus, metus sit amet mattis rhoncus, sapien dui laoreet odio, nec ultricies nibh augue a enim. Fusce in ligula. Quisque at magna et nulla commodo consequat. Proin accumsan imperdiet sem. Nunc porta. Donec feugiat mi at justo. Phasellus facilisis ipsum quis ante. In ac elit eget ipsum pharetra faucibus. Maecenas viverra nulla in massa.

7.2.1 Subsection 7.2 of section 2 in chapter 7

Aliquam lectus. Vivamus leo. Quisque ornare tellus ullamcorper nulla. Mauris porttitor pharetra tortor. Sed fringilla justo sed mauris. Mauris tellus. Sed non leo. Nullam elementum, magna in cursus sodales, augue est scelerisque sapien,

venenatis congue nulla arcu et pede. Ut suscipit enim vel sapien. Donec congue. Maecenas urna mi, suscipit in, placerat ut, vestibulum ut, massa. Fusce ultrices nulla et nisl.

Etiam ac leo a risus tristique nonummy. Donec dignissim tincidunt nulla. Vestibulum rhoncus molestie odio. Sed lobortis, justo et pretium lobortis, mauris turpis condimentum augue, nec ultricies nibh arcu pretium enim. Nunc purus neque, placerat id, imperdiet sed, pellentesque nec, nisl. Vestibulum imperdiet neque non sem accumsan laoreet. In hac habitasse platea dictumst. Etiam condimentum facilisis libero. Suspendisse in elit quis nisl aliquam dapibus. Pellentesque auctor sapien. Sed egestas sapien nec lectus. Pellentesque vel dui vel neque bibendum viverra. Aliquam porttitor nisl nec pede. Proin mattis libero vel turpis. Donec rutrum mauris et libero. Proin euismod porta felis. Nam lobortis, metus quis elementum commodo, nunc lectus elementum mauris, eget vulputate ligula tellus eu neque. Vivamus eu dolor.

7.3 REFERENCES

- [1] A. Liudi Mulyo, Y. Konno, J. S. Nilsen, A. T. J. van Helvoort, B.-O. Fimland, H. Weman, and K. Kishino. [Growth study of self-assembled GaN nanocolumns on silica glass by plasma assisted molecular beam epitaxy](#). *Journal of Crystal Growth* **480**, 67–73 (2017). Cited on page/s 89.
- [2] A. Liudi Mulyo, M. K. Rajpalke, H. Kuroe, P.-E. Vullum, H. Weman, B.-O. Fimland, and K. Kishino. [Vertical GaN nanocolumns grown on graphene intermediated with a thin AlN buffer layer](#). *Nanotechnology* **30** (1), 015604 (2018). Cited on page/s 89.
- [3] I. M. Hoiaas, A. Liudi Mulyo, P. E. Vullum, D.-C. Kim, L. Ahtapodov, B.-O. Fimland, K. Kishino, and H. Weman. [GaN/AlGaN Nanocolumn Ultraviolet Light-Emitting Diode Using Double-Layer Graphene as Substrate and Transparent Electrode](#). *Nano Letters* **19** (3), 1649–1658 (2019). Cited on page/s 89.
- [4] A. Liudi Mulyo, M. K. Rajpalke, P. E. Vullum, H. Weman, K. Kishino, and B.-O. Fimland. [The influence of AlN buffer layer on the growth of self-assembled GaN nanocolumns on graphene](#). *Scientific Reports* **10** (1), 853 (2020). Cited on page/s 89.
- [5] A. Liudi Mulyo *et al.* [The Influence of AlN Buffer Layer on the Growth of Self-Assembled GaN Nanocolumns on Graphene](#). *Unpublished* (n.d.). Cited on page/s 89.
- [6] A. Liudi Mulyo *et al.* [Utilization of Graphene as Substrate and Bottom Electrode for High-Density and Vertically-Aligned GaN/AlGaN Nanocolumns](#). *Unpublished* (n.d.). Cited on page/s 89.



APPENDIX A

Supporting information for chapter 4

A.1 DETAILED GROWTH INFORMATION

Lorem ipsum dolor sit amet, consectetuer adipiscing elit [?]. Ut purus elit, vestibulum ut, placerat ac, adipiscing vitae, felis ? . Curabitur dictum gravida mauris. Nam arcu libero, nonummy eget, consectetuer id, vulputate a, magna. Donec vehicula augue eu neque [?]. Pellentesque habitant morbi tristique senectus et netus et malesuada fames ac turpis egestas ? . Mauris ut leo. Cras viverra metus rhoncus sem [?]. Nulla et lectus vestibulum urna fringilla ultrices. Phasellus eu tellus sit amet tortor gravida placerat ? . Integer sapien est, iaculis in, pretium quis, viverra ac, nunc. Praesent eget sem vel leo ultrices bibendum [?]. Aenean faucibus. Morbi dolor nulla, malesuada eu, pulvinar at (??), mollis ac, nulla. Curabitur auctor semper nulla ? . Donec varius orci eget risus. Duis nibh mi, congue eu, accumsan eleifend, sagittis quis, diam. Duis eget orci sit amet orci dignissim rutrum [? ? ? ? ?].

TABLE A.1 | Detailed growth conditions of nanocolumns

| Nanocolumn segment/layer | Growth temperature, pyrometer reading (°C) | Beam equivalent pressure (Pa) | | | Si cell temperature (°C) | N ₂ plasma emission (sccm/mV) | Growth time (sec) |
|---|--|-------------------------------|------------------------|------------------------|--------------------------|--|-------------------|
| | | Al | Ga | Mg | | | |
| Al seeding with Si | 1 | 2.0 × 10 ⁻³ | - | - | 4 | - | 5 |
| Nitridation | 6 | - | - | - | - | 7.00/8.9 | 1 |
| n-AlN | 2 | 3.0 × 10 ⁻⁴ | - | - | 5 | 6.00/7.89 | 1 |
| n-GaN | 2 | - | 3.4 × 10 ⁻⁵ | - | 6 | 7.89/1.23 | 4 |
| n-Al _{0.56} Ga _{0.78} N | 9 | 1.2 × 10 ⁻³ | 4.0 × 10 ⁻⁵ | - | 6 | 7.00/8.9 | 1 |
| i-GaN | 2 | - | 3.1 × 10 ⁻² | - | - | 3.45/6.78 | 9 |
| p-Al _{1.23} Ga _{4.56} N | 7 | 8.9 × 10 ⁻¹ | 2.0 × 10 ⁻³ | 4.0 × 10 ⁻⁵ | - | 6.00/7.89 | 1 |
| p-GaN | 2 | - | 3.0 × 10 ⁻⁴ | 5.0 × 10 ⁻⁶ | - | 7.00/8.9 | 1 |

APPENDIX B

Supporting information for chapter 5

B.1 ADDITIONAL MICRO-RAMAN SPECTROSCOPY MEASUREMENTS

Lorem ipsum dolor sit amet, consectetuer adipiscing elit [?]. Ut purus elit, vestibulum ut, placerat ac, adipiscing vitae, felis ? . Curabitur dictum gravida mauris. Nam arcu libero, nonummy eget, consectetuer id, vulputate a, magna. Donec vehicula augue eu neque [?]. Pellentesque habitant morbi tristique senectus et netus et malesuada fames ac turpis egestas ? . Mauris ut leo. Cras viverra metus rhoncus sem [?]. Nulla et lectus vestibulum urna fringilla ultrices. Phasellus eu tellus sit amet tortor gravida placerat ? . Integer sapien est, iaculis in, pretium quis, viverra ac, nunc. Praesent eget sem vel leo ultrices bibendum [?]. Aenean faucibus. Morbi dolor nulla, malesuada eu, pulvinar at (??), mollis ac, nulla. Curabitur auctor semper nulla ? . Donec varius orci eget risus. Duis nibh mi, congue eu, accumsan eleifend, sagittis quis, diam. Duis eget orci sit amet orci dignissim rutrum [? ? ? ? ?].

TABLE B.1 | Summary of micro-Raman spectroscopy measurements for the as-grown nanocolumn sample carried out in different areas (of the same sample) from what is presented in ref fig:figures/paper-iv/fig-8. The table shows the median values of the D peak, G peak, and 2D peak, for the entire mapping (123 measurements), from the green patches (45 measurements), and from the purple areas (67 measurements).

| Median value | Area (number of measurements) | Position [cm ⁻¹] | Intensity [cps] | FWHM [cm ⁻¹] | Intensity ratio to G peak |
|--------------|-------------------------------|------------------------------|-----------------|--------------------------|---------------------------|
| D peak | Green patches (45) | 1 | 2 | 3 | 4 |
| | Full map (123) | 5 | 6 | 7 | 8 |
| | Purple areas (67) | 9 | 1 | 2 | 3 |
| G peak (*) | Green patches (45) | 4 | 5 | - | - |
| | Full map (123) | 6 | 7 | - | - |
| | Purple areas (67) | 8 | 9 | - | - |
| 2D peak | Green patches (45) | 1 | 2 | 3 | 4 |
| | Full map (123) | 5 | 6 | 7 | 8 |
| | Purple areas (67) | 9 | 1 | 2 | 3 |
| D' peak (**) | Green patches (45) | 4 | 5 | - | 6 |

APPENDIX C

Supplementary information for chapter 6

C.1 MICRO-PHOTOLUMINESCENCE SPECTRA OF HVPE-GAN AND NANOCOLUMN SAMPLES

This is an additional characterization from Subsection 6.2.1.

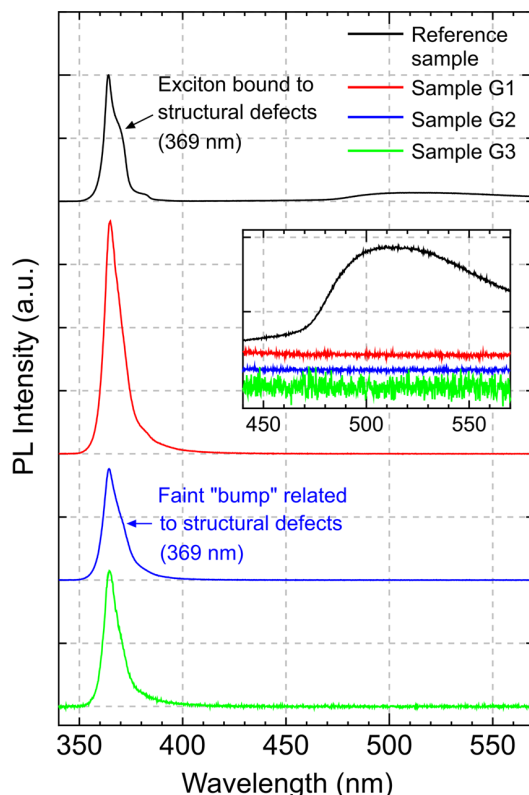


FIGURE C.1 | RT micro-photoluminescence spectra of reference sample (HVPE-freestanding GaN), samples G1, G2 and G3. Inset shows the magnified spectra in the wavelength range from 440 to 570 nm, highlighting the presence of broad green and yellow emission band in the reference sample (adapted with permission from ref. ? © Liudi Mulyo et al, 2020).

C.2 MICRO-RAMAN SPECTRA OF PRISTINE GRAPHENE AND NANOCOLUMN SAMPLES AFTER GROWTH

This is an extra measurement from subsection 6.2.1

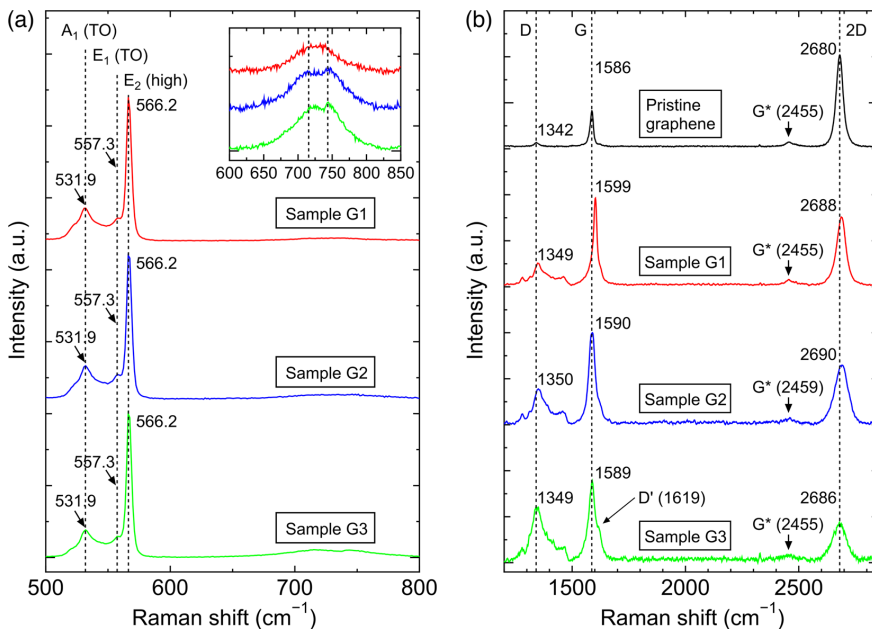


FIGURE C.2 | Micro-Raman spectroscopy of the nanocolumn samples, including the graphene for each respective sample. Raman spectra of (a) samples G1, G2 and G3 between 500 and 800 cm⁻¹, with the peak frequencies of the A₁ (TO), E₁ (TO) and E₂ (high) modes indicated by vertical dashed lines (inset: magnification from 600 to 850 cm⁻¹, with the identified peak frequencies at 715 and 743 cm⁻¹ of the possible SO and LPP modes, respectively [? ?], indicated by vertical dashed lines), and (b) pristine graphene, samples G1, G2 and G3 between 1100 and 3200 cm⁻¹. The dashed lines indicate D, G and 2D peak positions of pristine graphene (adapted with permission from ref. ? © Liudi Mulyo et al, 2020).

CURRICULUM VITAE

Author

PERSONAL INFORMATION

Family name, given name : Author
Nationality : Citizenship
Place, date of birth : City (Country), Month date^{st/nd/rd/th}, yyyy
Current address : Address, Postal code City, NO

EDUCATIONAL BACKGROUND AND RESEARCH EXPERIENCE

Doctor of Philosophy (Ph.D.) in Electronic Systems

Norwegian University of Science and Technology (NTNU), Trondheim, NO
month yyyy - month 2021

- ▶ Thesis title: The title of PhD thesis
- ▶ Advisors: Professor Supervisor and Professor Co-supervisor
- ▶ Additional information, like collaborative researcher at another Laboratory (name of the Professor) at University X, City, Country for total of xx months

Master of Science (M.Sc.) in Condensed Matter Physics

Norwegian University of Science and Technology (NTNU), Trondheim, NO
month yyyy - month 2013

- ▶ Thesis title: The title of MSc thesis
- ▶ Advisors: Professor Supervisor and Professor Co-supervisor

Bachelor of Engineering (B.Eng.) in Engineering Physics

Norwegian University of Science and Technology (NTNU), Trondheim, NO
month yyyy - month 2010

- ▶ Thesis title: The title of BEng thesis
- ▶ Advisors: Professor Supervisor and Professor Co-supervisor

TEACHING EXPERIENCE

Laboratory assistant for various courses, at **NTNU**: Nanoelectronics 2 (spring 2020 & 2021), Semiconductor Physics with Lab (spring 2017-2020), Physical Methods for Nanostructuring and Characterization (autumn 2017 & 2018), Chemical Methods for Synthesis and Characterization of Nanomaterial (autumn 2017 & 2018).

AWARDS

- Norges tekniske høgskoles fond, a travel grant for **ISSLED 2017** 2017
- NorFab travel grant for **MBE 2016** and **CSW 2017** 2017-2018
- NorFab project support, for research visit in University X 2018-2019
- PhD scholarship, NTNU 2017-2021

SKILLS

Scientific (laboratory) competency

- Experienced with the growth of semiconductor using molecular beam epitaxy technique.
- Skilled for material characterization techniques using scanning electron microscopy, photoluminescence, and Raman spectroscopy.
- Familiar with device fabrication tools, including mask/maskless aligner, e-beam/sputter deposition, plasma-enhanced chemical vapor deposition, wet etching, and inductively-coupled plasma reactive ion etching.
- Basic knowledge of e-beam lithography and X-ray diffraction.

Computer literacy

- Microsoft Windows, MacOS, and Debian-based Linux (competent)
- Microsoft Office, Inkscape, ImageJ, Ngraph, and L^AT_EX (intermediate)
- SketchUp, Blender, Python, MatLab, C++, HTML, and LabView (beginner)

Language fluency

- | | |
|-------------------------------|--------------------------|
| ► Indonesia (native) | ► Japanese (elementary) |
| ► English (full professional) | ► Norwegian (elementary) |

CONTACT INFORMATION

- | | | |
|----------|---|---|
| E-mail | : | author@outlook.com |
| Homepage | : | https://author.github.io |

Dissemination of research

PUBLICATIONS IN PEER REVIEWED JOURNALS

- [1] **Author 1**, Author 2, Author 3, Author 4, Author 5, Author 6, and Author 7. *Title of the paper*. *Journal of Crystal Growth* **480**, 67-73 (2017).
- [2] **Author 1**, Author 2, Author 3, Author 4, Author 5, Author 6, and Author 7. *Title of paper 2*. *Nanotechnology* **30** (1), 015604 (2018).
This article was chosen as cover image/featured article, see D.1.
- [3] Author 1*, **Author 2***, Author 3, Author 4, Author 5, Author 6, Author 7, and Author 8. *Title of paper 3*. *Nano Letters* **19** (3), 1649-1658 (2019).
***equal contributions**
- [4] **Author 1**, Author 2, Author 3, Author 4, Author 5, and Author 6. *Title of paper 4*. *Scientific Reports* **10**, 853 (2020).

MANUSCRIPT UNDER REVIEW

- [1] **Author 1**, Author 2*, Author 3*, Author 4, Author 5, Author 6, Author 7, Author 8, Author 9, and Author 10. *Title of manuscript*.
***equal contributions**



FIGURE D.1 | Our work published in Nanotechnology was selected as a cover image/featured article for the first issue of 2019 (4 January).

CONFERENCE PARTICIPATION (PRESENTATIONS)

Name of the author with [†] indicates the presenter. Half of the past meeting records (i.e., conference websites or pdf files of the conference programs) are still accessible online, and unfortunately half of them are no longer active (as of December 03 2020). For the latter, reader might notice that they are linked via [Internet Archive](#) or [my personal website](#).

- [1] **Author 1[†]**, Author 2, Author 3, Author 4, Author 5, and Author 6. *Title of the conference*. Contributed talk at [The 11th International Symposium on Semiconductor Light Emitting Devices \(ISSLED 2017\)](#), Banff, Canada, October 08-12 2017.
- [2] Author 1[†], **Author 2**, Author 3, Author 4, Author 5, and Author 6. *Title of the conference*. Contributed talk at [Nano@NTNU Symposium](#), Trondheim, Norway, December 06-07 2017.
- [3] **Author 1[†]**, Author 2, Author 3, Author 4, Author 5, and Author 6. *Title of the conference*. Poster presentation at [Nano@NTNU Symposium](#), Trondheim, Norway, December 06-07 2017.
No website or pdf file of the conference program is associated with this item.
- [4] Author 1[†], **Author 2**, Author 3, Author 4, Author 5, Author 6, Author 7, and Author 8. *Title of the conference*. Contributed talk at [Nanowire Week](#), Hamilton, Canada, June 11-15 2018.
- [5] Author 1, **Author 2**, Author 3, Author 4, Author 5, Author 6, Author 7, and Author 8[†]. *Title of the conference*. Poster presentation at [The International Workshop on Nitride Semiconductors](#), Kanazawa, Japan, November 11-16 2018.
- [6] **Author 1**, Author 2, Author 3, Author 4, Author 5, Author 6[†], and Author 7. *Title of the conference*. Poster presentation at [The International Workshop on Nitride Semiconductors](#), Kanazawa, Japan, November 11-16 2018.
- [7] **Author 1[†]**, Author 2, Author 3, Author 4, Author 5, Author 6, and Author 7. *Title of the conference*. Contributed talk at [The 10th annual workshop of Norwegian PhD Network on Nanotechnology for Microsystems](#), Tromsø, Norway, June 17-19 2019.
- [8] **Author 1**, Author 2, Author 3, Author 4, Author 5, and Author 6[†]. *Title of the conference*. Poster presentation at [The 13th International Conferences on Nitride Semiconductors](#), Bellevue, Washington (Seattle), USA, July 07-12 2019.

Copyright permissions

Below is the complete list of the copyright figures shown in this Doctoral thesis, mainly from chapter 1 to chapter 4.

- § [Figure 4.1¹](#) is reproduced with permission from: ¹page 23
[Offshore Wind Farms and Isolated Oil and Gas Platforms: Perspectives and Possibilities. ASME OMAE 2022 vol, pp \(2022\).](#)
Copyright © 2022 ASME.
- § [Figure 4.2²](#) is reproduced with permission from: ²page 24
[Offshore Wind Farms and Isolated Oil and Gas Platforms: Perspectives and Possibilities. ASME OMAE 2022 vol, pp \(2022\).](#)
Copyright © 2022 ASME.
- § [Figure 4.3³](#) is reproduced with permission from: ³page 26
[Offshore Wind Farms and Isolated Oil and Gas Platforms: Perspectives and Possibilities. ASME OMAE 2022 vol, pp \(2022\).](#)
Copyright © 2022 ASME.
- § [Figure 4.4⁴](#) is adapted with permission from: ⁴page 28
[Offshore Wind Farms and Isolated Oil and Gas Platforms: Perspectives and Possibilities. ASME OMAE 2022 vol, pp \(2022\).](#)
Copyright © 2022 Daniel Mota.
- § [Figure 4.5⁵](#) is reproduced with permission from: ⁵page 30
[Offshore Wind Farms and Isolated Oil and Gas Platforms: Perspectives and Possibilities. ASME OMAE 2022 vol, pp \(2022\).](#)
Copyright © 2022 ASME.
- § [Figure 4.6⁶](#) is reproduced with permission from: ⁶page 31
[Offshore Wind Farms and Isolated Oil and Gas Platforms: Perspectives and Possibilities. ASME OMAE 2022 vol, pp \(2022\).](#)
Copyright © 2022 ASME.
- § [Figure 4.7⁷](#) is reproduced with permission from: ⁷page 33
[Offshore Wind Farms and Isolated Oil and Gas Platforms: Perspectives and Possibilities. ASME OMAE 2022 vol, pp \(2022\).](#)
Copyright © 2022 ASME.

⁸page 37 § [Figure 4.8](#)⁸ is adapted from:

[Offshore Wind Farms and Isolated Oil and Gas Platforms: Perspectives and Possibilities. ASME OMAE 2022 vol, pp \(2022\).](#)

Copyright © 2022 Daniel Mota.

⁹page 38 § [Figure 4.9](#)⁹ is reproduced with permission from:

[Offshore Wind Farms and Isolated Oil and Gas Platforms: Perspectives and Possibilities. ASME OMAE 2022 vol, pp \(2022\).](#)

Copyright © 2022 ASME.

¹⁰page 39 § [Figure 4.10](#)¹⁰ is reproduced with permission from:

[Offshore Wind Farms and Isolated Oil and Gas Platforms: Perspectives and Possibilities. ASME OMAE 2022 vol, pp \(2022\).](#)

Copyright © 2022 ASME.

COLOPHON

This thesis was typeset using L^AT_EX and the book documentclass. Main text is contained within the dimension of 115 mm (width)/197.2 mm (length), where the horizontal (top:bottom) and vertical (left:right) margin ratios are 1:1. The width of the margin notes is 12 mm. Style of this thesis is inspired by Friedrich Wiemer's thesis *Security Arguments and Tool-based Design of Block Ciphers* [<https://hss-opus.ub.rub.de/opus4/frontdoor/deliver/index/docId/7044/file/diss.pdf>].

Sebastian Kosch's *Crimson* [<https://github.com/skosch/Crimson>] is set as the running text (11 pt) typeface. Matthew Carter's *Charter* acts as the title (14.4 pt), section (10 pt), subsection (10 pt), and header (8 pt) typefaces. Hermann Zapf's *Palatino* serves as the page (9 pt) typeface. Christian Robertson's *Roboto* [<https://tug.org/FontCatalogue/roboto/>] is utilized for the figure caption (8 pt) typeface. Libertine Open Fonts Project's *Linux Libertine* [<https://tug.org/FontCatalogue/linuxlibertine/>] and Linus Romer's *Miama Nueva* [<https://tug.org/FontCatalogue/miamanueva/>] are used for math/equation (11 pt) and calligraphical (14.4 pt) typefaces. The *textgreek* package [<https://www.ctan.org/pkg/textgreek>] provides Greek letters in normal font (being not *italicized* as in \$math\$ mode).

Six different color palettes exploited throughout this thesis are listed as follows: RGB: 0, 80, 158 , RGB: 125, 0, 45 , RGB: 255, 248, 220 , RGB: 231, 231, 231 , RGB: 0, 65, 120 , and RGB: 128, 128, 128 .

The references were processed by BibTeX/natbib -backref option enabled-with modified unsrtnat bibliography style. Further details on the packages utilized to make this thesis, along with the L^AT_EX source (template) of this thesis can be found on <https://andreasliudimulyo.github.io/#latex>.

Most of the graphics in this thesis were generated using Inkscape [<https://inkscape.org>] and Ngraph [<https://forest.watch.impress.co.jp/library/software/ngraph/>].

Final Version as of Tuesday 27th September, 2022 at 17:25:26.